# Supporting Information

# Synthesis of γ-Oxo-α-amino Acids via Radical Acylation with Carboxylic Acids

Kay Merkens,‡ Francisco José Aguilar Troyano,‡ Khadijah Anwar, Adrián Gómez-Suárez*

*Organic Chemistry, Bergische Universität Wuppertal, Gaußstr. 20, 42119 Wuppertal (Germany)*

**Corresponding to: Email: gomezsuarez@uni-wuppertal.de*

## Table of Contents

## LED’s emission spectra & standard reaction set up

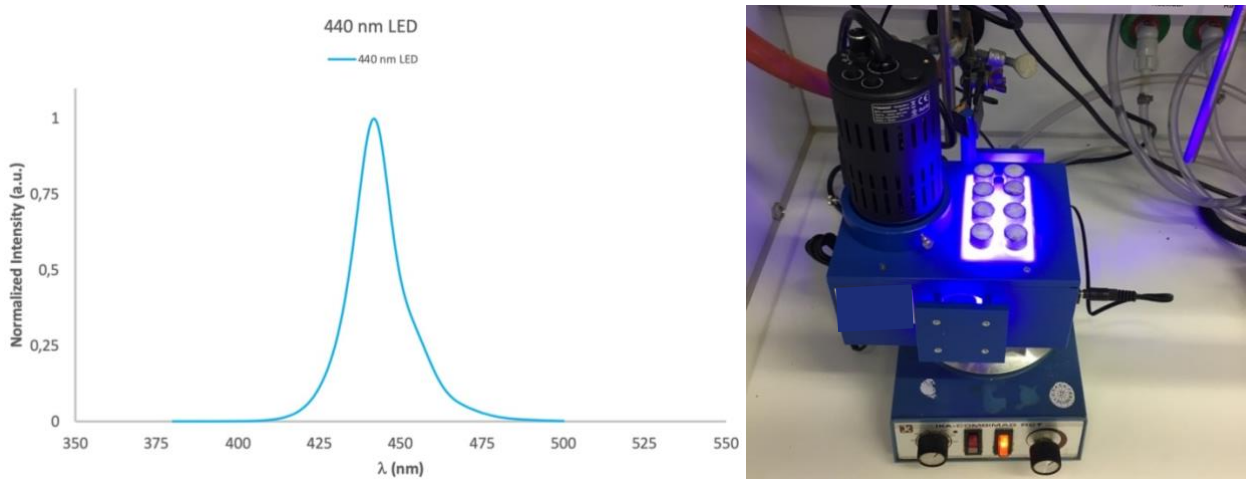


**Figure S1.** LED lamp reaction equipment

## Optimization of the reaction conditions

### General protocol

A 4 mL vial was charged with Dha derivative **I**, an acid, the photocatalyst, phosphine, and, if solid, the corresponding base, then sealed with a septum cap. The vial was put under vacuum for 5 min and refilled with $N_2$. Afterwards, degassed solvent and the base, if liquid, were added subsequently. The reaction mixture was then sparged with $N_2$ for 2-5 min and irradiated with blue LEDs ($\lambda_{max}$ = 440 or 450 nm) for the stated time. Afterwards, methyl laureate (25 µL, 0.1 mmol, 1.0 equiv.) was added as the internal standard, and the reaction was diluted with EtOAc. An aliquot of the mixture was then analysed by GC-FID and the yield or conversion calculated from the corresponding calibration curve.

### Optimization of acylation with benzoic acid

**Table S1.** Screening of solvents and bases for the acylation with benzoic acid

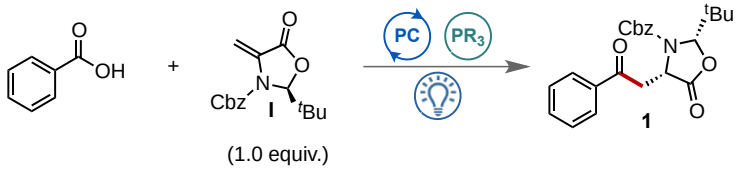


| Entry | PC (mol%) | Acid (equiv.) | Solvent (M) | $PPh_3$ (equiv.) | Base (equiv.) | Time (h) | T (ºC) | **I** left (%) | Yield **1** (%) |
|---|---|---|---|---|---|---|---|---|---|
| **1** | **Ir-F** (1) | 1.5 | 1,4-dioxane (0.2) | 2 | 2,6-lutidine (2.0) | 16 | 25 | 0 | Quant. |
| **2** | **Ir-F** (1) | 1.5 | DMF (0.2) | 2 | 2,6-lutidine (2.0) | 16 | 25 | 10 | 78 |
| **3** | **Ir-F** (1) | 2 | DMF (0.2) | 2.5 | 2,6-lutidine (2.5) | 16 | 25 | 2 | 68 |
| **4** | **Ir-F** (1) | 2 | DMF (0.5) | 2.5 | 2,6-lutidine (2.5) | 16 | 25 | 0 | 28 |
| **5** | **Ir-F** (1) | 1.5 | 1,4-dioxane (0.1) | 1.5 | 2,6-lutidine (1.5) | 16 | 25 | 7 | 84 |
| **6** | **Ir-F** (1) | 1.5 | 1,4-dioxane (0.2) | 1.5 | 2,6-lutidine (1.5) | 16 | 25 | 5 | 95 |
| **7** | **Ir-F** (1) | 1.5 | MeCN (0.1) | 1.5 | 2,6-lutidine (1.5) | 16 | 25 | 0 | Quant |
| **8** | **Ir-F** (1) | 1.5 | 1,4-dioxane (0.2) | 1.8 | $Cs_2CO_3$ (2.0) | 16 | 25 | 60 | 35 |
| **9** | **Ir-F** (1) | 1.5 | 1,4-dioxane (0.2) | 1.8 | $K_2HPO_4$ (2.0) | 16 | 25 | 21 | 70 |
| **10** | **Ir-F** (1) | 1.5 | 1,4-dioxane (0.2) | 1.8 | $KH_2PO_4$ (2.0) | 16 | 25 | 76 | 10 |
| **11** | **-** | 1.5 | 1,4-dioxane (0.2) | 1.8 | 2,4,6-collidine (2.0) | 24 | 25 | Quant | 0 |
| **12*** | **Ir-F** (1) | 1.5 | 1,4-dioxane (0.2) | 1.8 | 2,4,6-collidine (2.0) | 24 | 25 | Quant | 0 |
| **13** | **4CzIPN** (1) | 1.5 | 1,4-dioxane (0.2) | 1.8 | 2,4,6-collidine (2.0) | 24 | 25 | Quant | 0 |

** No irradiation*

### Optimization of acylation with nicotinic acid

**Table S2.** Screening of solvents and bases for the acylation with nitcotinic acid

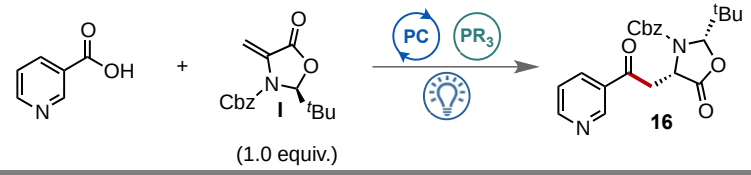


(1.0 equiv.)

| Entry | PC (mol%) | Acid (equiv.) | Solvent (M) | $PPh_3$ (equiv.) | Base (equiv.) | Time (h) | T (ºC) | **I** left (%) | Yield **16** (%) |
|---|---|---|---|---|---|---|---|---|---|
| **1** | **Ir-F** (1) | 1.5 | 1,4-dioxane(0.1) | 1.5 | 2,6-lutidine (1.5) | 16 | 25 | 86 | 24 |
| **2** | **Ir-F** (1) | 1.5 | 1,4-dioxane (0.1) | 1.5 | 2,4,6-collidine (1.5) | 16 | 25 | 29 | 46 |
| **3** | **Ir-F** (1) | 1.5 | 1,4-dioxane (0.2) | 2 | 2,6-lutidine (2.0) | 16 | 25 | 40 | 41 |
| **4** | **Ir-F** (1) | 1.5 | 1,4-dioxane (0.2) | 1.8 | 2,4,6-collidine (2.0) | 24 | 25 | 20 | 56 |
| **5** | **Ir-F** (1) | 1.5 | DMF (0.2) | 2 | 2,6-lutidine (2.0) | 16 | 25 | 16 | 39 |
| **6** | **Ir-F** (1) | 2 | DMF (0.2) | 2.5 | 2,6-lutidine (2.5) | 16 | 25 | 23 | 37 |
| **7** | **Ir-F** (1) | 2 | DMF (0.5) | 2.5 | 2,6-lutidine (2.5) | 16 | 25 | 19 | 33 |
| **8** | **Ir-F** (1) | 2 | DMF (0.5) | 2.5 | 2,6-lutidine (2.5) | 16 | 42 | 5 | 32 |
| **9** | **Ir-F** (1) | 1.5 | MeCN (0.1) | 1.5 | 2,6-lutidine (1.5) | 16 | 25 | 21 | 55 |
| **10** | **Ir-F** (1) | 1.5 | MeCN (0.2) | 1.5 | 2,4,6-collidine (1.5) | 60 | 25 | 9 | 58 |
| **11** | **Ir-F** (1) | 1.5 | $CH_2Cl_2$ (0.1) | 1.5 | 2,6-lutidine (1.5) | 16 | 25 | 46 | 26 |

## Optimization of acylation with hydrocinnamic acid

**Table S3.** Screening of solvents and bases for the acylation with hydrocinnamic acid

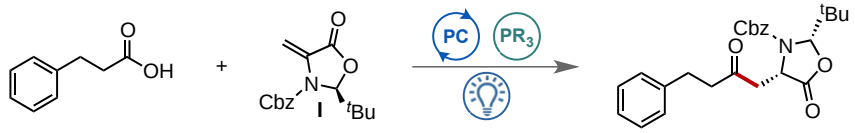


(1.0 equiv.)

| Entry | PC (mol%) | Acid (equiv.) | Solvent (M) | $PR_3$ (equiv.) | Base (equiv.) | Time (h) | T (ºC) | **I** left (%) | Yield (%) |
|---|---|---|---|---|---|---|---|---|---|
| **1** | **Ir-F** (1) | 1.5 | 1,4-dioxane (0.2) | $PPh_3$ (2.0) | 2,6-lutidine (2.0) | 16 | 25 | 89 | 0 |
| **2** | **Ir-F** (1) | 2 | DMF (0.2) | $PPh_3$ (2.5) | 2,6-lutidine (2.5) | 16 | 42 | 43 | 2 |
| **3** | **Ir-F** (1) | 2 | DMF (0.2) | $PPh_3$ (2.5) | 2,6-lutidine (2.5) | 16 | 25 | 84 | 0 |
| **4** | **Ir-F** (1) | 2 | DMSO (0.2) | $PPh_3$ (2.5) | 2,6-lutidine (2.5) | 16 | 25 | 79 | 0 |
| **5** | **Ir-F** (1) | 2 | Acetone (0.2) | $PPh_3$ (2.5) | 2,6-lutidine (2.5) | 16 | 25 | 89 | 0 |
| **6** | **Ir-F** (1) | 2 | MeCN (0.2) | $PPh_3$ (2.5) | 2,6-lutidine (2.5) | 16 | 25 | 95 | 0 |
| **7** | **Ir-F** (1) | 2 | DCM (0.2) | $PPh_3$ (2.5) | 2,6-lutidine (2.5) | 16 | 25 | 93 | 0 |
| **8** | **Ir-F** (1) | 2 | DME (0.2) | $PPh_3$ (2.5) | 2,6-lutidine (2.5) | 16 | 25 | 81 | 0 |
| **9** | Ir-F (1) | 1.5 | 1,4-dioxane (0.2) | $PPhMe_2$ (1.5) | 2,6-lutidine (1.5) | 16 | 25 | 94 | 0 |
| **10** | Ir-F (1) | 1.5 | 1,4-dioxane (0.2) | $PPh_2OEt$ (1.5) | 2,6-lutidine (1.5) | 16 | 25 | 88 | 0 |
| **11** | Ir-F (1) | 1.5 | 1,4-dioxane (0.2) | $POMe_2Ph$ (1.5) | 2,6-lutidine (1.5) | 16 | 25 | 75 | 0 |
| **12** | Ir-F (1) | 1.5 | 1,4-dioxane (0.5) | $PPh_3$ (1.8) | 2,4,6-collidine (2.0) | 18 | 45 | 77 | 0 |
| **13** | Ir-F (1) | 1.5 | 1,4-dioxane (0.5) | $PMePh_2$ (1.8) | 2,4,6-collidine (2.0) | 18 | 45 | 50 | 0 |

## UV/Vis absorption spectra

UV/Vis absorption spectra were recorded using a Mettler Toledo UV5 spectrophotometer. The samples were measured in UV quartz cuvettes (chamber volume = 1.4 mL, H × W × D = 46 mm × 12.5 mm, 12.5 mm) fitted with a PTFE stopper. Stock solutions of $PPh_3$, 2,4,6-collidine, **I**, benzoic acid and the reaction mixture with and without **Ir-F**, were prepared with the same concentration used in the reaction in the presence of air, using 1,4-dioxane as solvent.

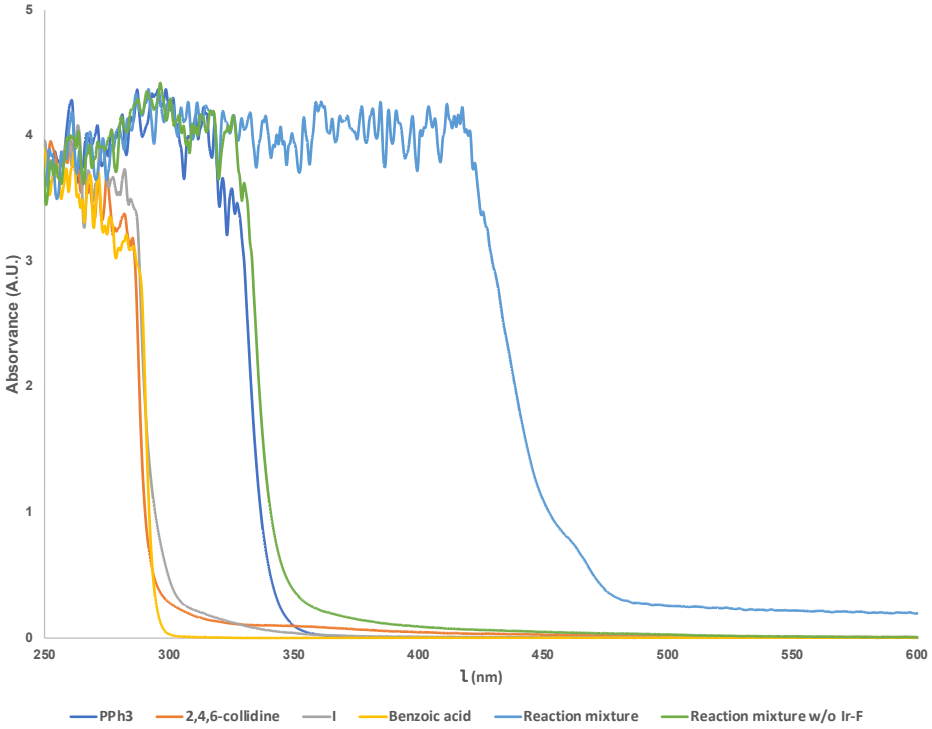


**Figure S2.** UV/Vis absorption spectrum of reaction components

## Reaction in the presence of TEMPO

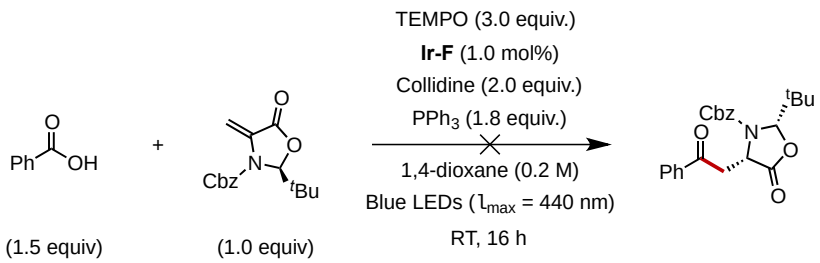


**Figure S3**. Scheme of reaction in the presence of TEMPO

A 4 mL vial was charged with benzoic acid (22.5 mg, 0.15 mmol, 1.5 equiv.), **I** (29 mg, 0.1 mmol, 1.0 equiv.), $PPh_3$ (47 mg, 0.27 mmol, 1.8 equiv.), **Ir-F** (1.1 mg, 1 µmol, 1 mol%), and TEMPO (46.8 mg, 0.3 mmol, 3.0 equiv.), and sealed with a septum cap. The vial was put under vacuum for 1 min and refilled with $N_2$ (x 3). Afterwards, 2,4,6-collidine (25 µL, 0.2 mmol, 2.0 equiv.) and degassed 1,4-dioxane (0.5 mL, 0.2 M) were added. The reaction mixture was then sparged with $N_2$ for 2-5 min and irradiated with blue LEDs ($\lambda_{max}$ = 440 nm) for 16 h. Afterwards, the reaction was diluted with EtOAc (1 mL) and methyl laureate (25 µL, 0.1 mmol, 1.0 equiv.) was added as internal standard. An aliquot of the mixture was then analysed by GC-FID. No product formation was observed.

## Quantum yield determination

### Determination of the light intensity at 440 nm

Following the procedure of Yoon,[1] the photon flux of the LED ($\lambda_{max}$ = 440 nm) was determined by standard ferrioxalate actinometry.[2] A 0.15 M solution of ferrioxalate was prepared by dissolving potassium ferrioxalate trihydrate (0.73 g) in $H_2SO_4$ (10 mL of a 0.05 M

solution). A buffered solution of 1,10-phenanthroline was prepared by dissolving 1,10-phenanthroline (25 mg) and sodium acetate (5.6 g) in $H_2SO_4$ (25 mL of a 0.50 M solution). Both solutions were stored in the dark. To determine the photon flux of the LED, the ferrioxalate solution (1.0 mL) was placed in a cuvette and irradiated for 120 seconds at $\lambda_{max}$ = 440 nm. After irradiation, the phenanthroline solution (175 µL) was added to the cuvette and the mixture was allowed to stir in the dark for 1 h to allow the ferrous ions to fully coordinate to the phenanthroline. The absorbance of the solution was measured at 510 nm. A non-irradiated sample was also prepared and the absorbance was measured at 510 nm. Conversion was calculated using eq. 1.

$$\text{mol } Fe^{2+} = \frac{V\Delta A(510\text{ nm})}{l\varepsilon} \quad \text{(eq. 1)}$$

where V is the total volume (0.001175 L) of the solution after addition of phenanthroline, ∆A is the difference in absorbance at 510 nm between the irradiated and non-irradiated solutions, l is the path length (1.00 cm), and ε is the molar absorptivity of the ferrioxalate actinometer at 510 nm (11,100 $Lmol^{-1}cm^{-1}$).[3] With this data, the photon flux was calculated using eq. 2.

$$\text{Photon flux} = \frac{\text{mol } Fe^{2+}}{\Phi t f} \quad \text{(eq. 2)}$$

where Φ is the quantum yield for the ferrioxalate actinometer (1.01 at $\lambda_{ex}$ = 437 nm),[4] t is the irradiation time (120 s), and f is the fraction of light absorbed at $\lambda_{ex}$ = 437 nm by the ferrioxalate actinometer. This value was calculated using eq. 3 where A (440 nm) is the absorbance of the ferrioxalate solution at 440 nm. An absorption spectrum gave an A (440 nm) value of > 3, indicating that the fraction of absorbed light (f) is > 0.999.

$$f = 1 - 10^{-A(440\,nm)} \quad \text{(eq. 3)}$$

The photon flux was thus calculated (as an average of three experiments) to be 8.24081 x $10^{-10}$ einsteins $s^{-1}$

**Determination of the reaction quantum yield**

**Using GP-A:** A reaction under the standard conditions using **1** (29 mg, 0.1 mmol, 1 equiv.) and benzoic acid (18.3 mg, 0.15 mmol, 1.5 equiv.) was irradiated at 440 nm for 3600 sec. Afterwards, the reaction was diluted with EtOAc (1 mL) and methyl laureate (25 µL, 0.1 mmol, 1.0 equiv.) was added as internal standard. An aliquot of the mixture was then analysed by GC-FID and the yield/conversion was calculated from the corresponding calibration curve. This afforded **2** in 40 % yield (4 x $10^{-5}$ mol). The reaction quantum yield (Φ) was determined using eq. 4, where the photon flux 8.24081 x $10^{-10}$ einsteins $s^{-1}$ (determined by actinometry as described above), t is the reaction time (3600 s) and f is the fraction of incident light absorbed by the reaction mixture, determined using eq. 3. An absorption spectrum of the reaction mixture gave an absorbance value of 2.19444 at 437 nm, thus f was determined to be a value of 0.9936.

$$\Phi = \frac{\text{mol of product formed}}{\text{Photon flux}tf} \quad \text{(eq. 4)}$$

Hence, the reaction quantum yield (Φ) was thus determined to be 13.57.

## Alternative mechanistic hypothesis

Quantum yield determinations suggest that there is also a significant contribution from a radical-chain pathway (Φ = 13.5), which made us reconsider the mechanistic proposal. Based on further experiments, it seems likely that 2,4,6-collidine plays a crucial role in the chain process: when the reaction is carried out either using superstoichiometric inorganic bases ($Cs_2CO_2$, $K_2HPO_4$ or $KH_2PO_4$) or in the absence of base, **1** is obtained in diminished yields, while when a catalytic amount of 2,4,6-collidine is employed (20 mol%) the reaction affords **1** in good yields (20% yield after 1 h, 79% yield after 3 h) and with a Φ = 6.8 after 1 h. Based on this information, we propose the following mechanistic pathway, where 2,4,6-collidine plays a crucial role as radical-chain carrier:

First, the excited photocatalyst (***Ir**$^{III}$, $^*E_{1/2}$ = +1.21 V versus SCE)[5] undergoes reductive quenching by $PPh_3$ ($E_{1/2}$ = +0.98 V versus SCE)[6] to generate a phosphoranyl radical cation (**III**) and a **Ir**$^{II}$ species. **III** reacts with the corresponding carboxylic acid to afford intermediate **IV**, which readily undergoes β-scission to deliver $OPPh_3$ and the key acyl radical **V**. Subsequent radical addition of the latter to **I** affords α-amino radical **VI**. After intermediate **VI** is generated, two path-ways are possible:

a) reduction of **VI** by the reduced **Ir**$^{II}$ ($E_{1/2}$ = −1.37 V vs SCE)[5] and protonation to deliver the desired product and complete the photocatalytic cycle.
b) a HAT or PCET between **VI** and pyridinium species **VII** would generate a highly oxidizing pyridinium radical cation (**VIII**) ($E_{1/2}$ collidine ≥ +2 V vs SCE),[7] which would act as a chain carrier by oxidizing $PPh_3$ to generate the key phosphoranyl radical cation **III** and regenerate the base.

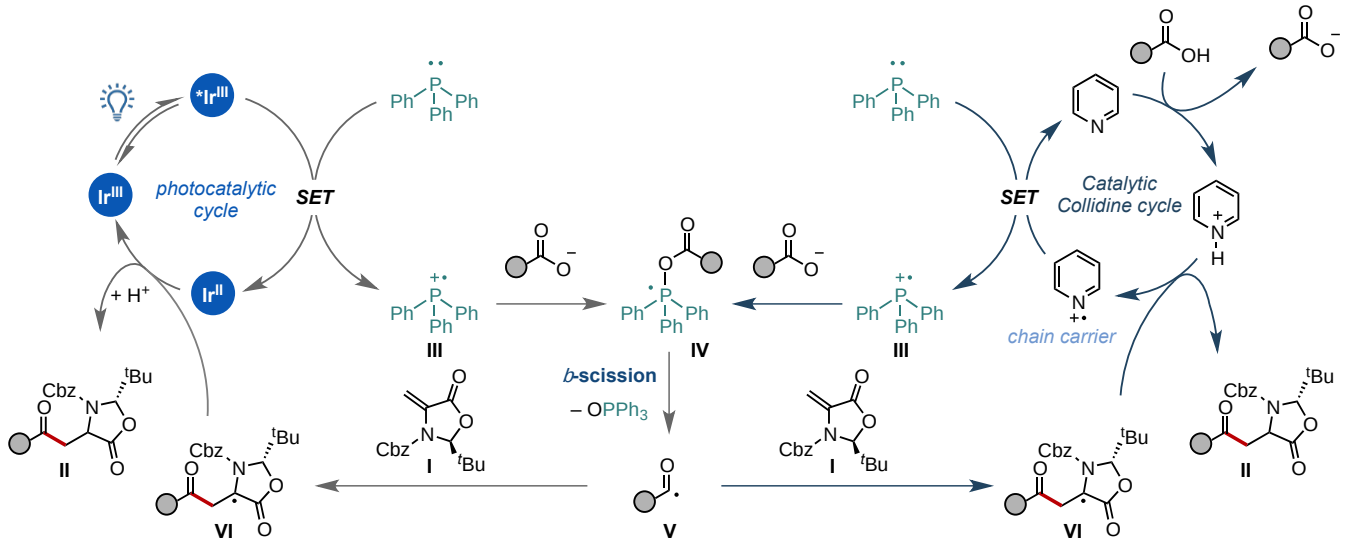


**Figure S4.** Alternative mechanistic hypothesis.

## $^{1}H$, $^{13}C$ and $^{19}F$ NMR Spectra

**(2S,4S)-2-(tert-butyl)-5-oxo-4-(2-oxo-2-phenylethyl)oxazolidine-3-carboxylate (1)**

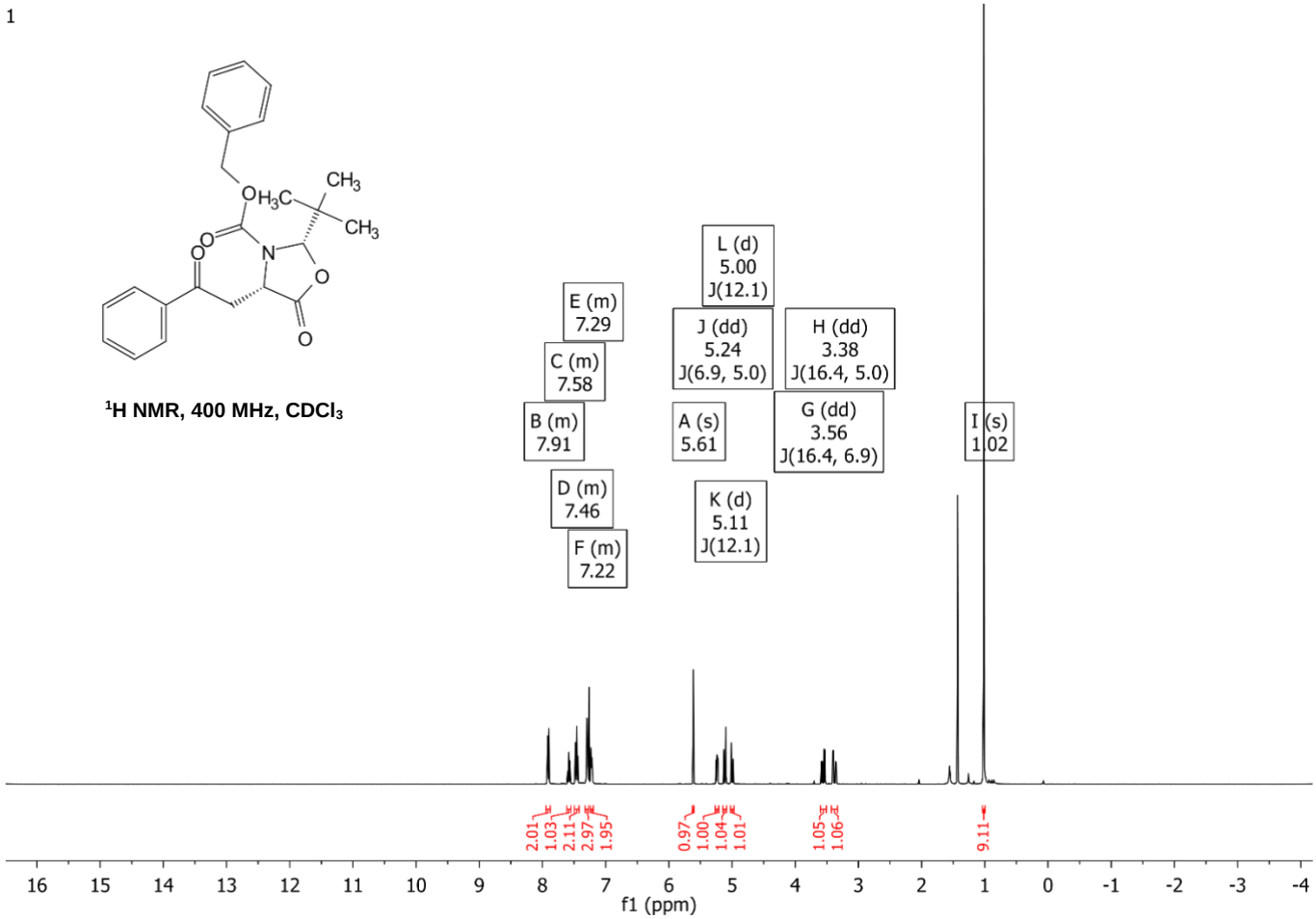


**$^{1}H$ NMR, 400 MHz, $CDCl_3$**

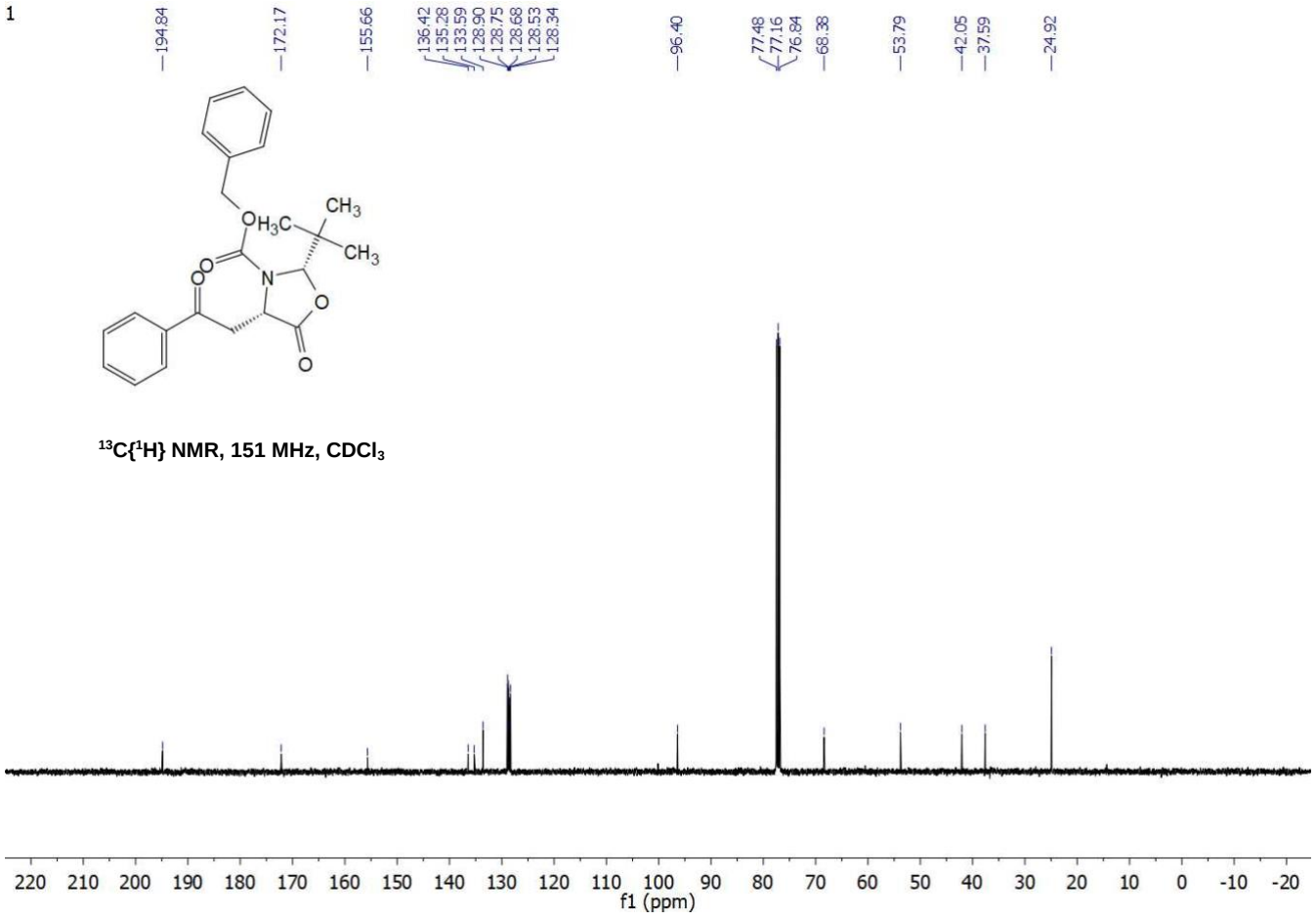


**$^{13}C\{^{1}H\}$ NMR, 151 MHz, $CDCl_3$**

**Benzyl (2R,4R)-2-(tert-butyl)-5-oxo-4-(2-oxo-2-phenylethyl-2-13C)oxazolidine-3-carboxylate (1-13)**

1-13



**$^{1}$H NMR, 400 MHz, $CDCl_3$**

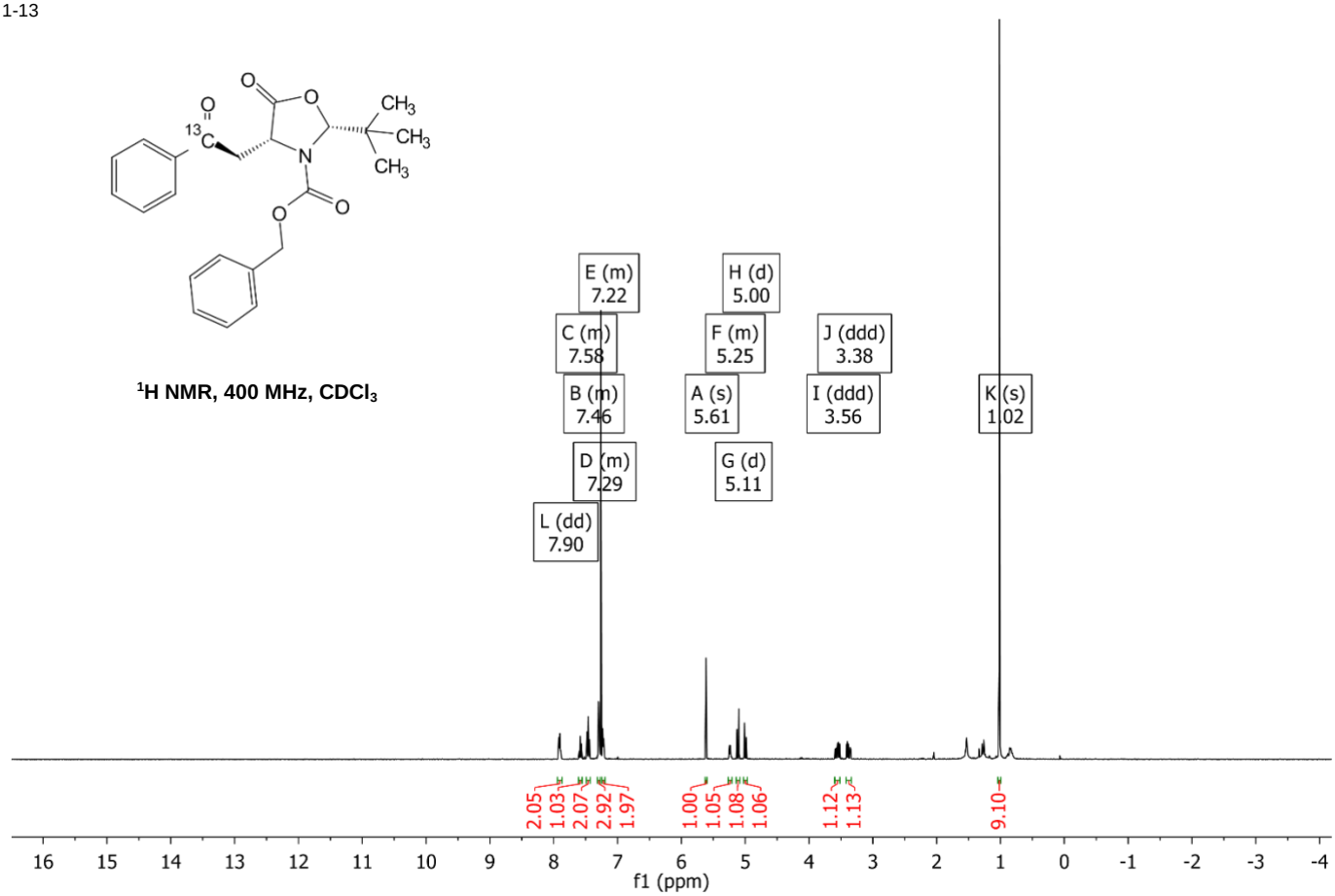




**$^{13}C\{^{1}H\}$ NMR, 151 MHz, $CDCl_3$**

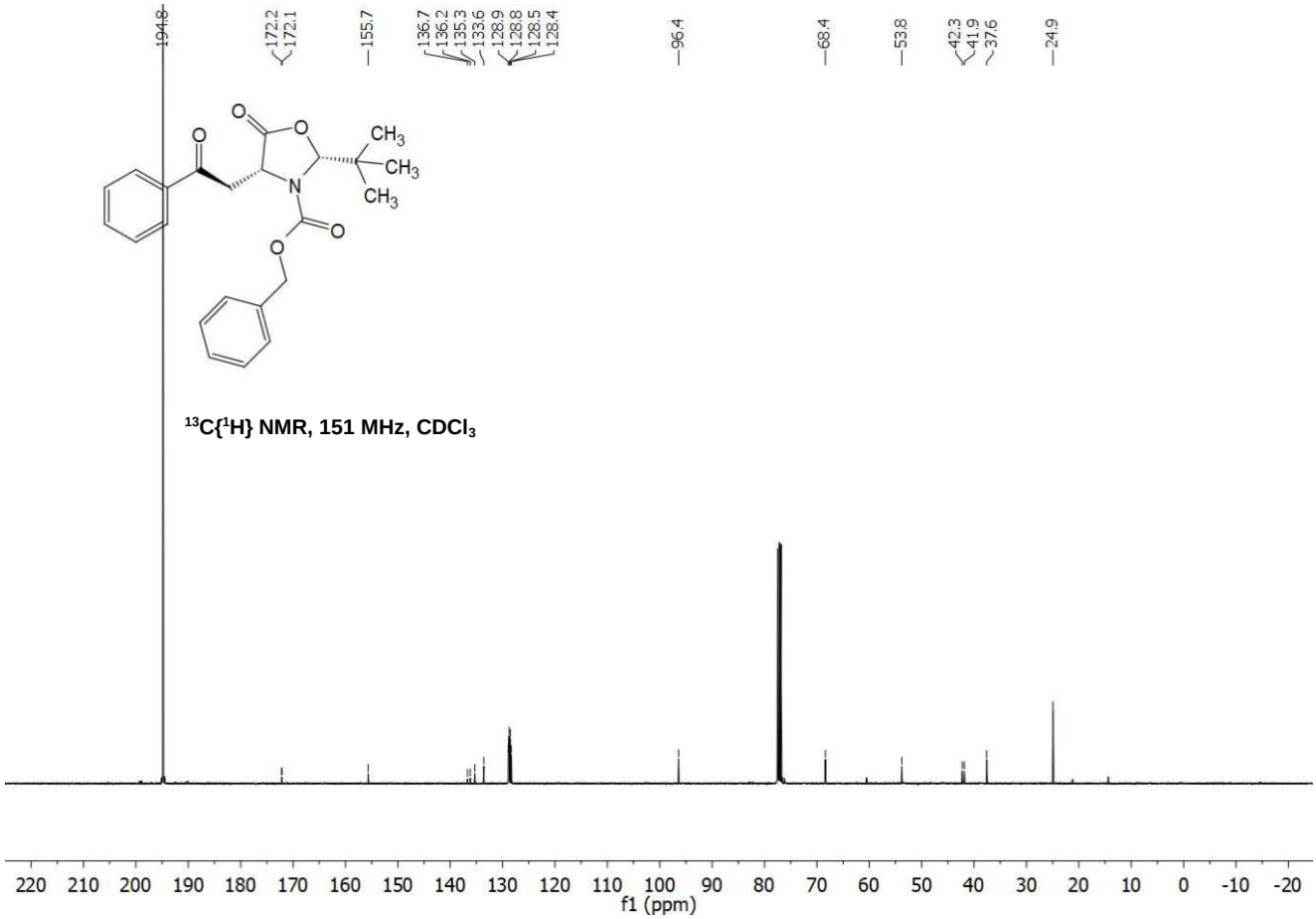

**Methyl 2-(bis(tert-butoxycarbonyl)amino)-4-oxo-4-phenylbutanoate (1A)**

1A

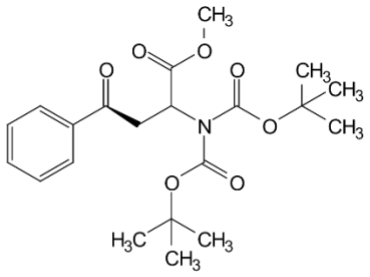

**$^{1}$H NMR, 400 MHz, $CDCl_3$**

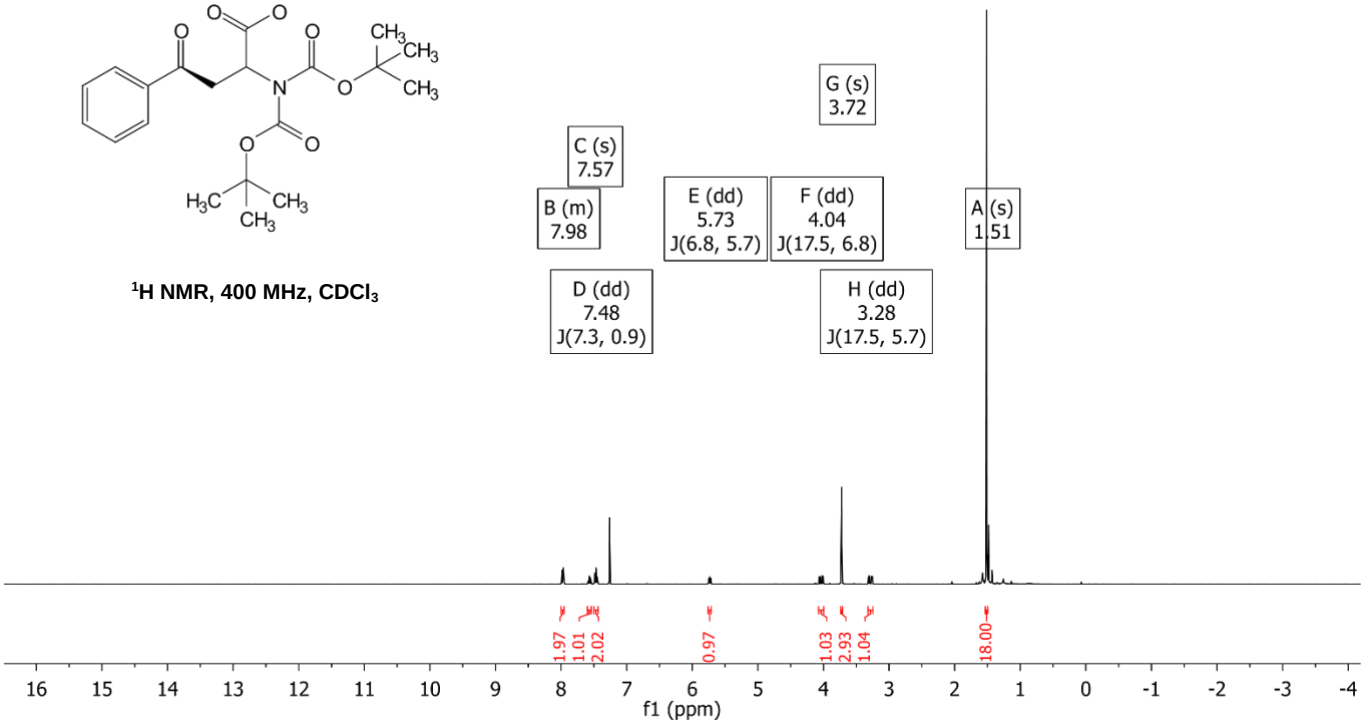


1A


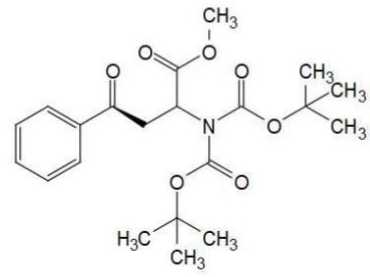

**$^{13}$C{$^{1}$H} NMR, 151 MHz, $CDCl_3$**

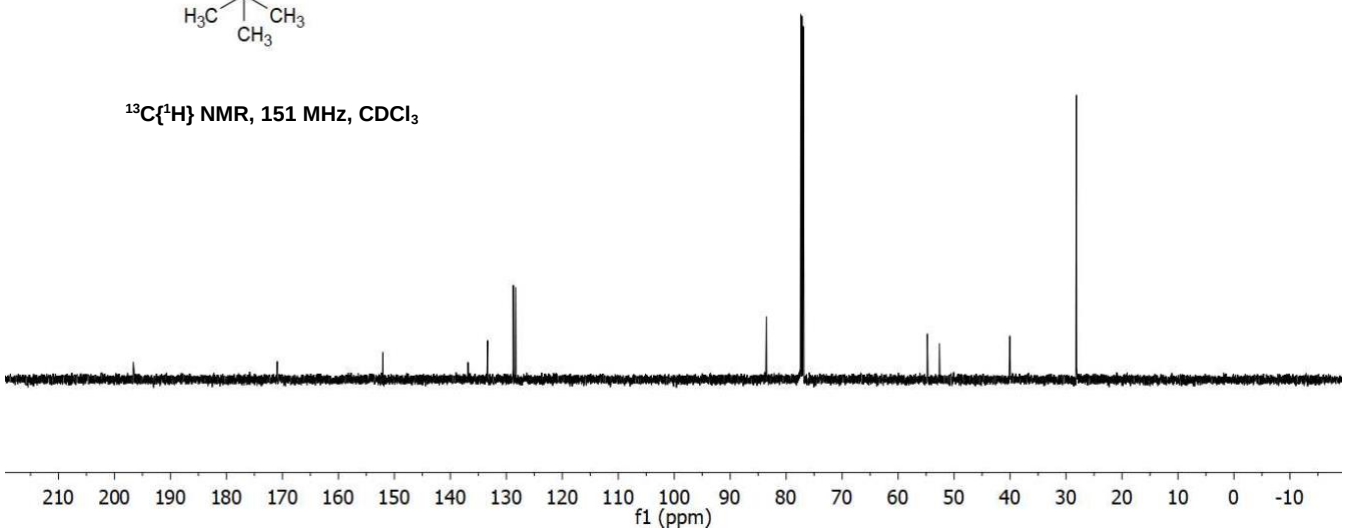

**Benzyl (2S,4S)-2-(tert-butyl)-4-(2-(4-methoxyphenyl)-2-oxoethyl)-5-oxooxazolidine-3-carboxylate (3)**

3

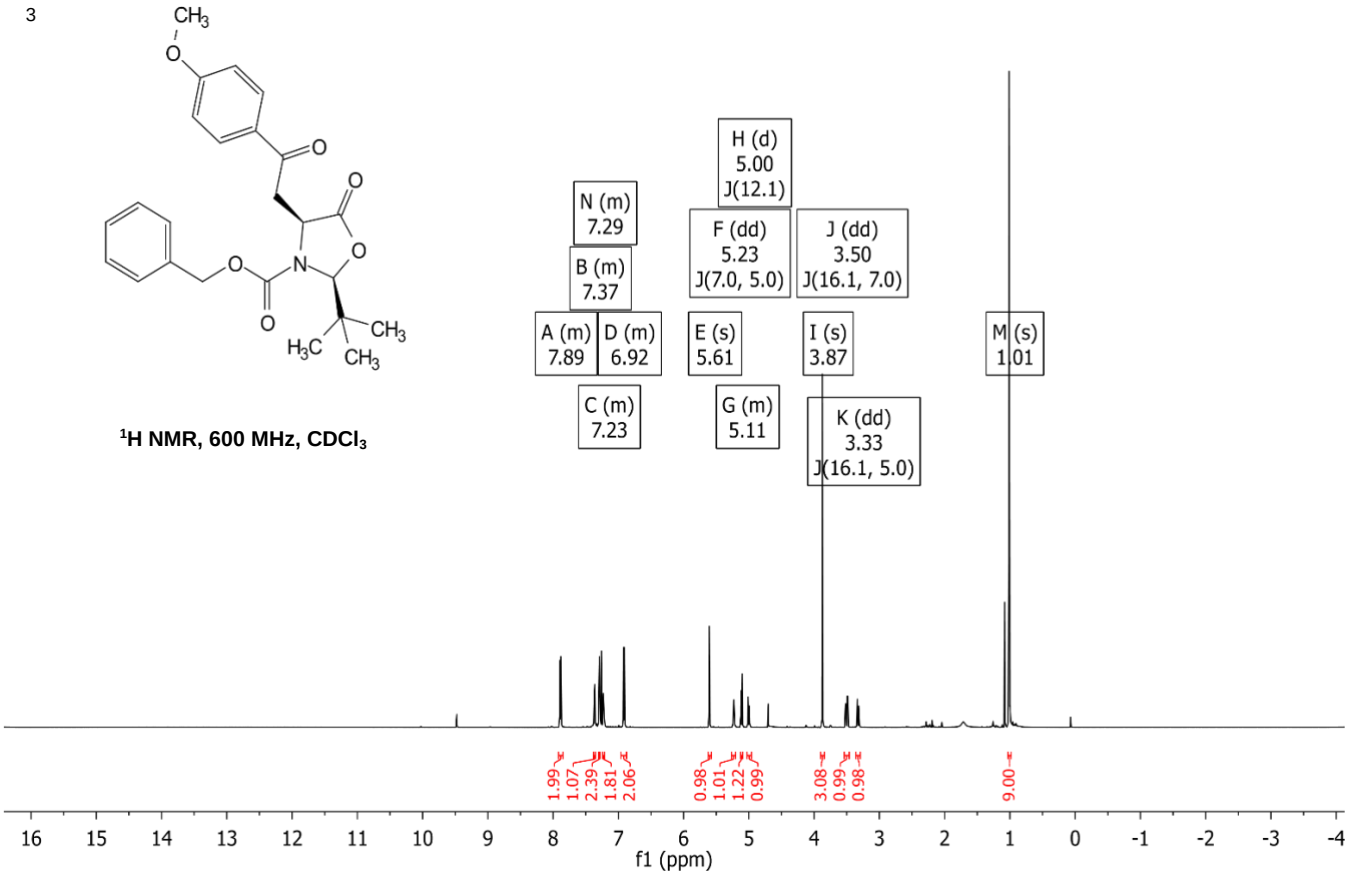


**$^{1}$H NMR, 600 MHz, $CDCl_3$**

3

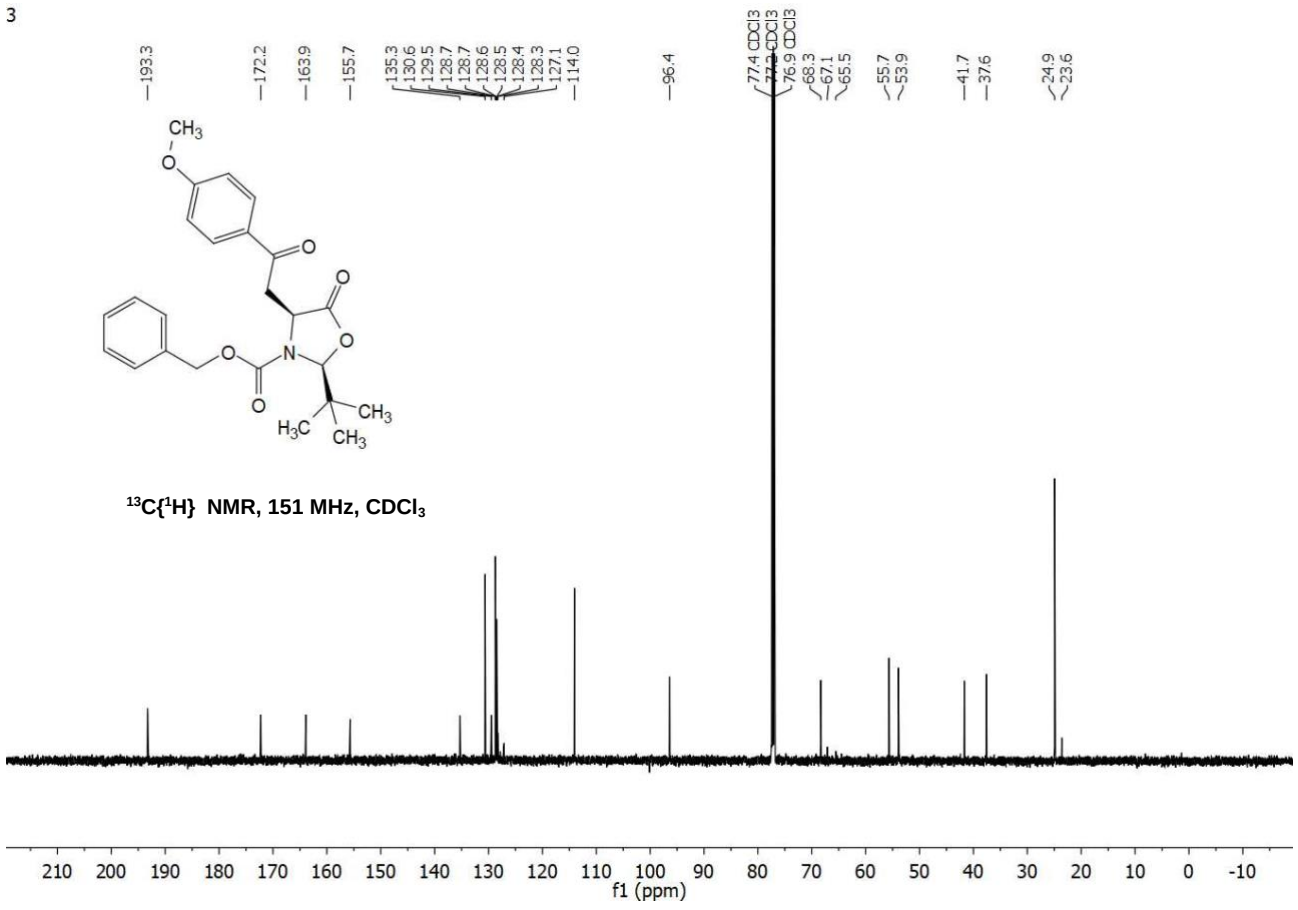


**$^{13}$C{$^{1}$H} NMR, 151 MHz, $CDCl_3$**

**Benzyl (2S,4S)-4-(2-(4-((tert-butoxycarbonyl)amino)phenyl)-2-oxoethyl)-2-(tert-butyl)-5-oxooxazolidine-3-carboxylate (4)**

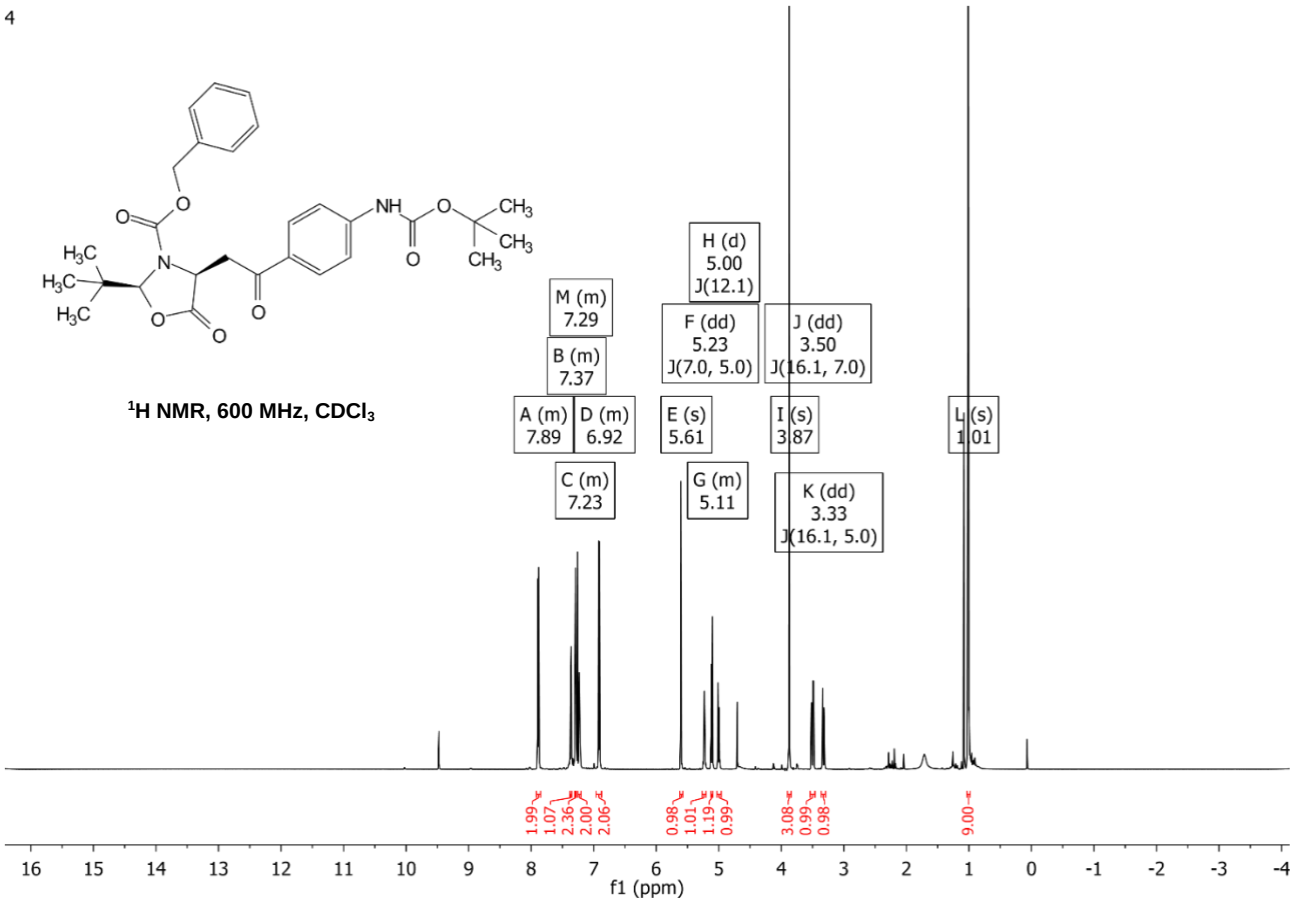


**$^{1}$H NMR, 600 MHz, $CDCl_3$**

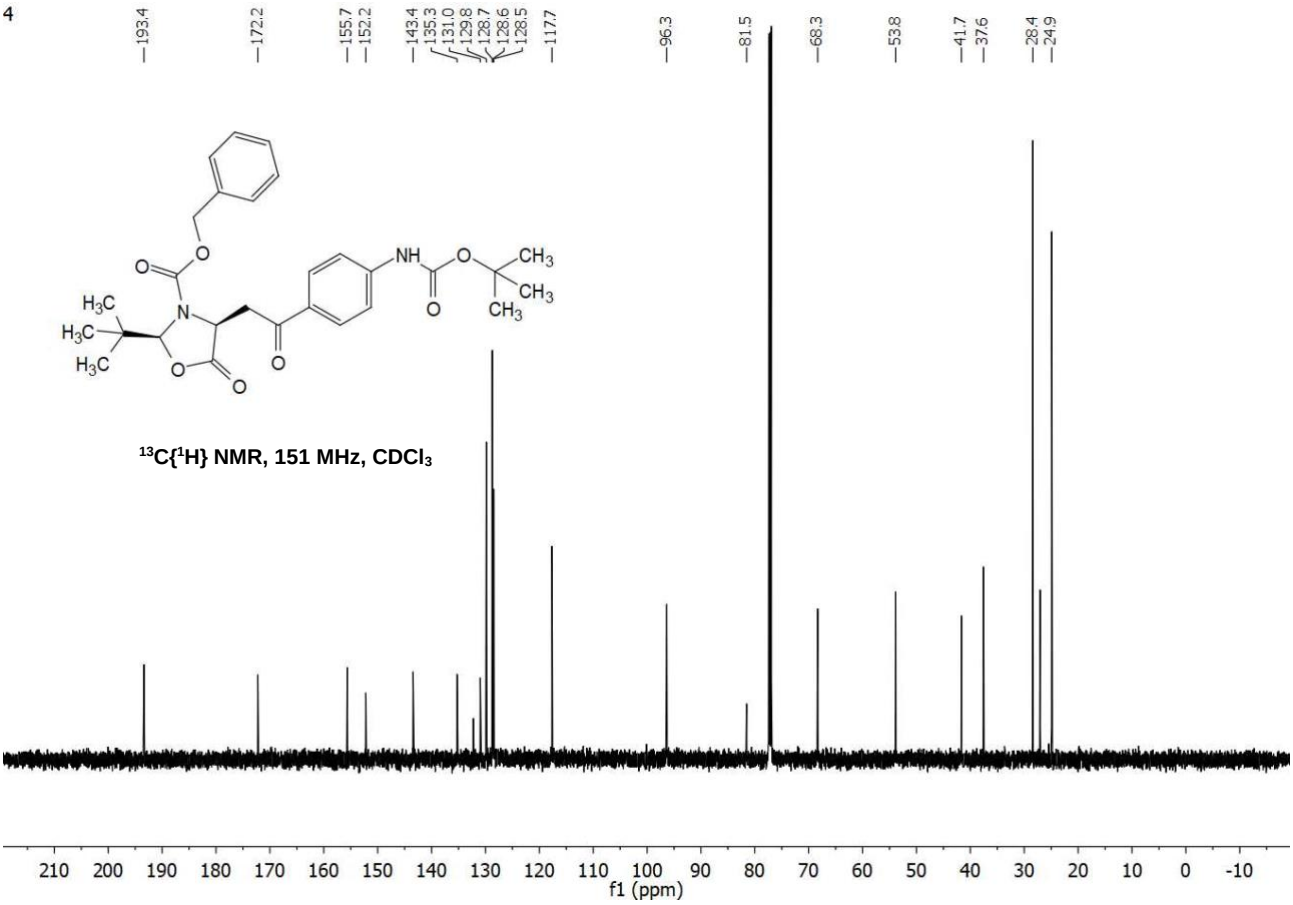


**$^{13}$C{$^{1}$H} NMR, 151 MHz, $CDCl_3$**

**Benzyl (2S,4S)-2-(tert-butyl)-5-oxo-4-(2-oxo-2-(p-tolyl)ethyl)oxazolidine-3-carboxylate (5)**

5

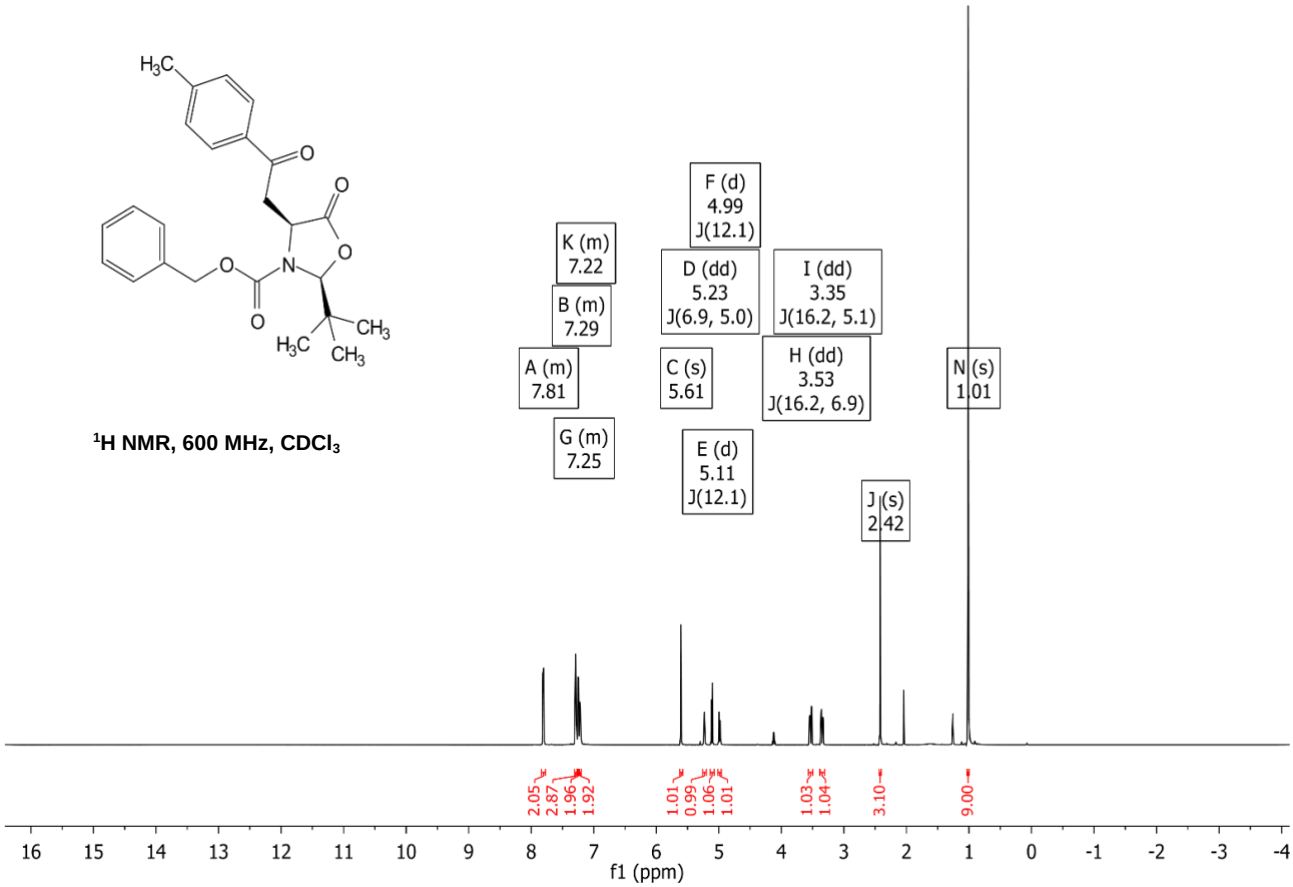


$^{1}$H NMR, 600 MHz, $CDCl_3$

5

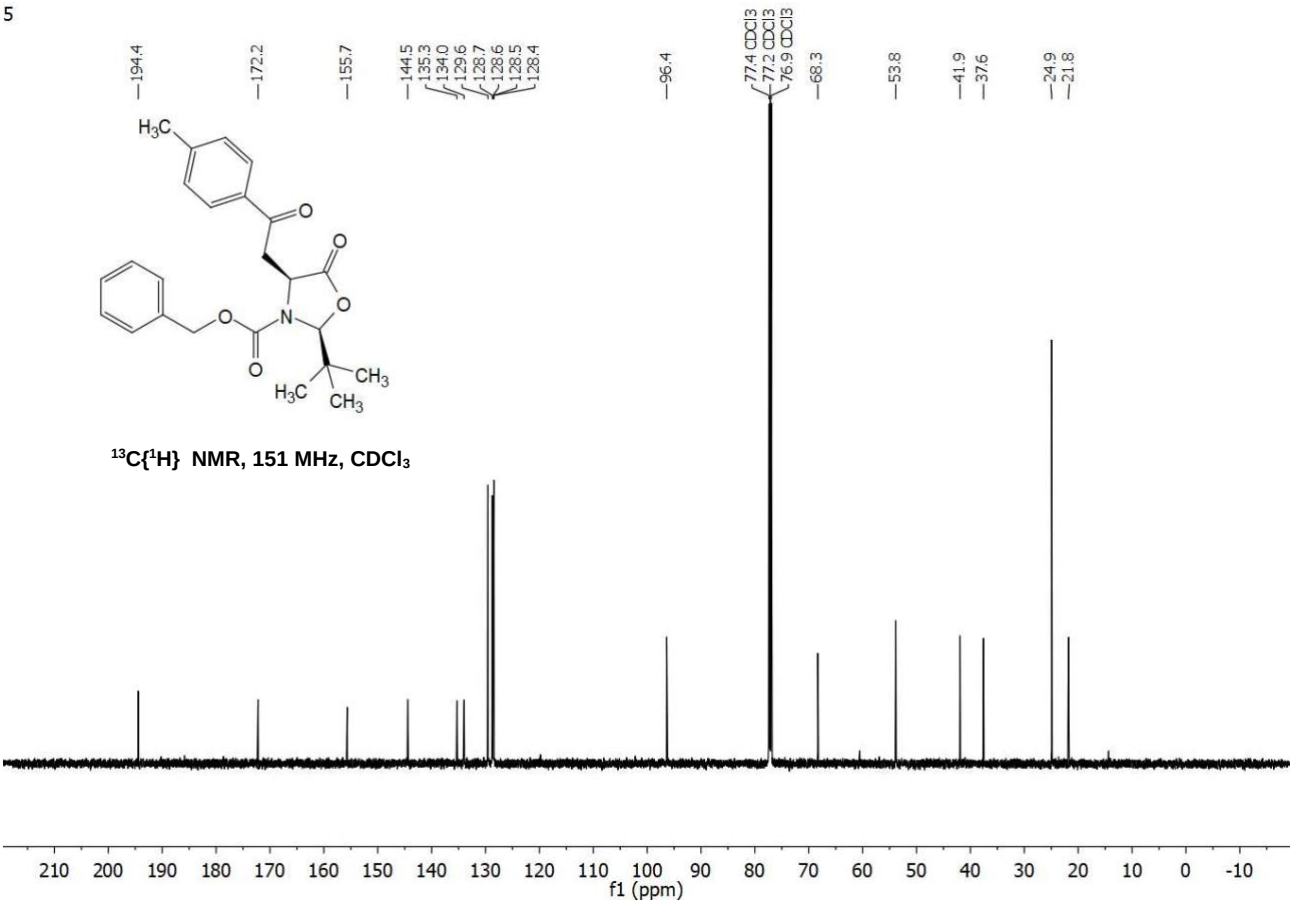


$^{13}C\{^{1}H\}$ NMR, 151 MHz, $CDCl_3$

**Benzyl (2S,4S)-4-(2-(4-bromophenyl)-2-oxoethyl)-2-(tert-butyl)-5-oxooxazolidine-3-carboxylate (6)**

6

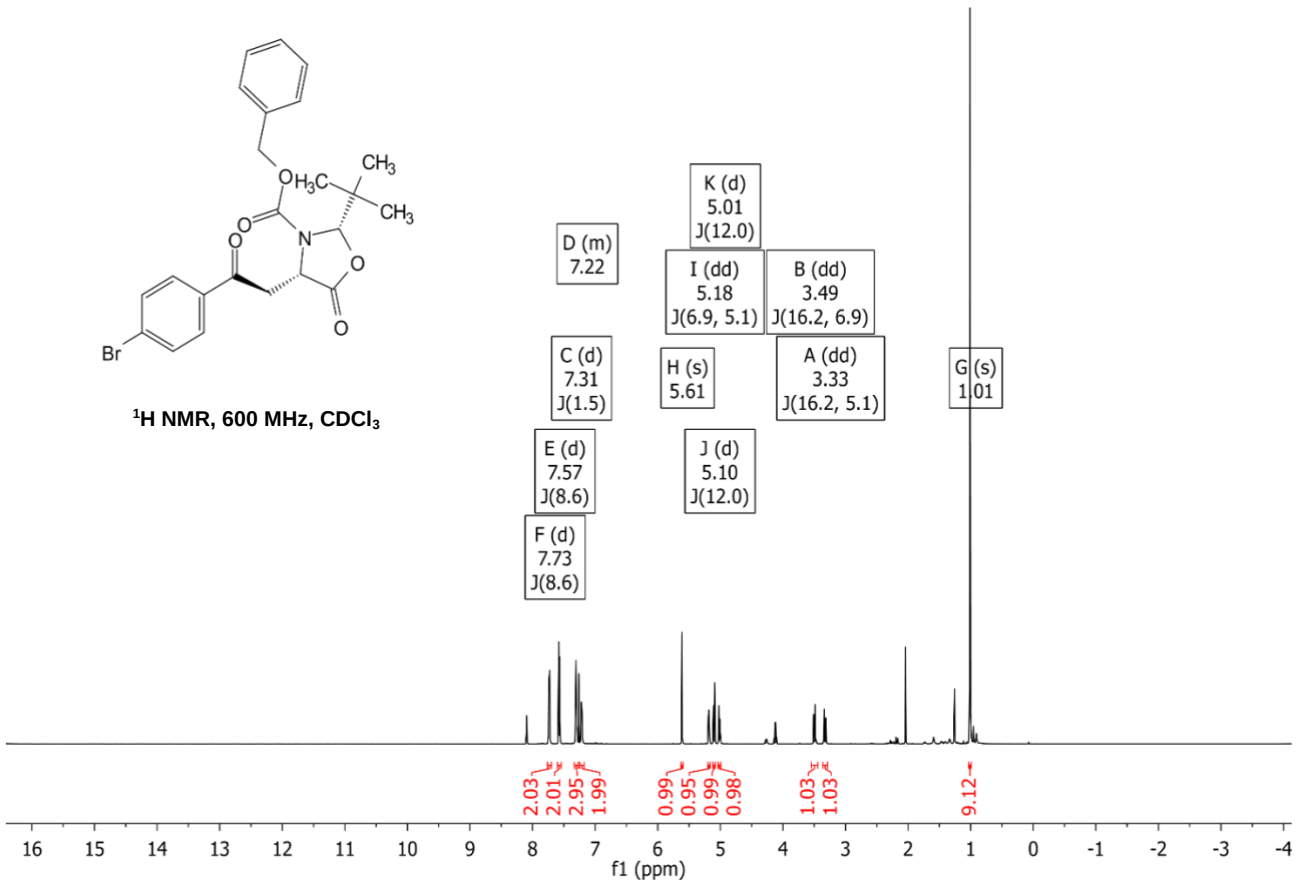


**$^{1}$H NMR, 600 MHz, $CDCl_3$**

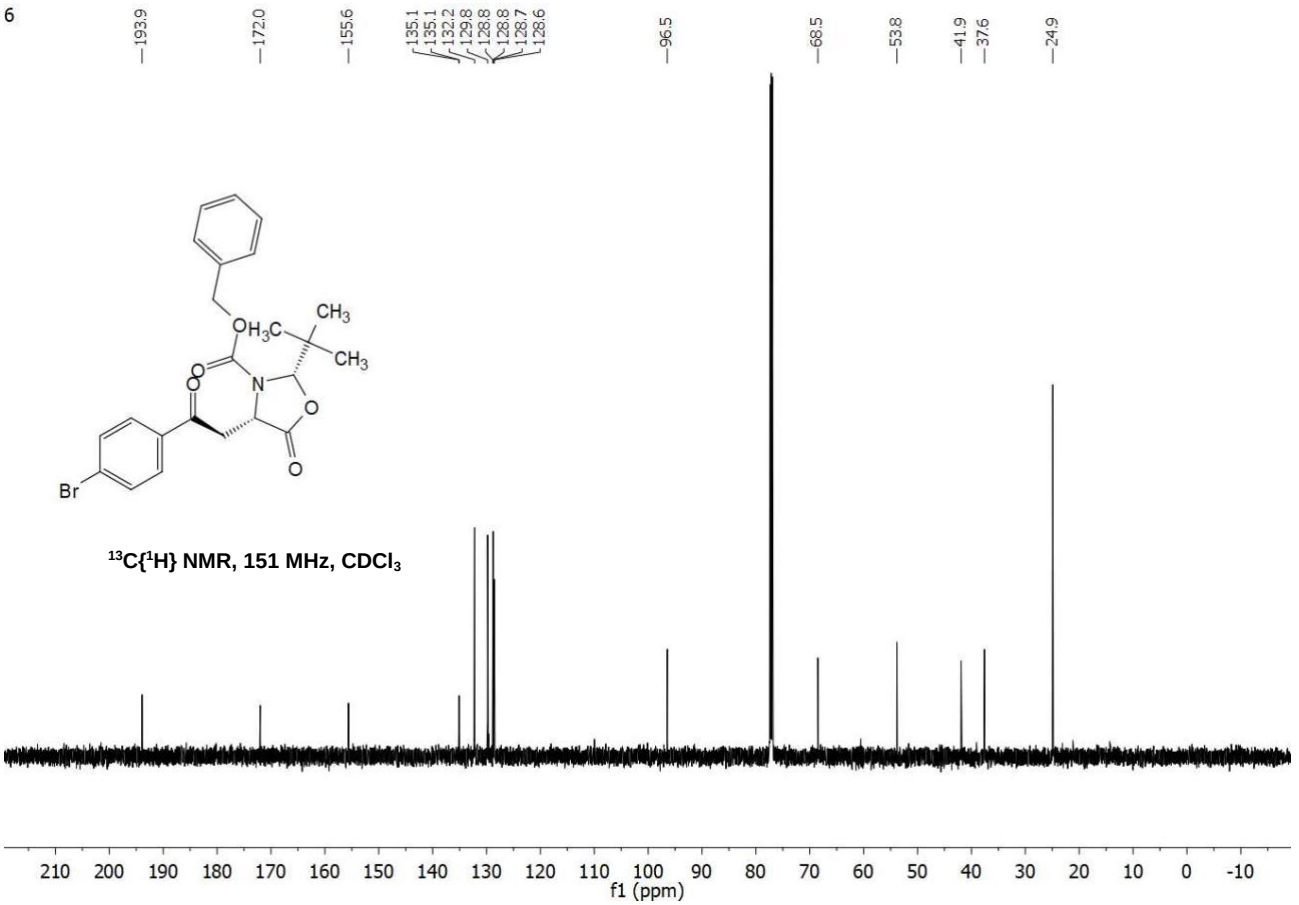


**$^{13}$C{$^{1}$H} NMR, 151 MHz, $CDCl_3$**

**Benzyl (2S,4S)-2-(tert-butyl)-4-(2-(4-fluorophenyl)-2-oxoethyl)-5-oxooxazolidine-3-carboxylate (7)**

7



**$^{1}$H NMR, 400 MHz, $CDCl_3$**

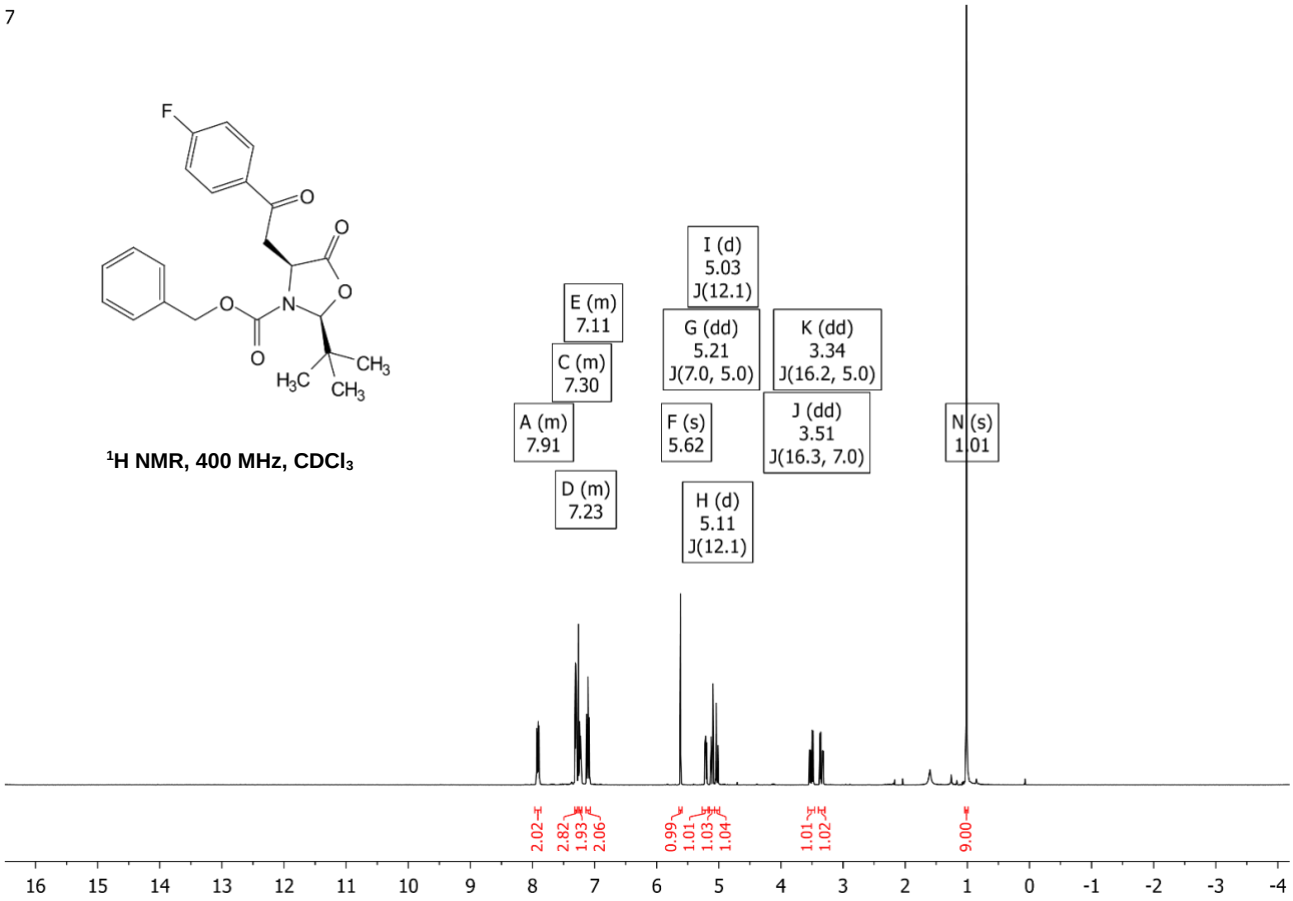


7



**$^{13}$C{$^{1}$H} NMR, 101 MHz, $CDCl_3$**

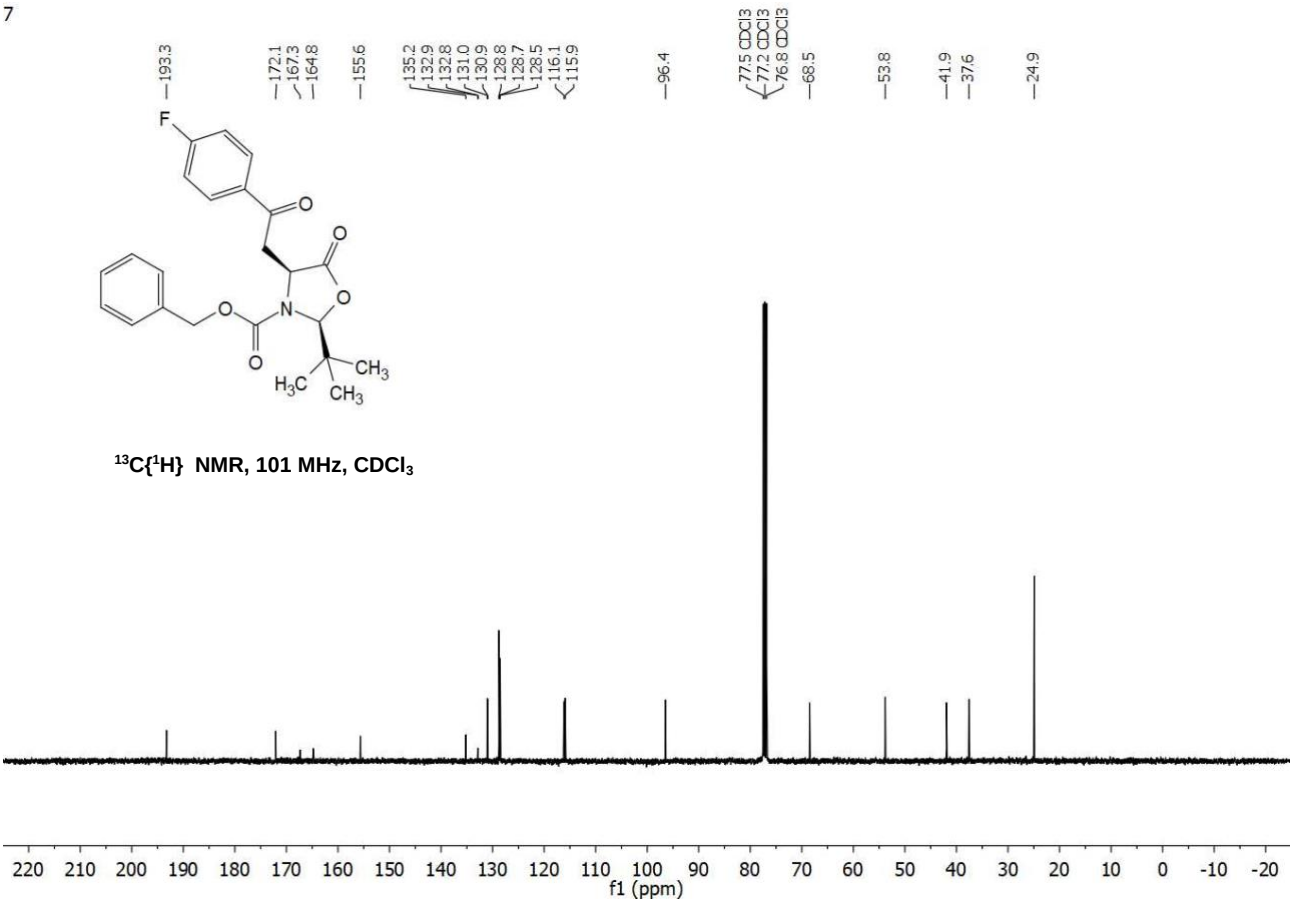

7




**$^{19}F\{^{1}H\}$ NMR, 376 MHz, $CDCl_3$**

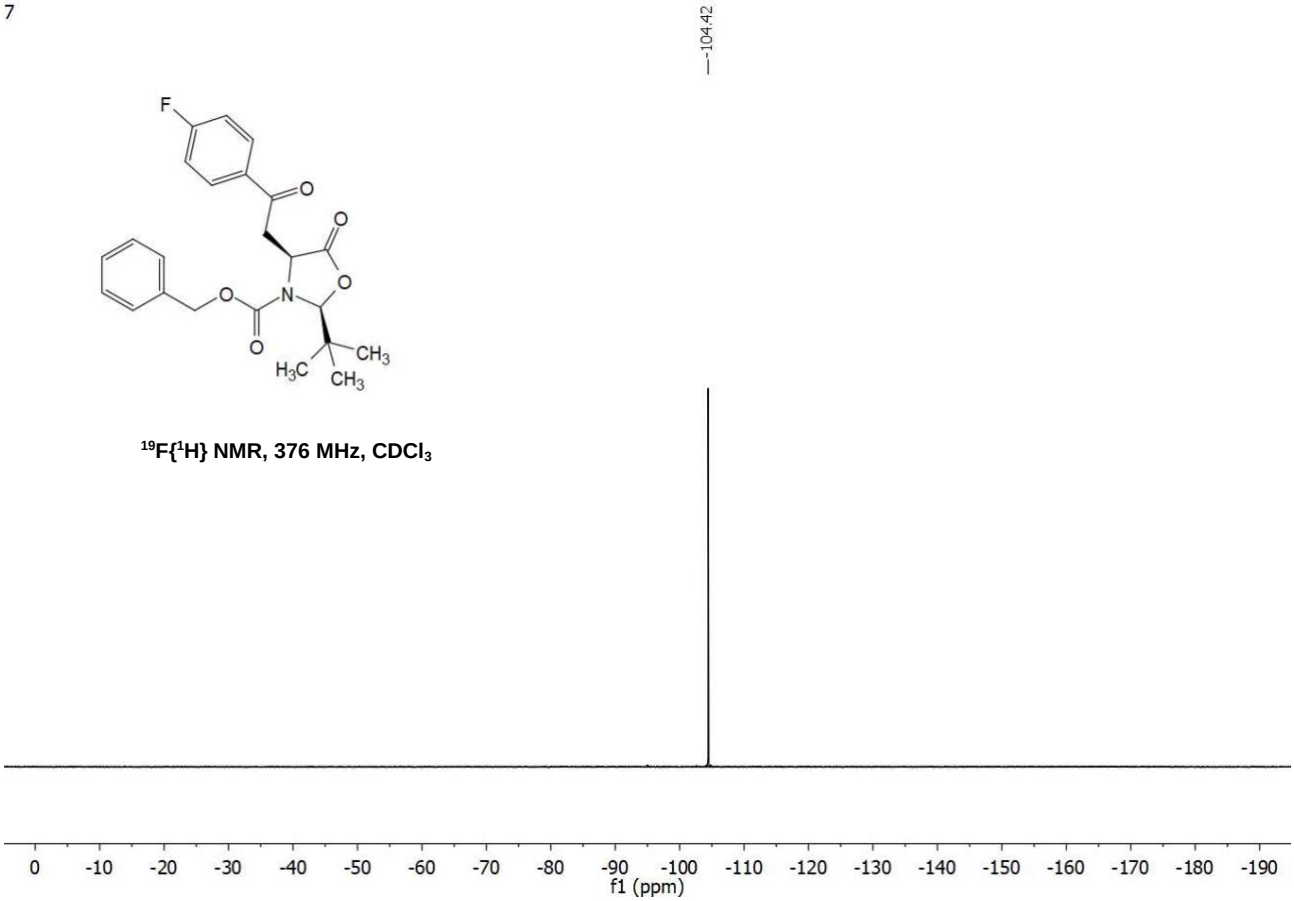

**Benzyl (2S,4S)-2-(tert-butyl)-4-(2-(4-cyanophenyl)-2-oxoethyl)-5-oxooxazolidine-3-carboxylate (8)**

8

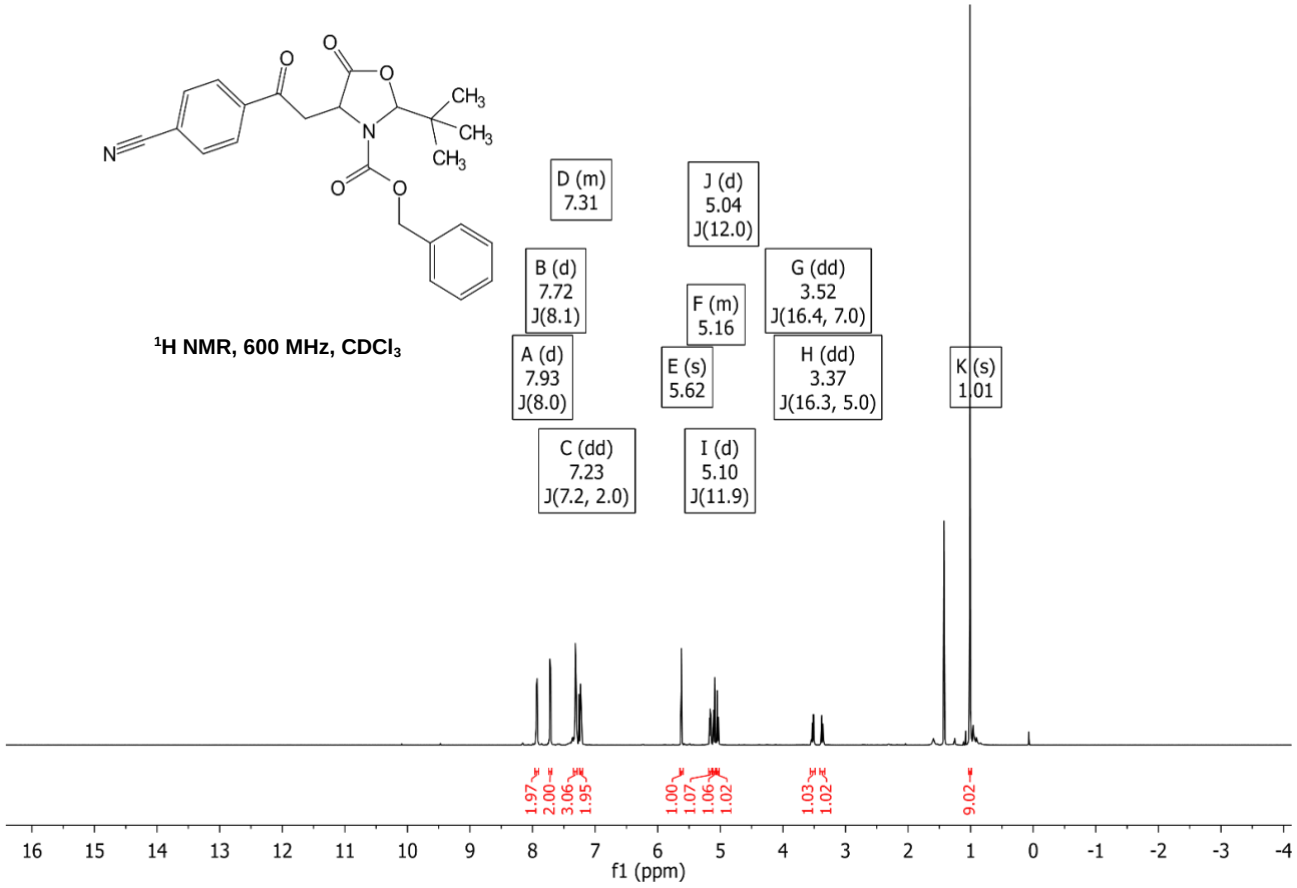


**$^{1}$H NMR, 600 MHz, CDCl$_3$**

8

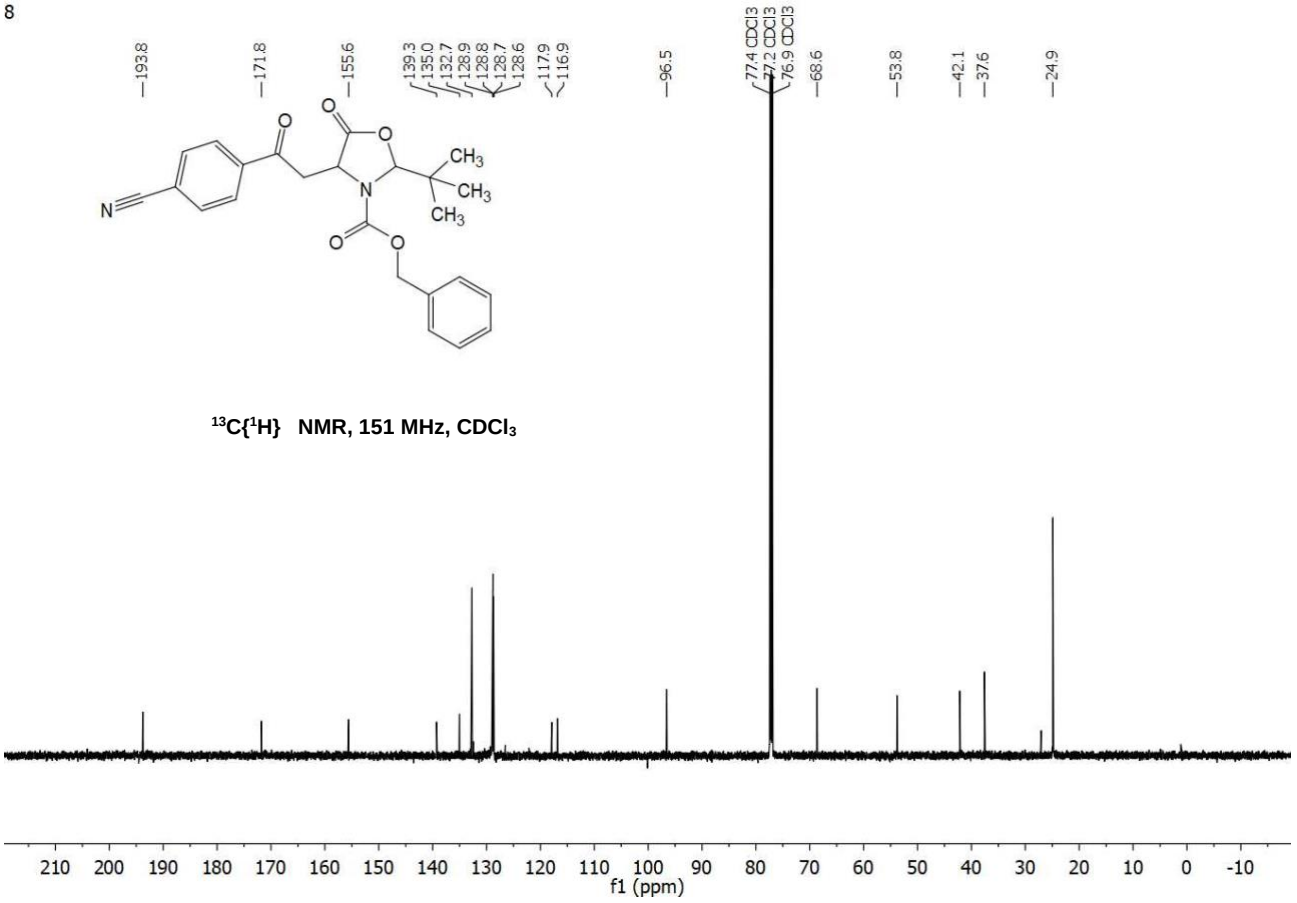


**$^{13}$C{$^{1}$H} NMR, 151 MHz, CDCl$_3$**

**Benzyl (2S,4S)-2-(tert-butyl)-5-oxo-4-(2-oxo-2-(4-(trifluoromethyl)phenyl)ethyl)oxazolidine-3-carboxylate (9)**

9

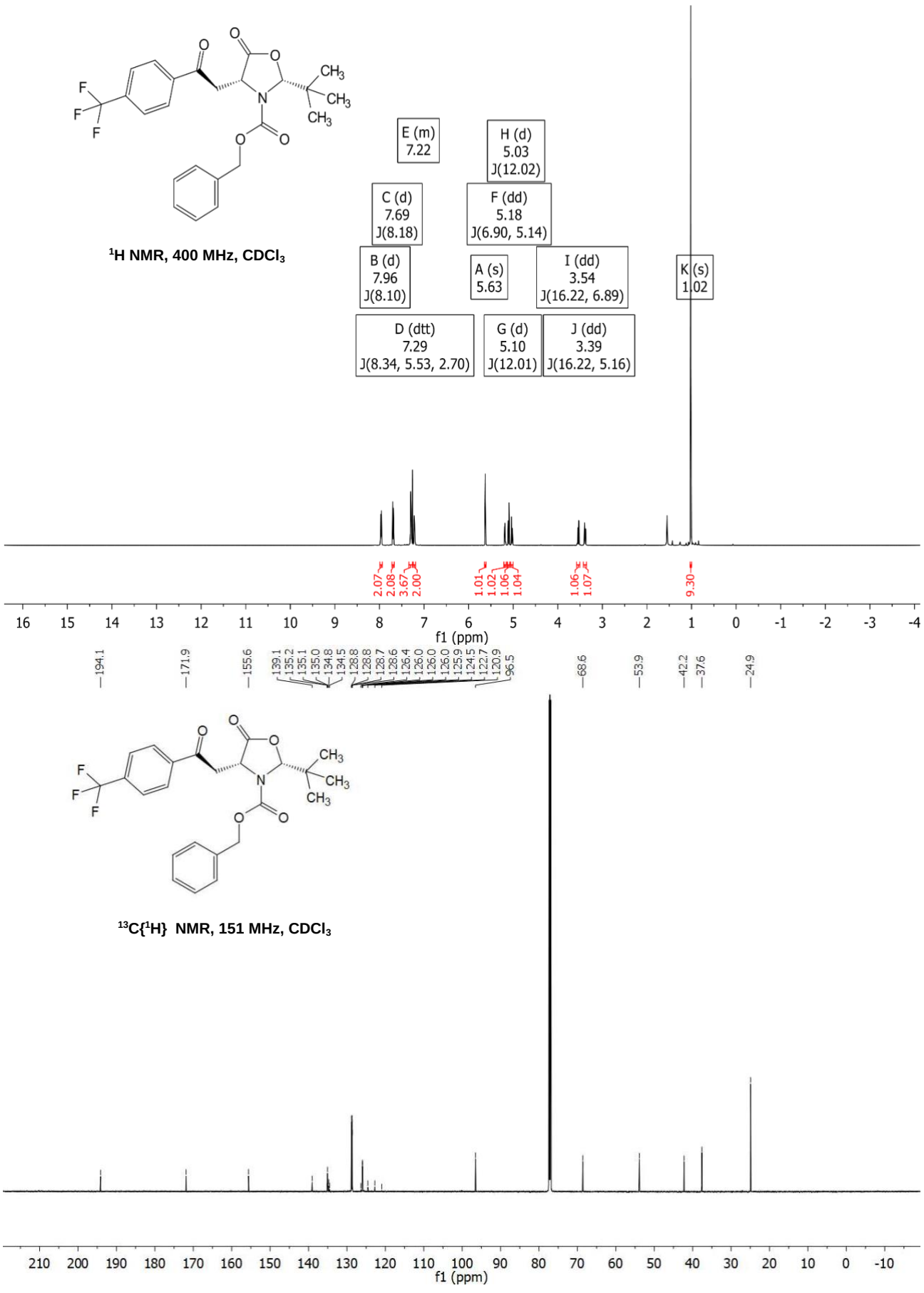


**$^{1}$H NMR, 400 MHz, $CDCl_3$**




**$^{13}C\{^{1}H\}$ NMR, 151 MHz, $CDCl_3$**

9

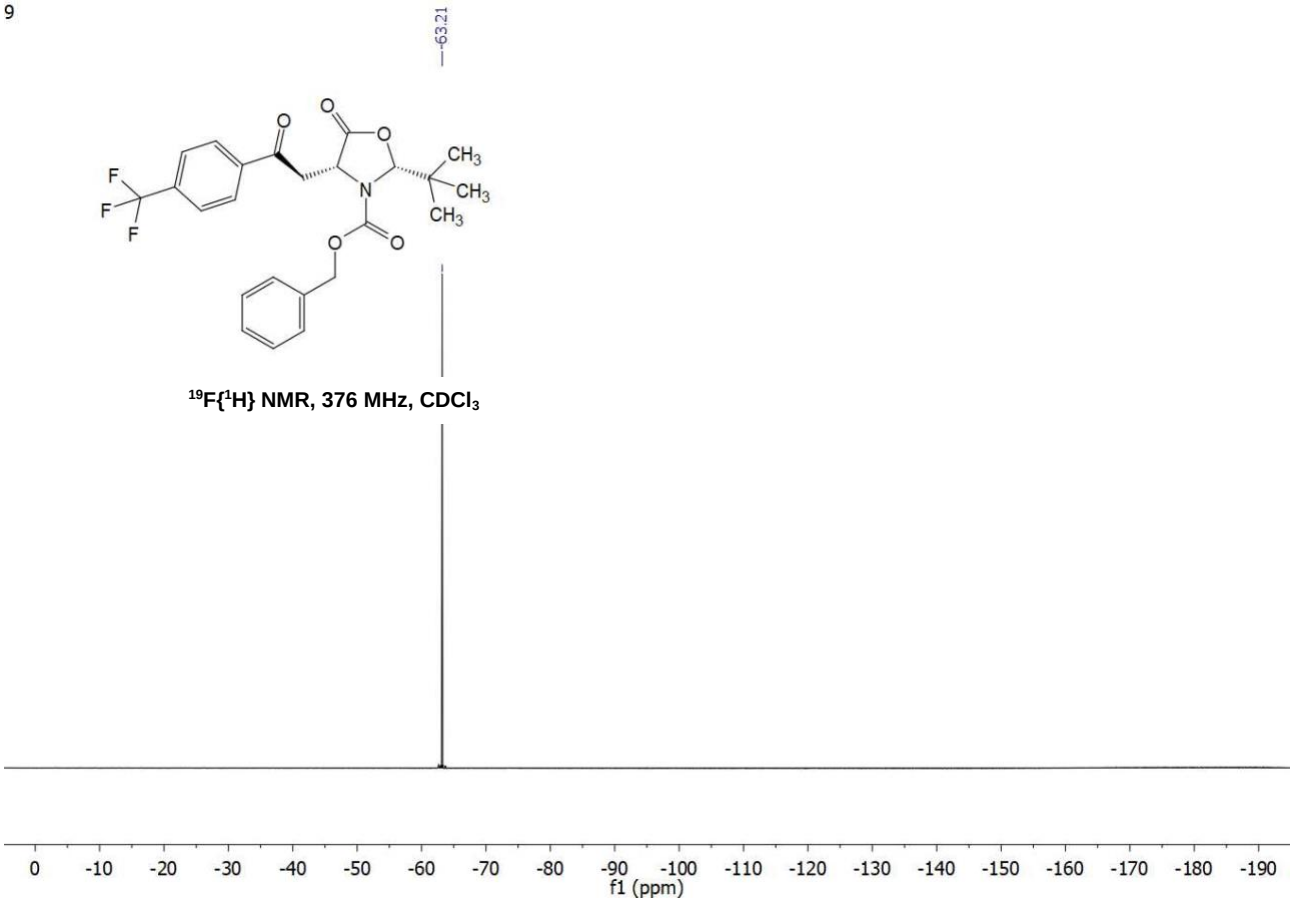


**$^{19}F\{^{1}H\}$ NMR, 376 MHz, $CDCl_3$**

**Benzyl (2S,4S)-2-(tert-butyl)-4-(2-(4-formylphenyl)-2-oxoethyl)-5-oxooxazolidine-3-carboxylate (10)**

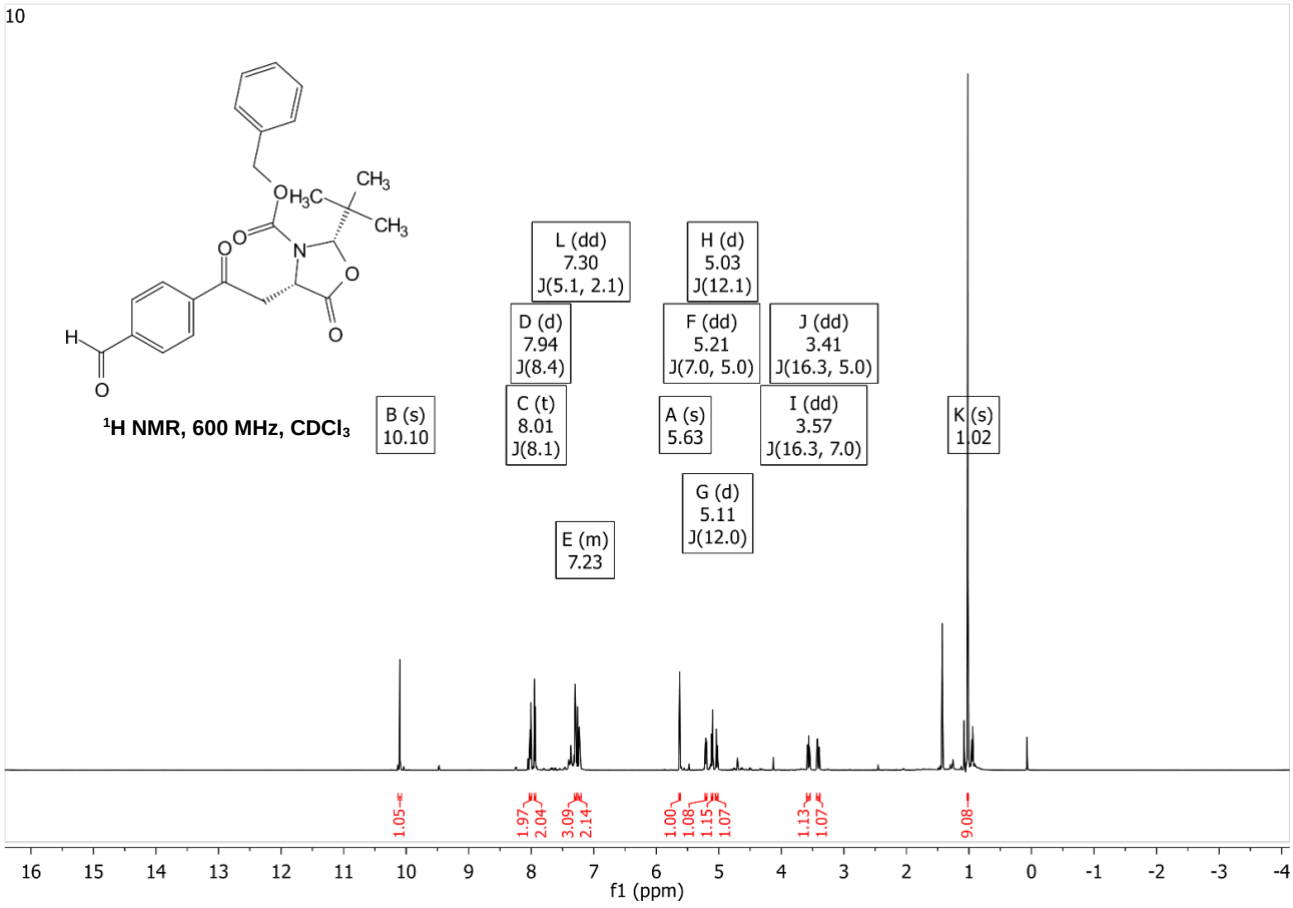


$^{1}$H NMR, 600 MHz, $CDCl_3$

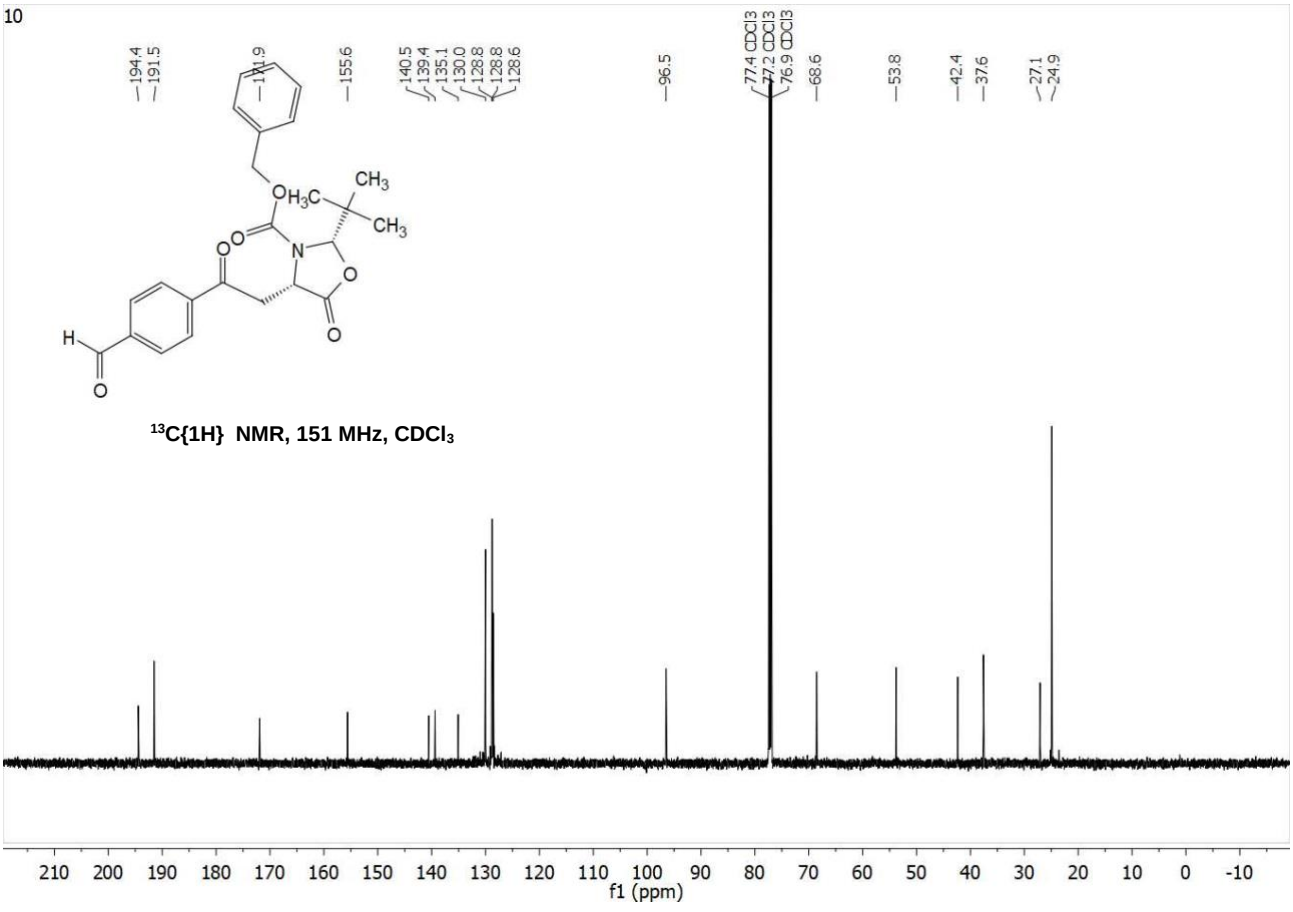


$^{13}$C{1H} NMR, 151 MHz, $CDCl_3$

**(2S,4S)-benzyl 4-(2-(benzo[d][1,3]dioxol-5-yl)-2-oxoethyl)-2-(tert-butyl)-5-oxooxazolidine-3-carboxylate (11)**

11

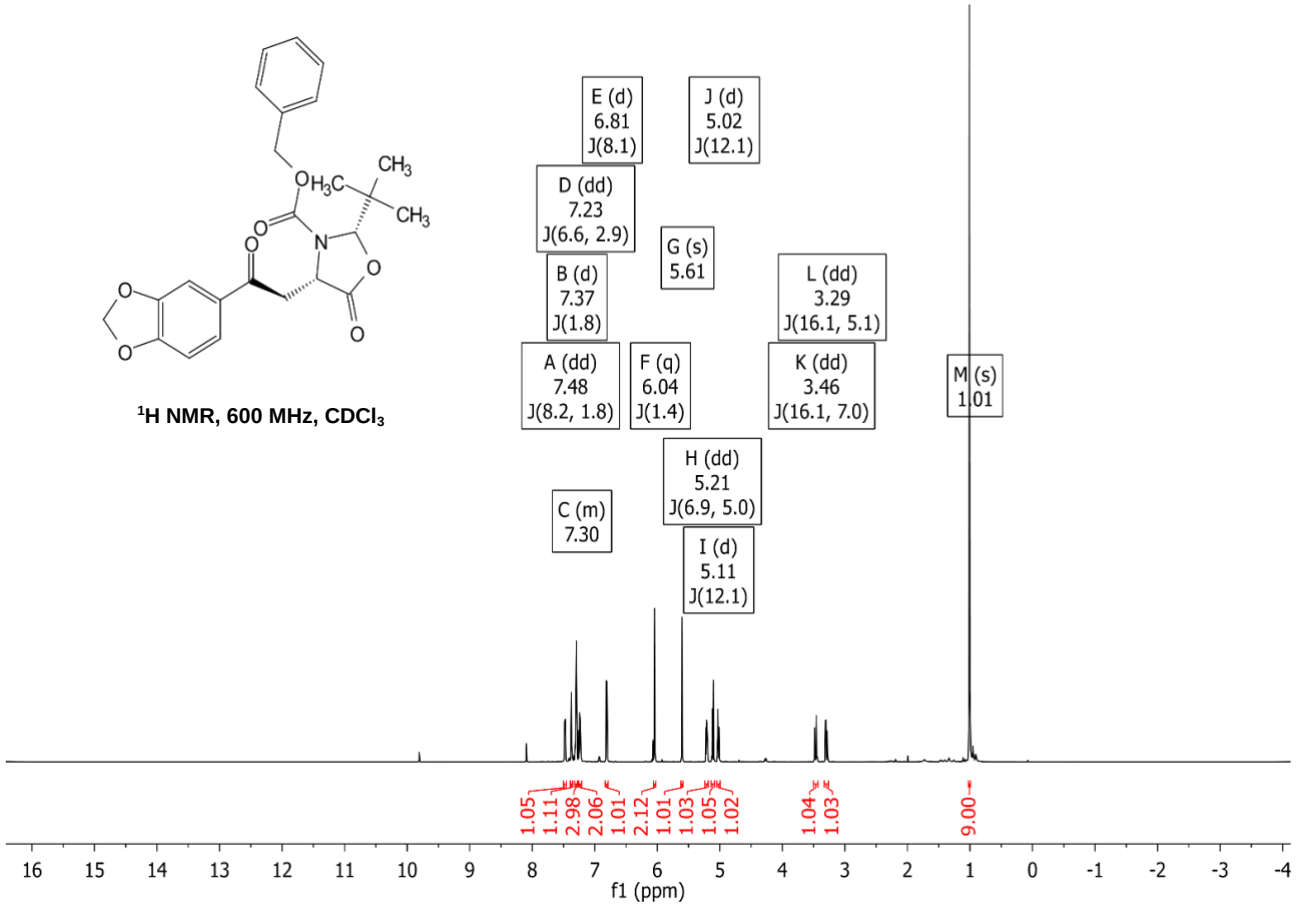


**$^{1}$H NMR, 600 MHz, $CDCl_3$**

11

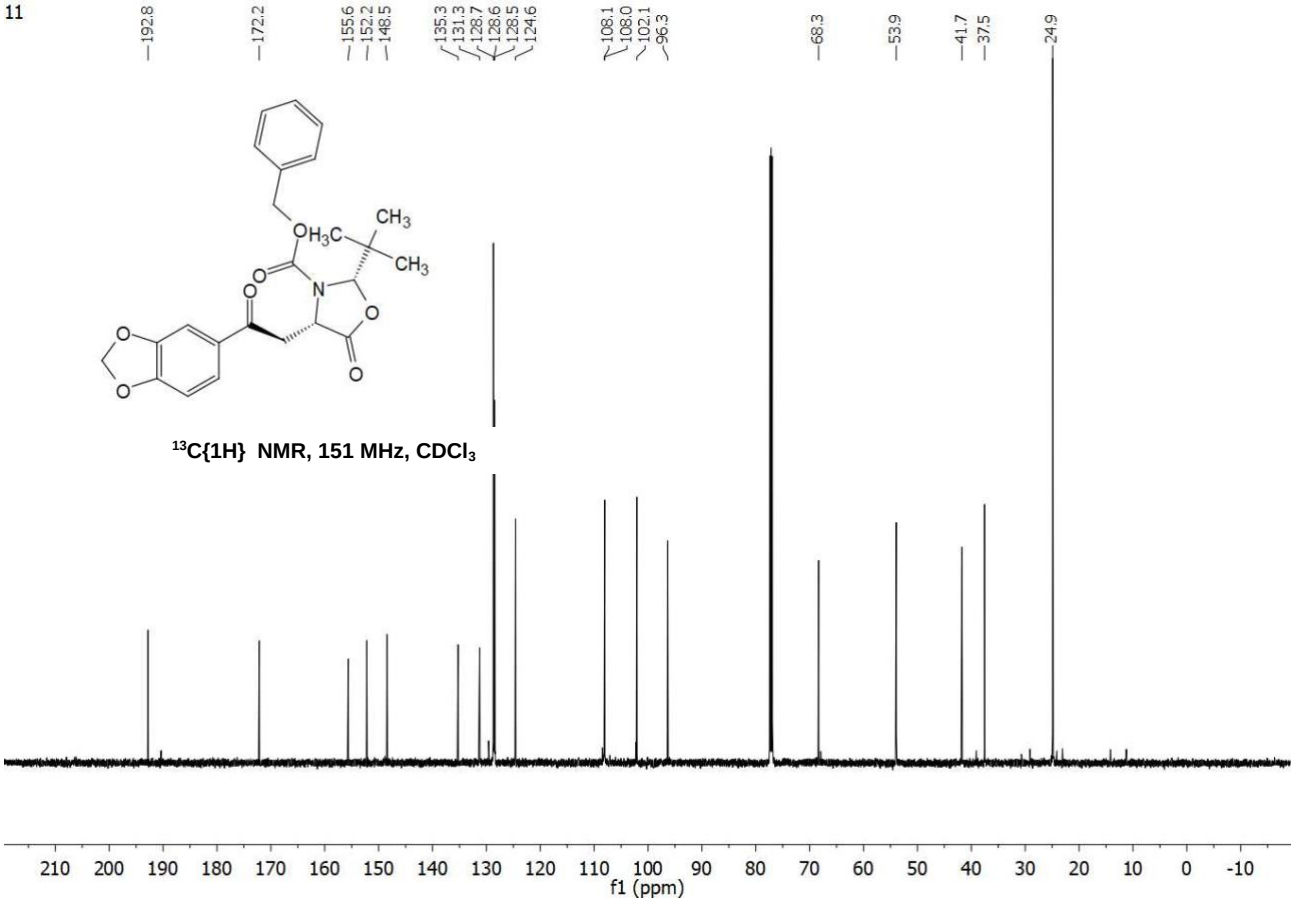


**$^{13}$C{1H} NMR, 151 MHz, $CDCl_3$**

**Benzyl (2S,4S)-2-(tert-butyl)-4-(2-(2-chlorophenyl)-2-oxoethyl)-5-oxooxazolidine-3-carboxylate (12)**

12

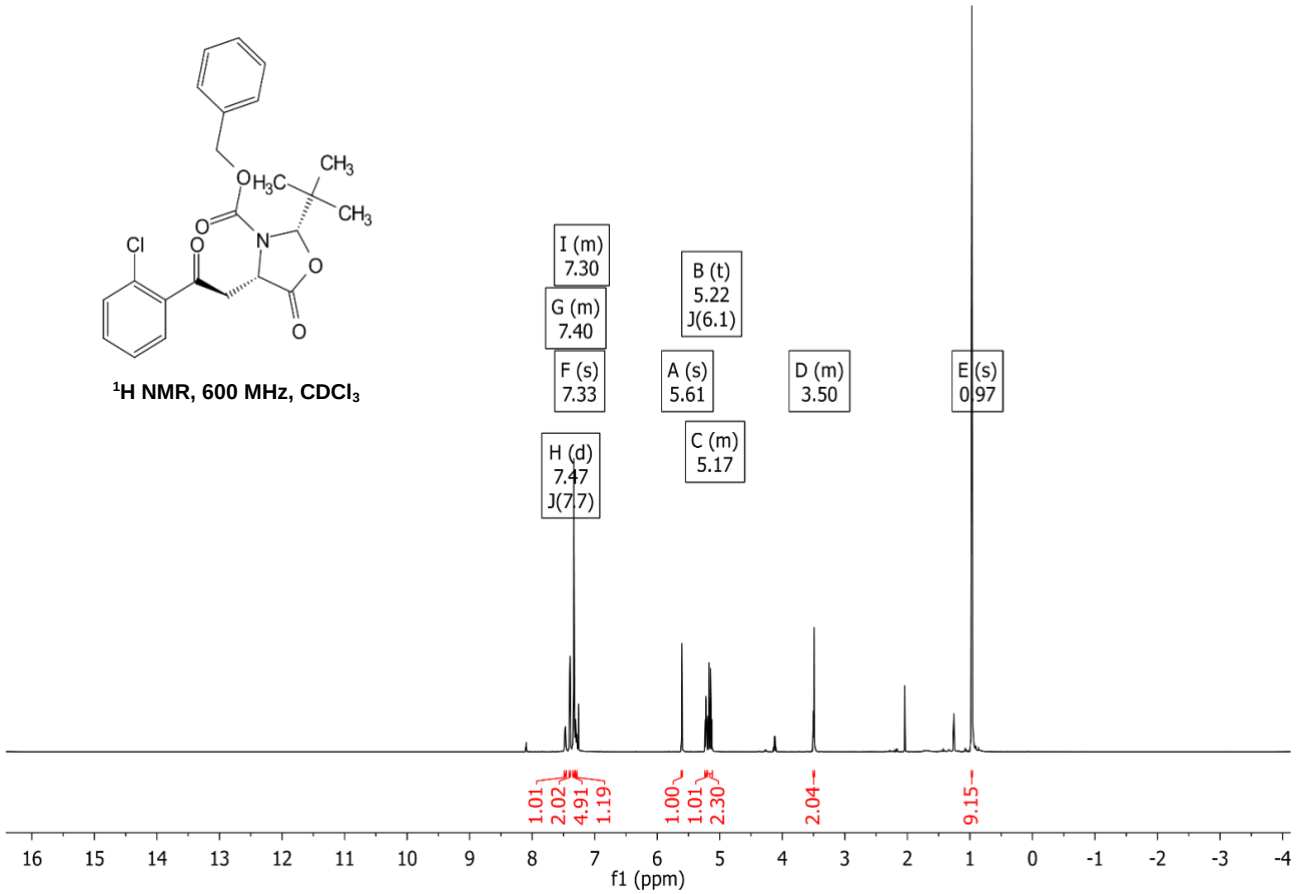


**$^{1}$H NMR, 600 MHz, $CDCl_3$**

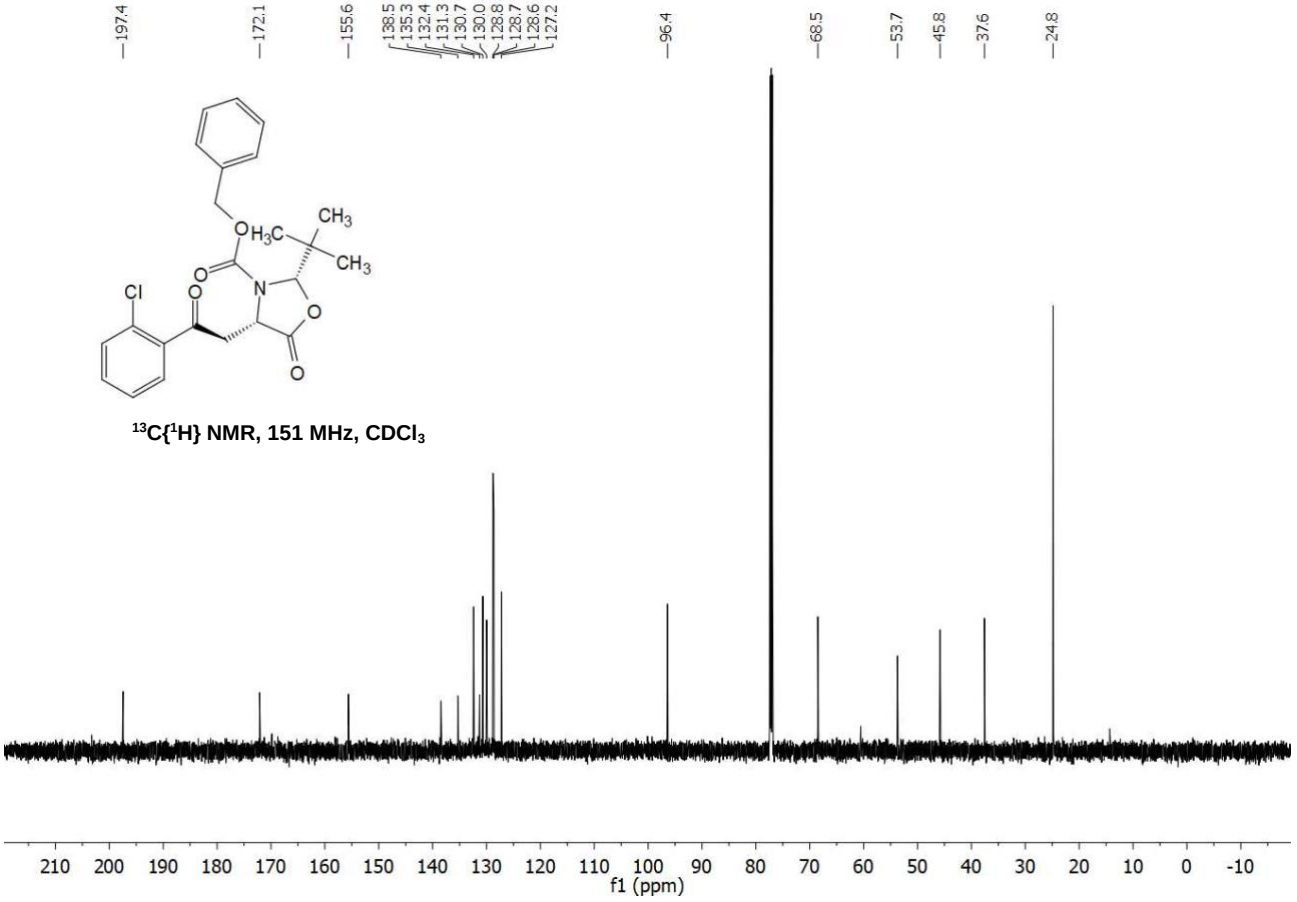


**$^{13}$C{$^{1}$H} NMR, 151 MHz, $CDCl_3$**

**Benzyl (2S,4S)-4-(2-(2-acetoxyphenyl)-2-oxoethyl)-2-(tert-butyl)-5-oxooxazolidine-3-carboxylate (13)**

13

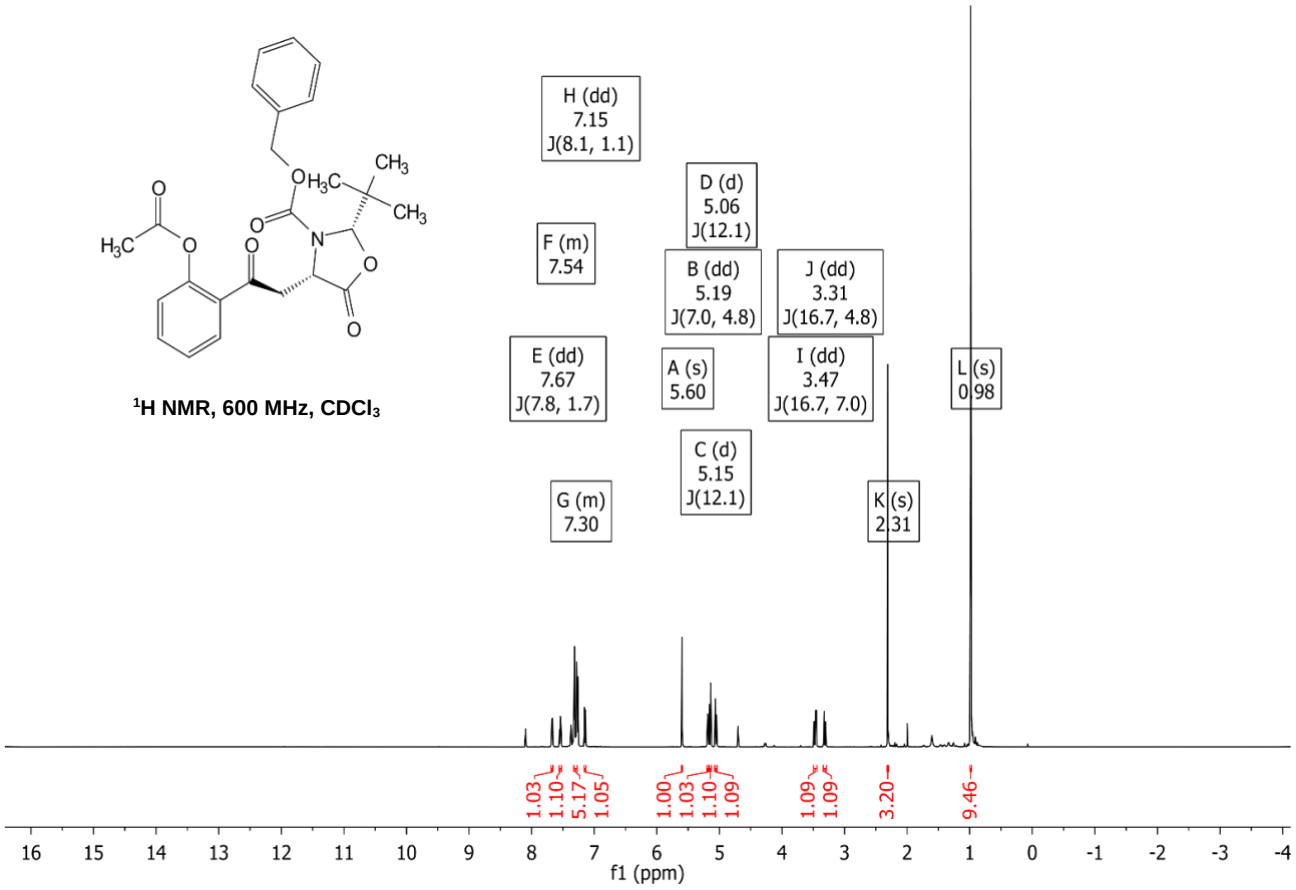


**$^{1}$H NMR, 600 MHz, $CDCl_3$**

13

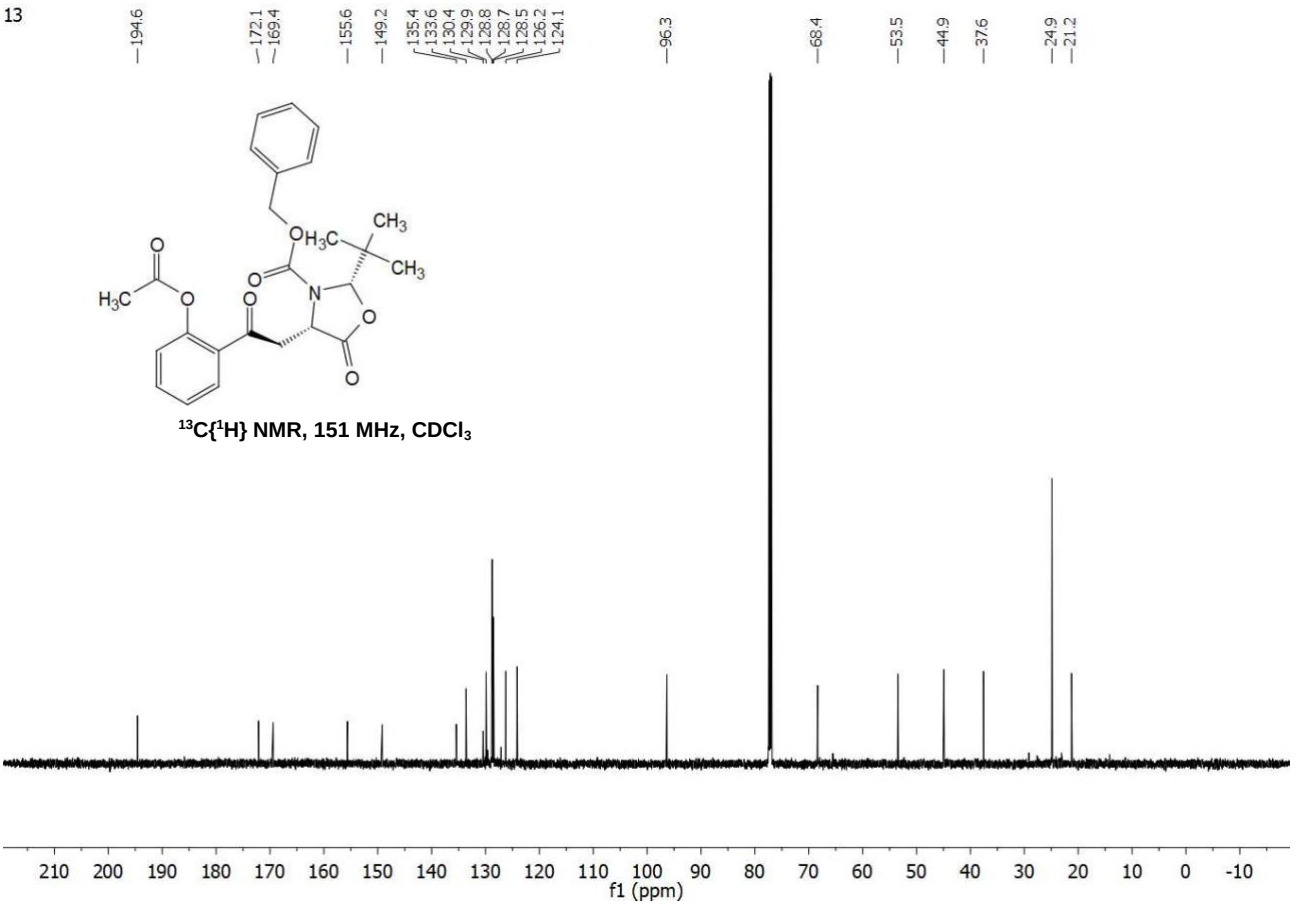


**$^{13}$C{$^{1}$H} NMR, 151 MHz, $CDCl_3$**

**Benzyl (2S,4S)-2-(tert-butyl)-4-(2-(3-(5-(2-fluorophenyl)-1,2,4-oxadiazol-3-yl)phenyl)-2-oxoethyl)-5-oxooxazolidine-3-carboxylate (14)**

**14**

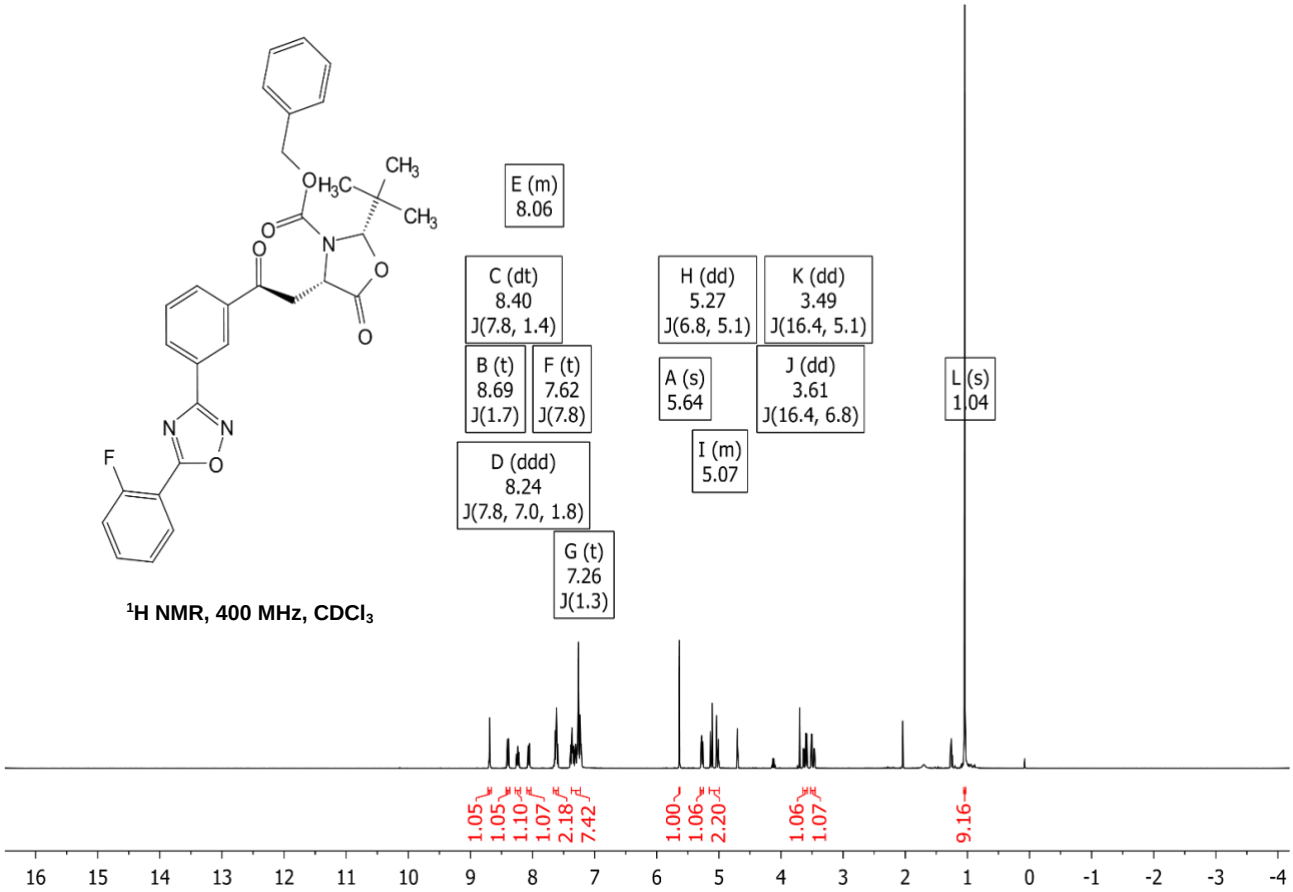


**$^{1}$H NMR, 400 MHz, $CDCl_3$**

**14**

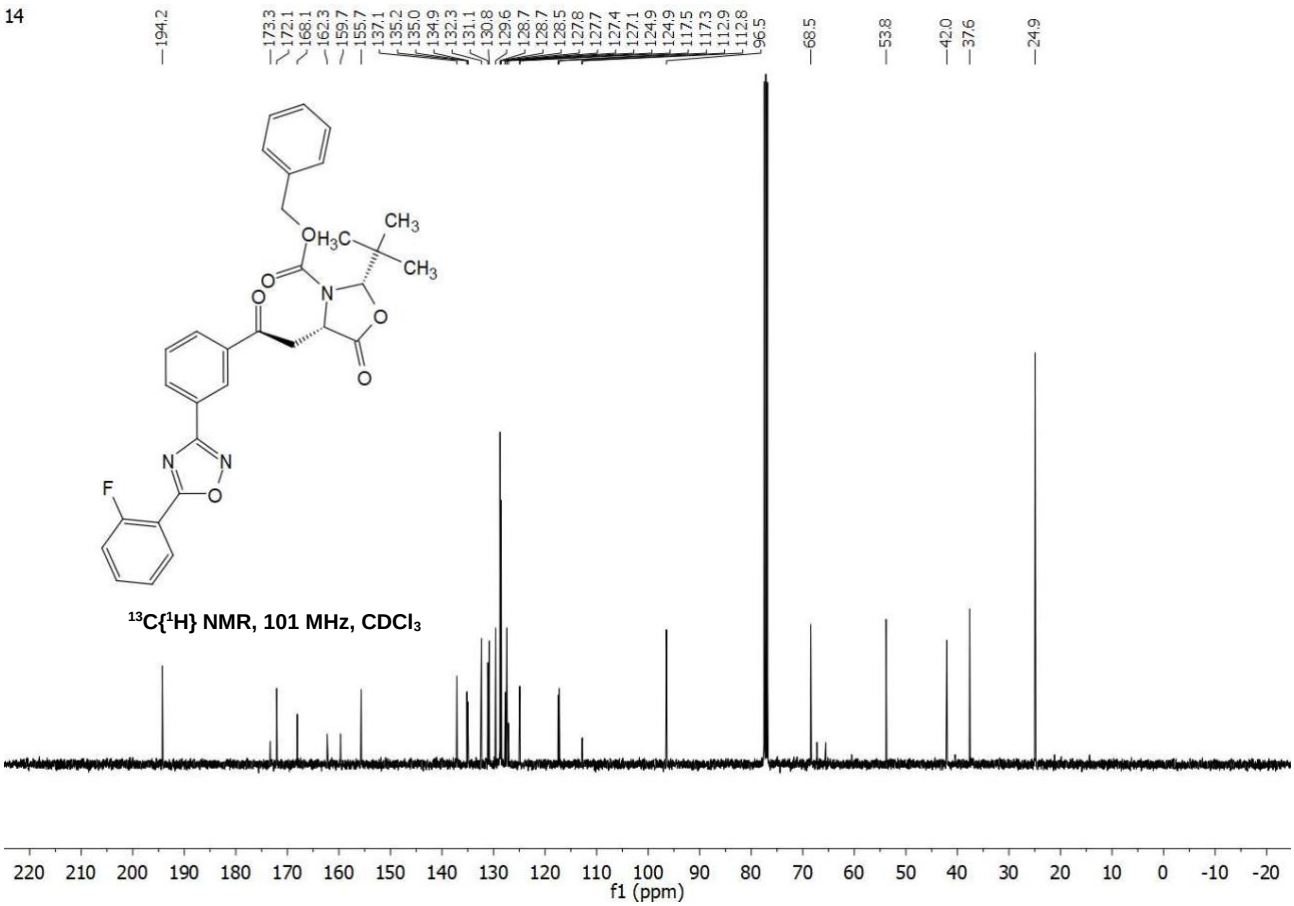


**$^{13}$C{$^{1}$H} NMR, 101 MHz, $CDCl_3$**

14



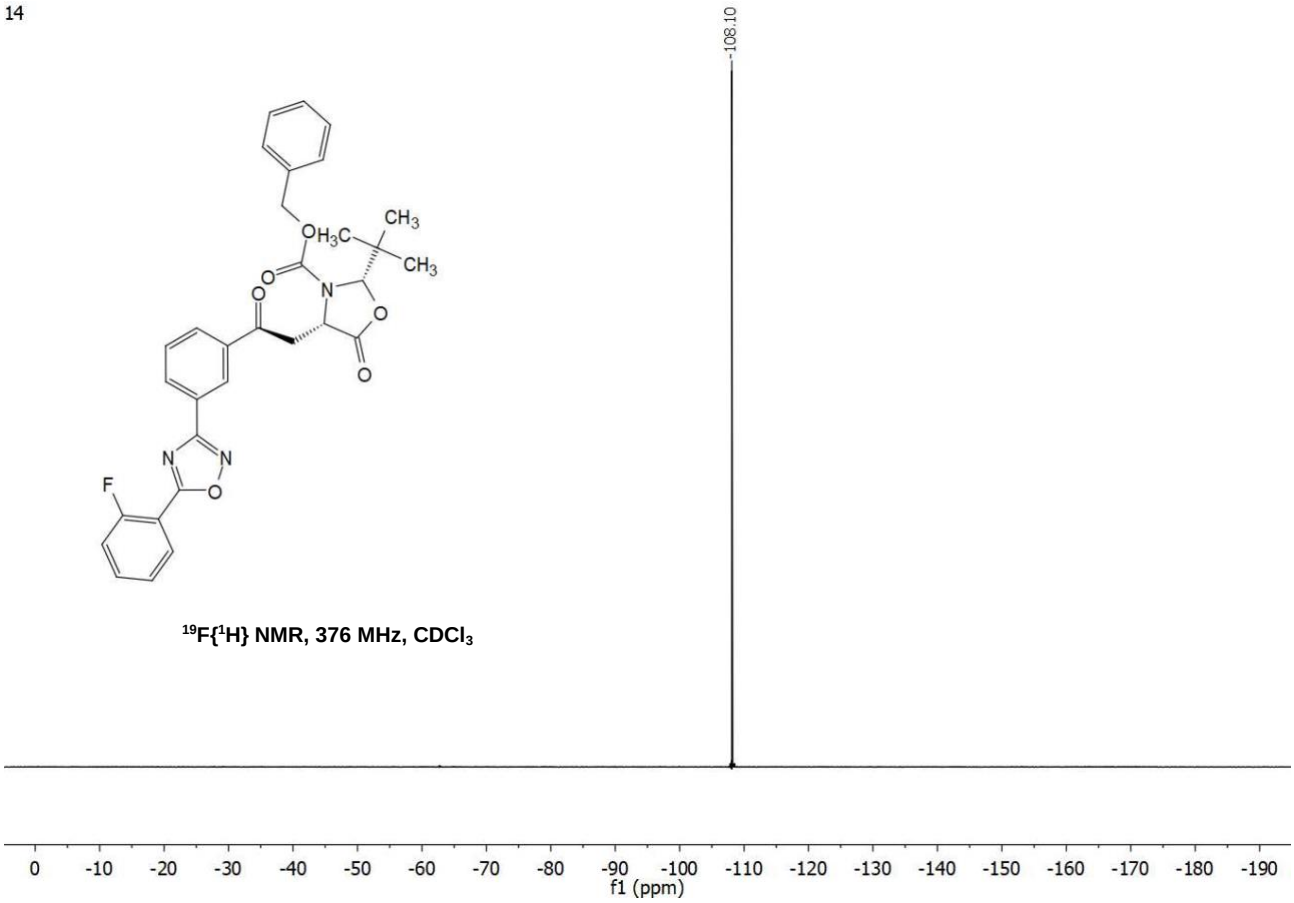


**$^{19}F\{^{1}H\}$ NMR, 376 MHz, $CDCl_3$**

**Benzyl (2S,4S)-2-(tert-butyl)-5-oxo-4-(2-oxo-2-(3-(4,4,5,5-tetramethyl-1,3,2-dioxaborolan-2-yl)phenyl)ethyl)oxazolidine-3-carboxylate (15)**

15

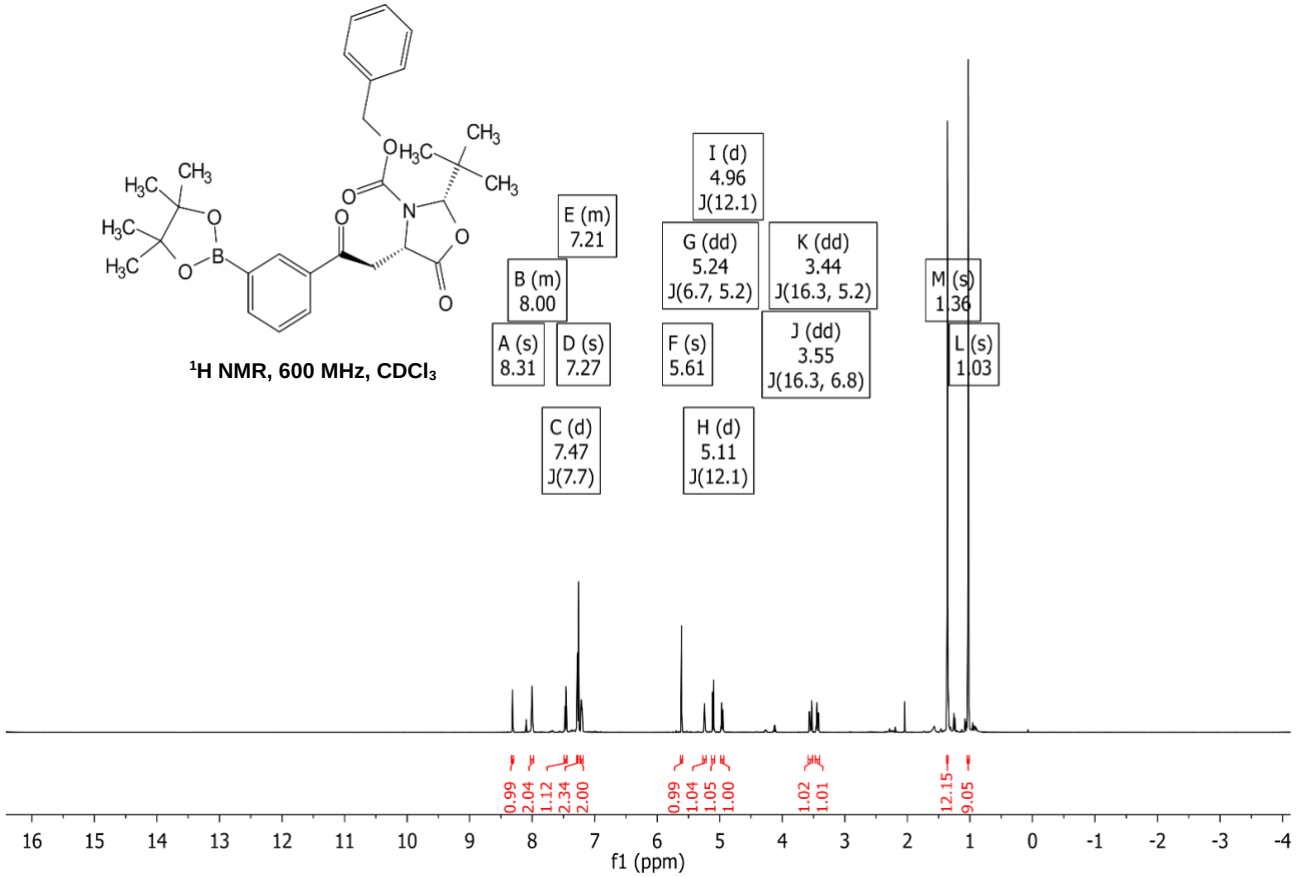


**$^{1}$H NMR, 600 MHz, $CDCl_3$**

15

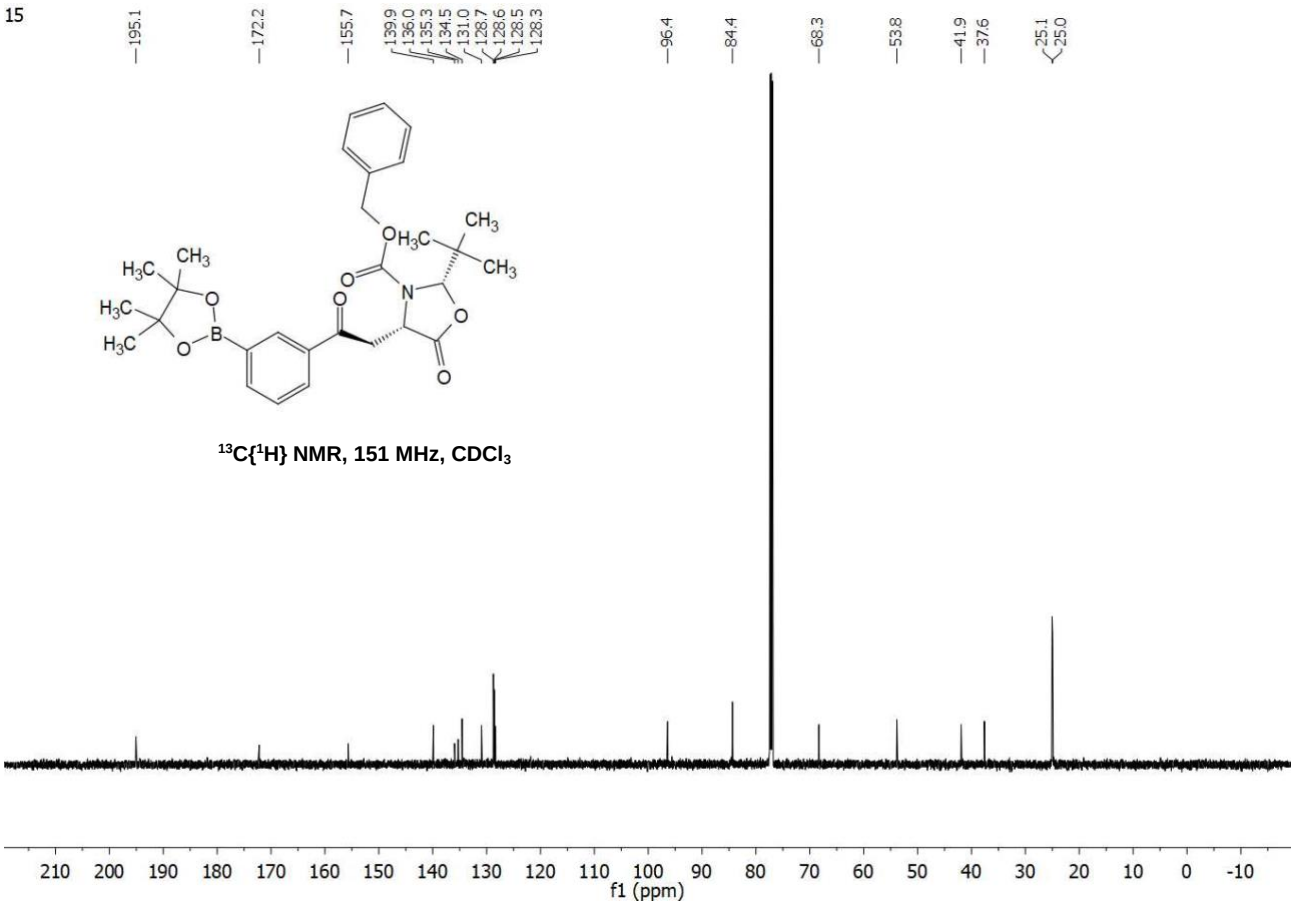


**$^{13}$C{$^{1}$H} NMR, 151 MHz, $CDCl_3$**

**Benzyl (2S,4S)-2-(tert-butyl)-5-oxo-4-(2-oxo-2-(pyridin-3-yl)ethyl)oxazolidine-3-carboxylate (16)**

16

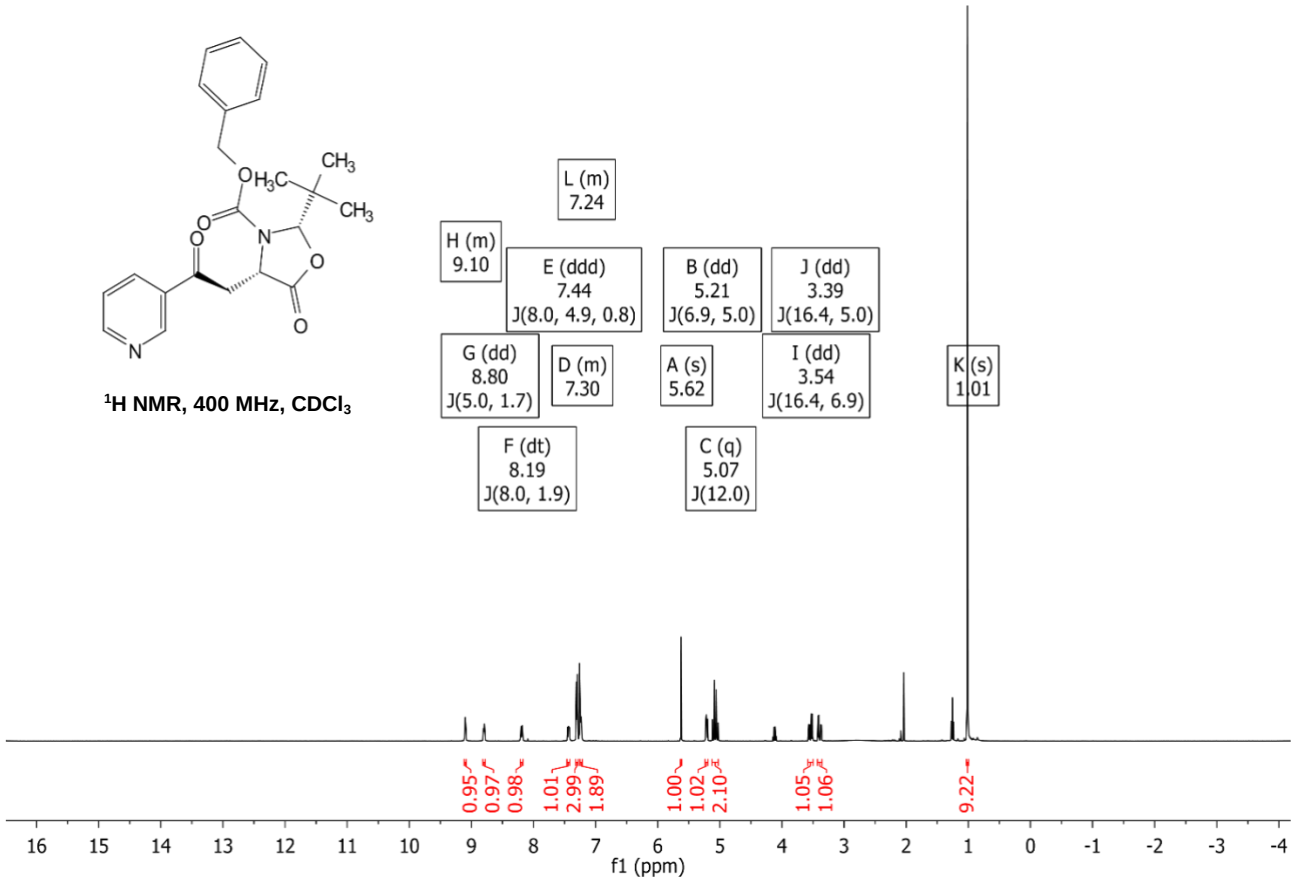


**$^{1}$H NMR, 400 MHz, $CDCl_3$**

16

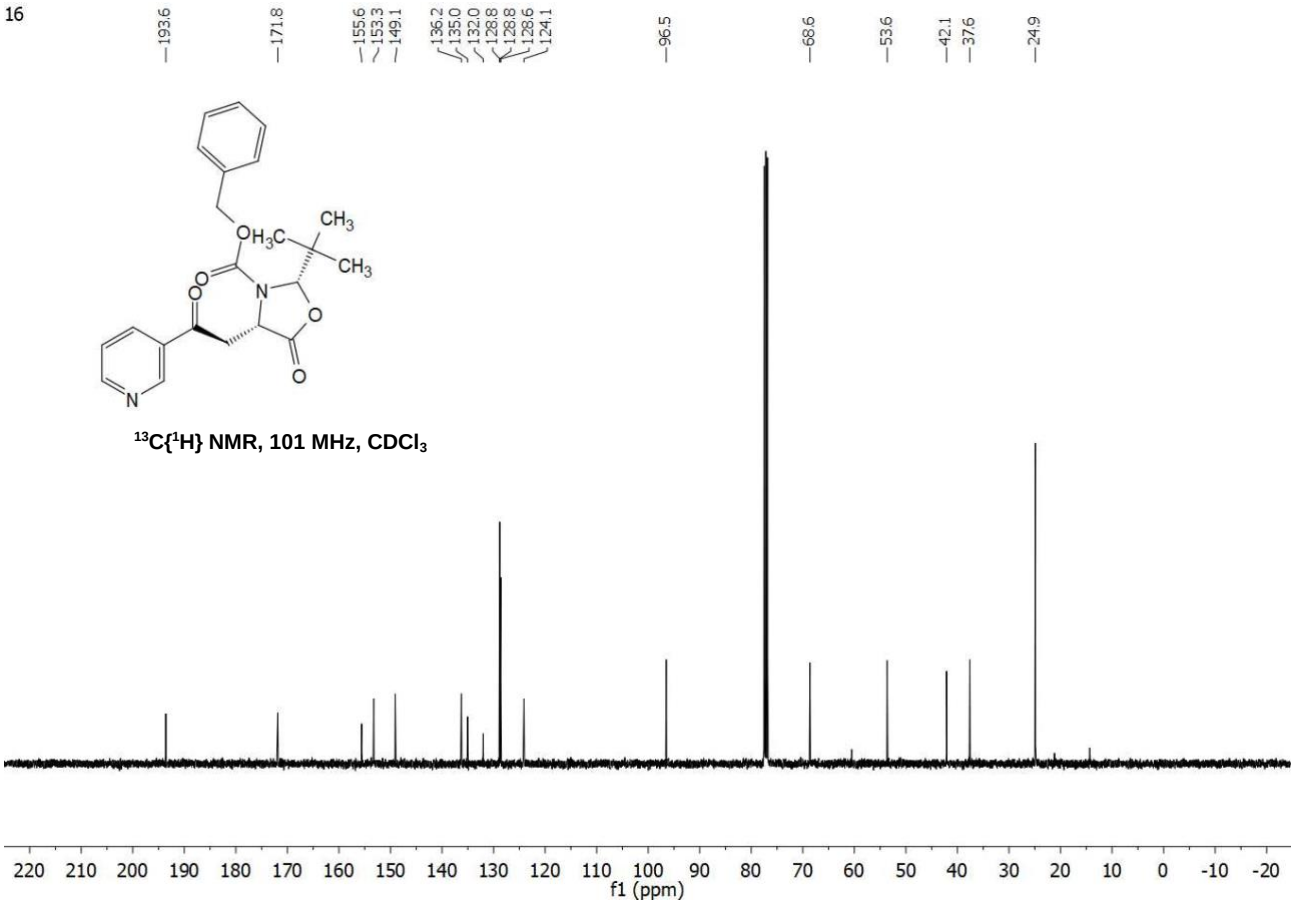


**$^{13}$C{$^{1}$H} NMR, 101 MHz, $CDCl_3$**

**Benzyl (2S,4S)-2-(tert-butyl)-4-(2-(1,3-dimethyl-1H-pyrazolo[3,4-b]pyridin-5-yl)-2-oxoethyl)-5-oxooxazolidine-3-carboxylate (17)**

17

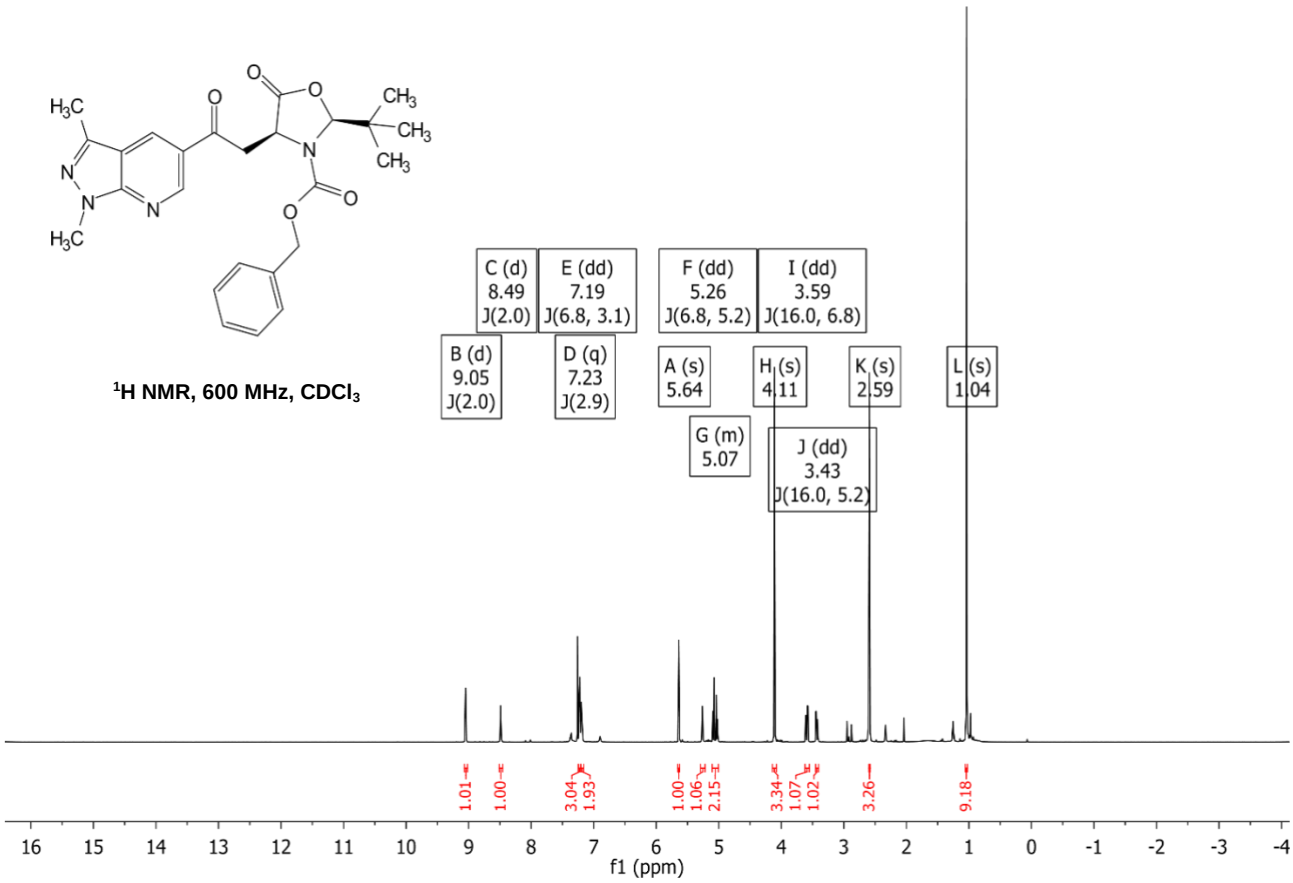


**$^{1}$H NMR, 600 MHz, $CDCl_3$**

17

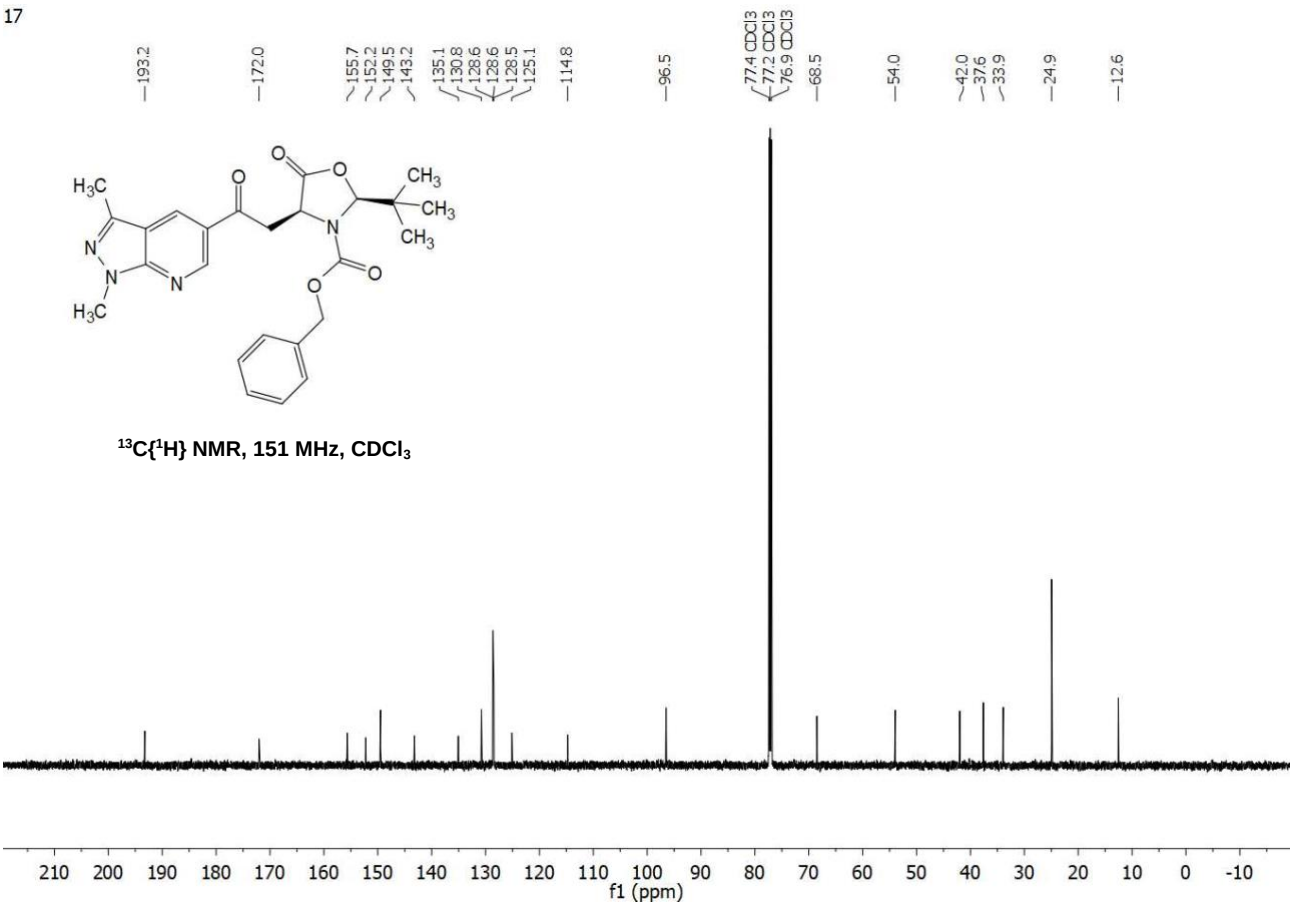


**$^{13}C\{^{1}H\}$ NMR, 151 MHz, $CDCl_3$**

**benzyl (2S,4S)-2-(tert-butyl)-4-(2-(4-chloro-1,3-dimethyl-1H-pyrazolo[3,4-b]pyridin-5-yl)-2-oxoethyl)-5-oxooxazolidine-3-carboxylate (17')**

17'



**$^{1}$H NMR, 400 MHz, $CDCl_3$**

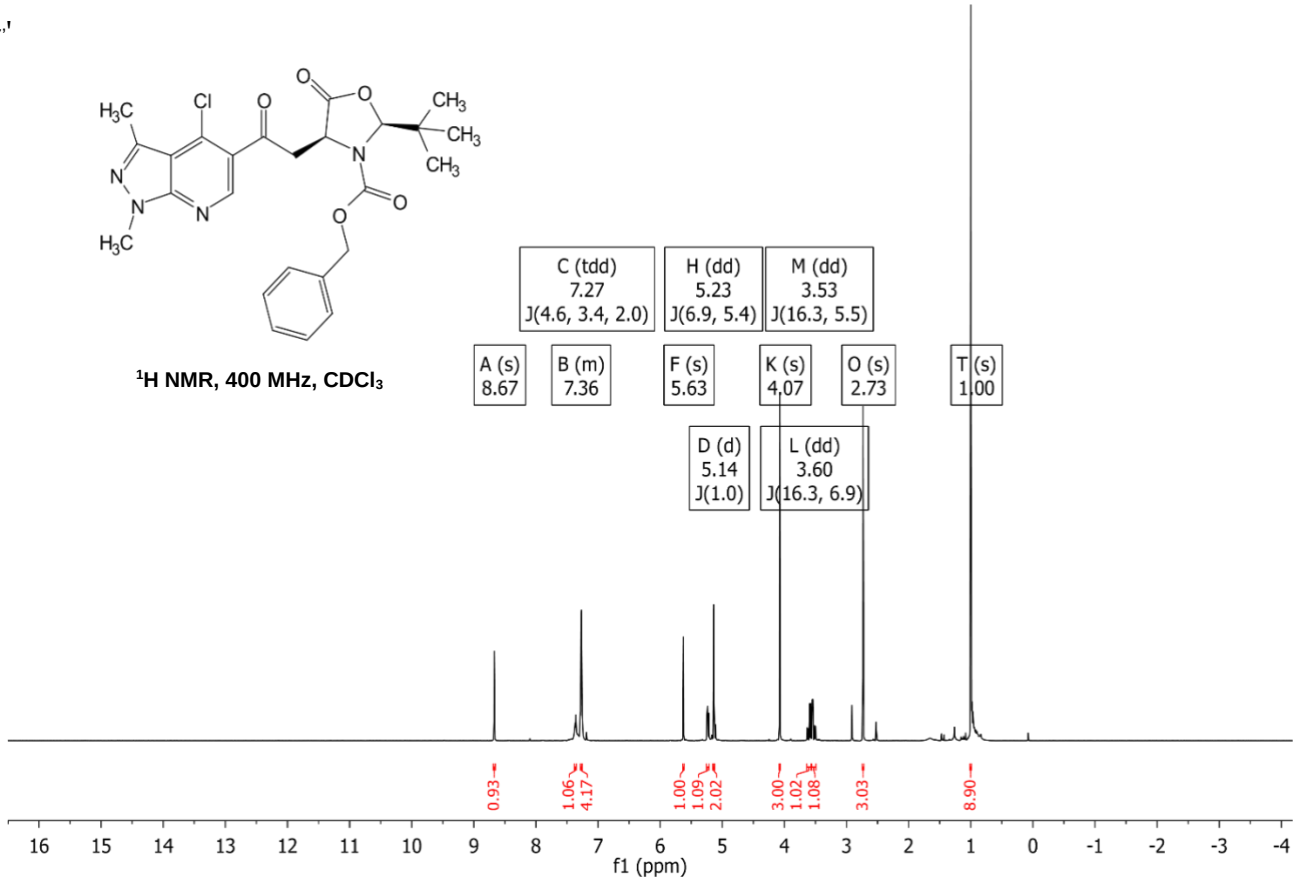


17'



**$^{13}$C{$^{1}$H} NMR, 101 MHz, $CDCl_3$**

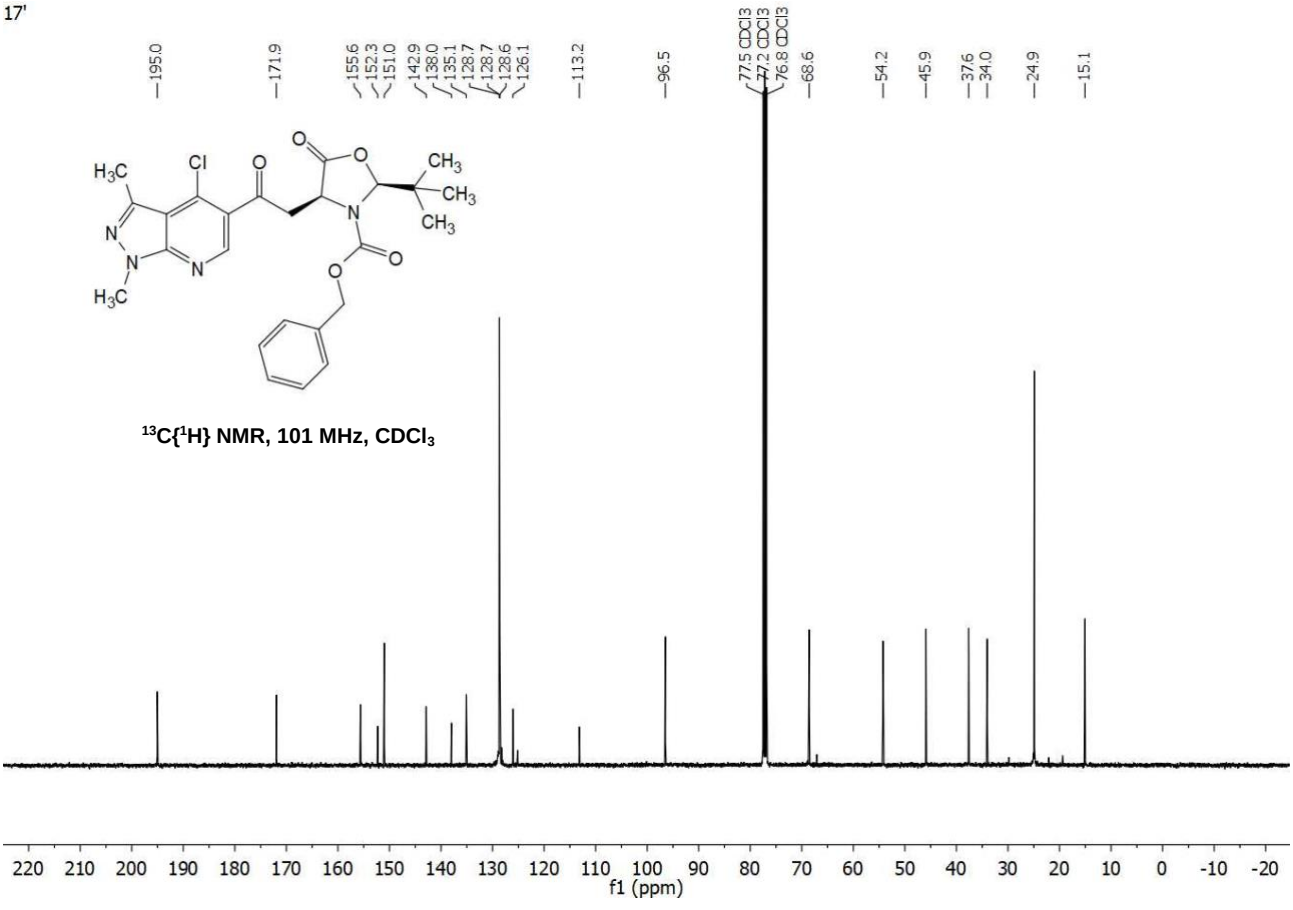

**Benzyl (2S,4S)-2-(tert-butyl)-5-oxo-4-(2-oxo-2-(1H-pyrrol-2-yl)ethyl)oxazolidine-3-carboxylate (20)**

20



**$^{1}$H NMR, 600 MHz, $CDCl_3$**

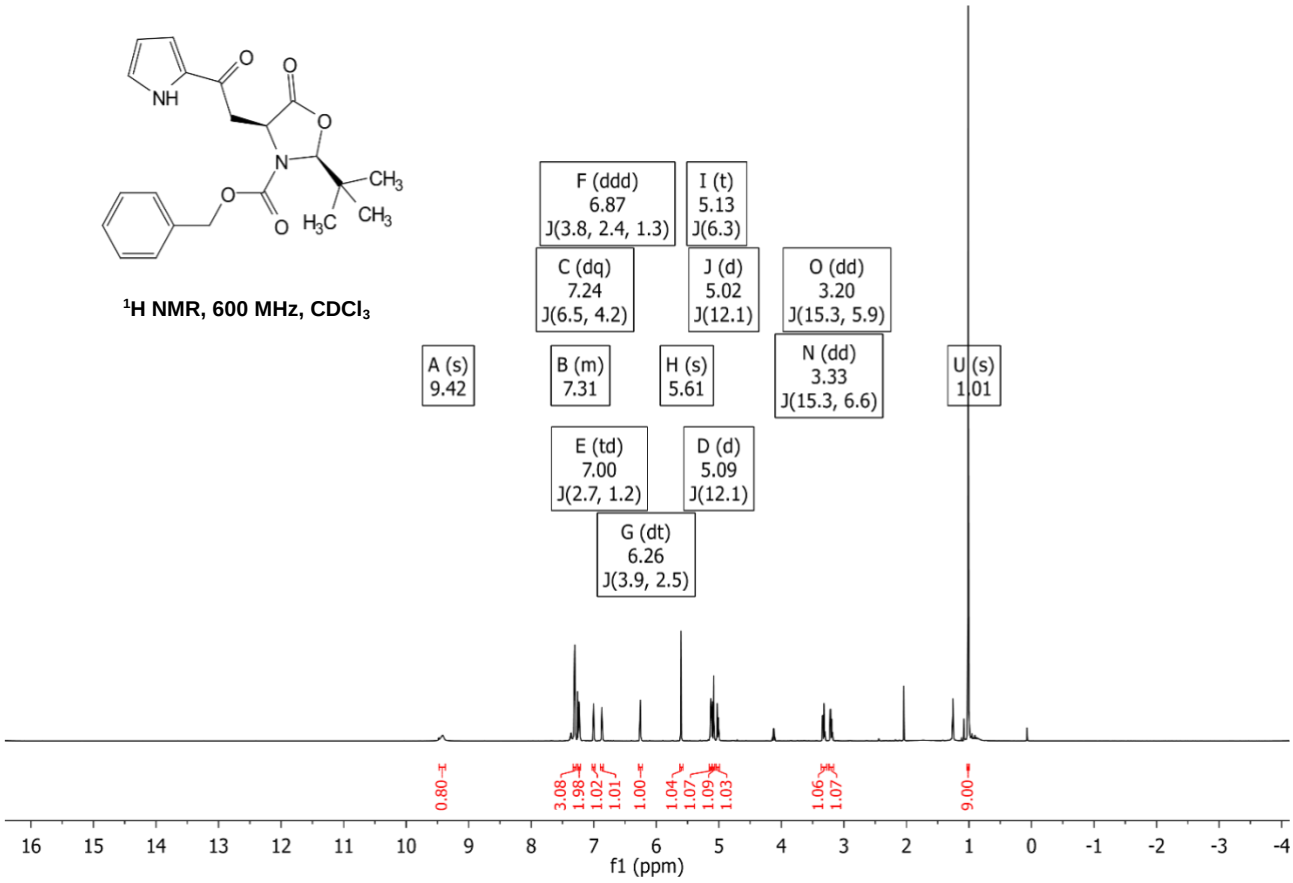


20



**$^{13}$C{$^{1}$H} NMR, 151 MHz, $CDCl_3$**

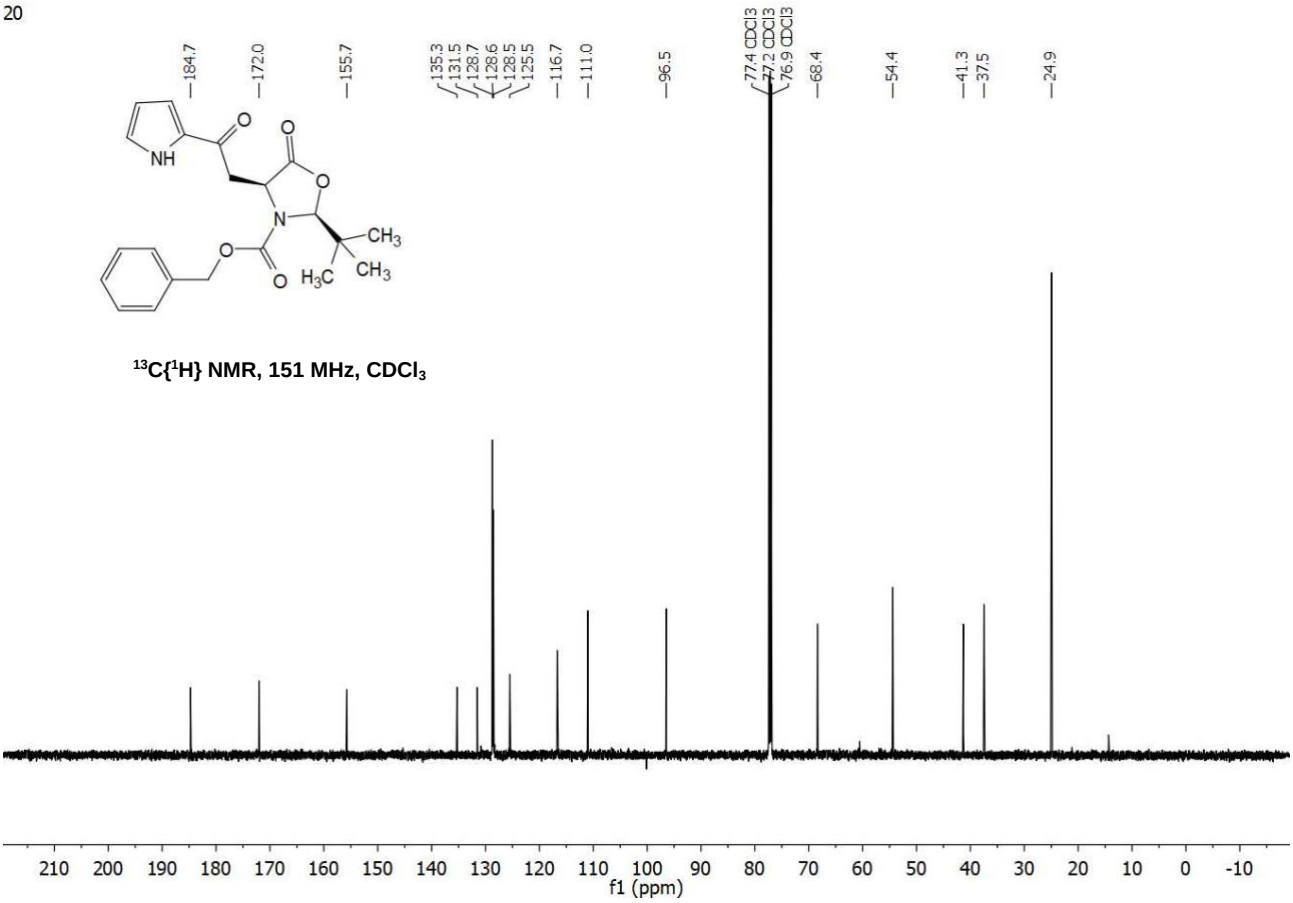

**Benzyl (2S,4S)-2-(tert-butyl)-4-(2-(furan-2-yl)-2-oxoethyl)-5-oxooxazolidine-3-carboxylate (21)**

21



**$^{1}$H NMR, 400 MHz, $CDCl_3$**

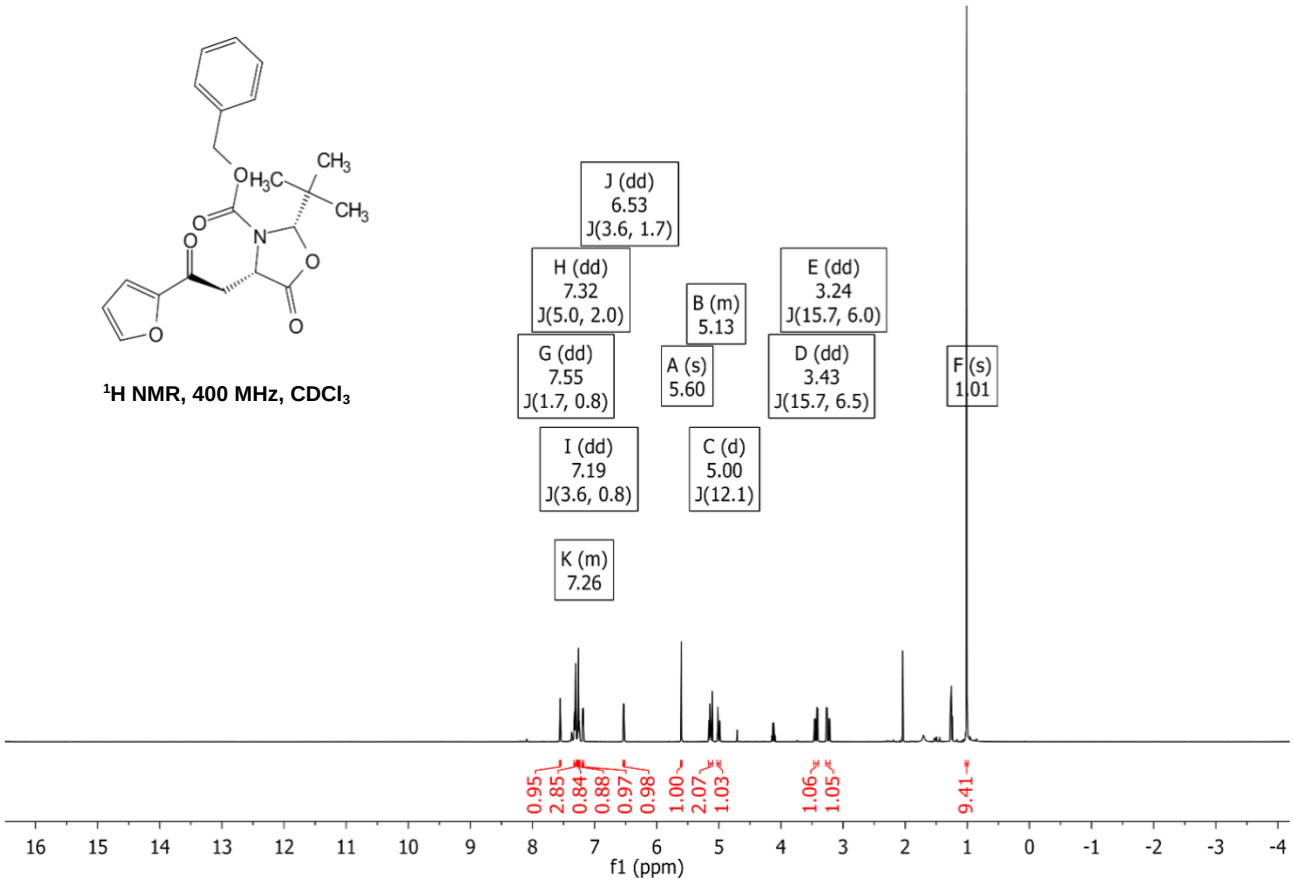


21



**$^{13}$C{$^{1}$H} NMR, 101 MHz, $CDCl_3$**

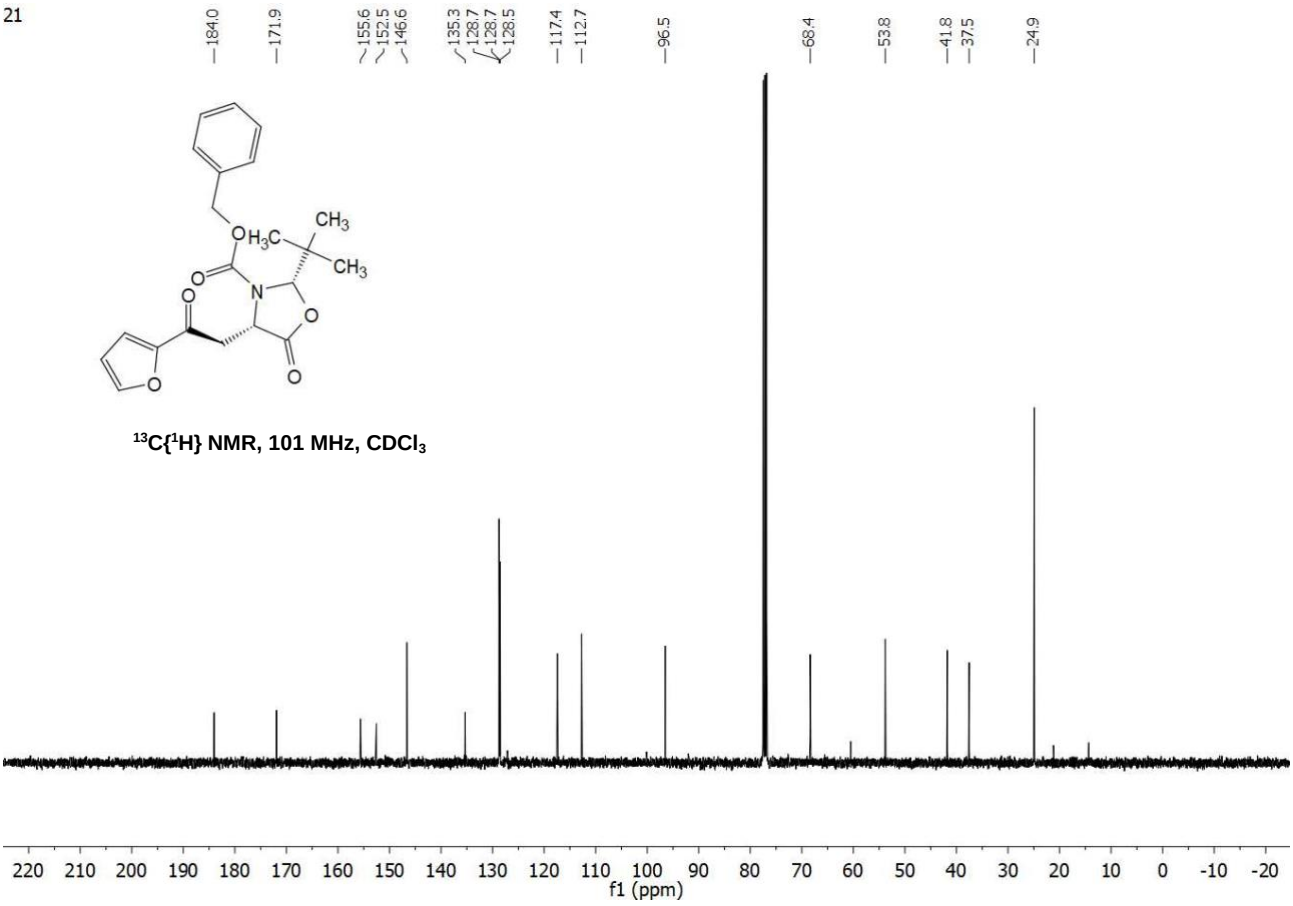

**Benzyl (2S,4S)-2-(tert-butyl)-5-oxo-4-(2-oxo-2-(thiophen-2-yl)ethyl)oxazolidine-3-carboxylate (22)**

22

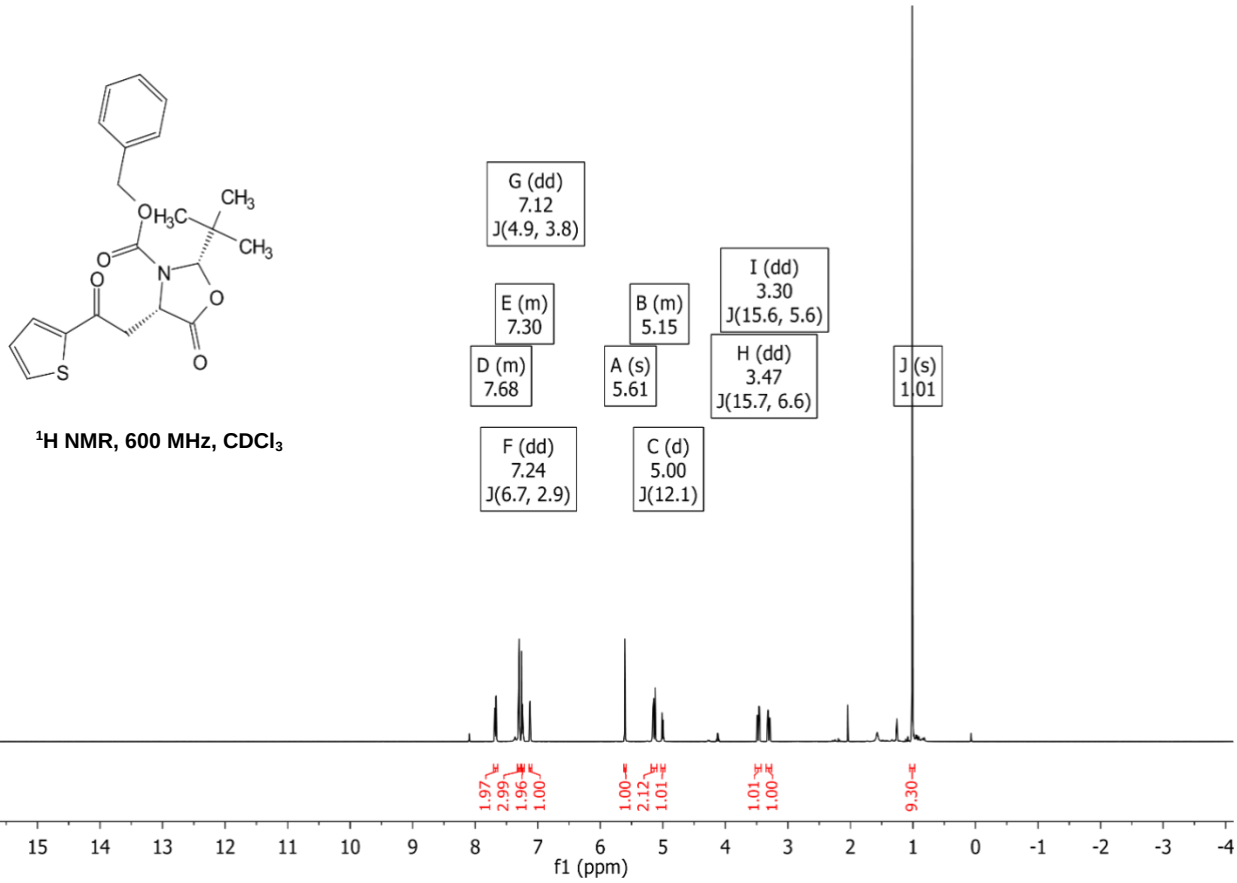


**$^{1}$H NMR, 600 MHz, $CDCl_3$**

22

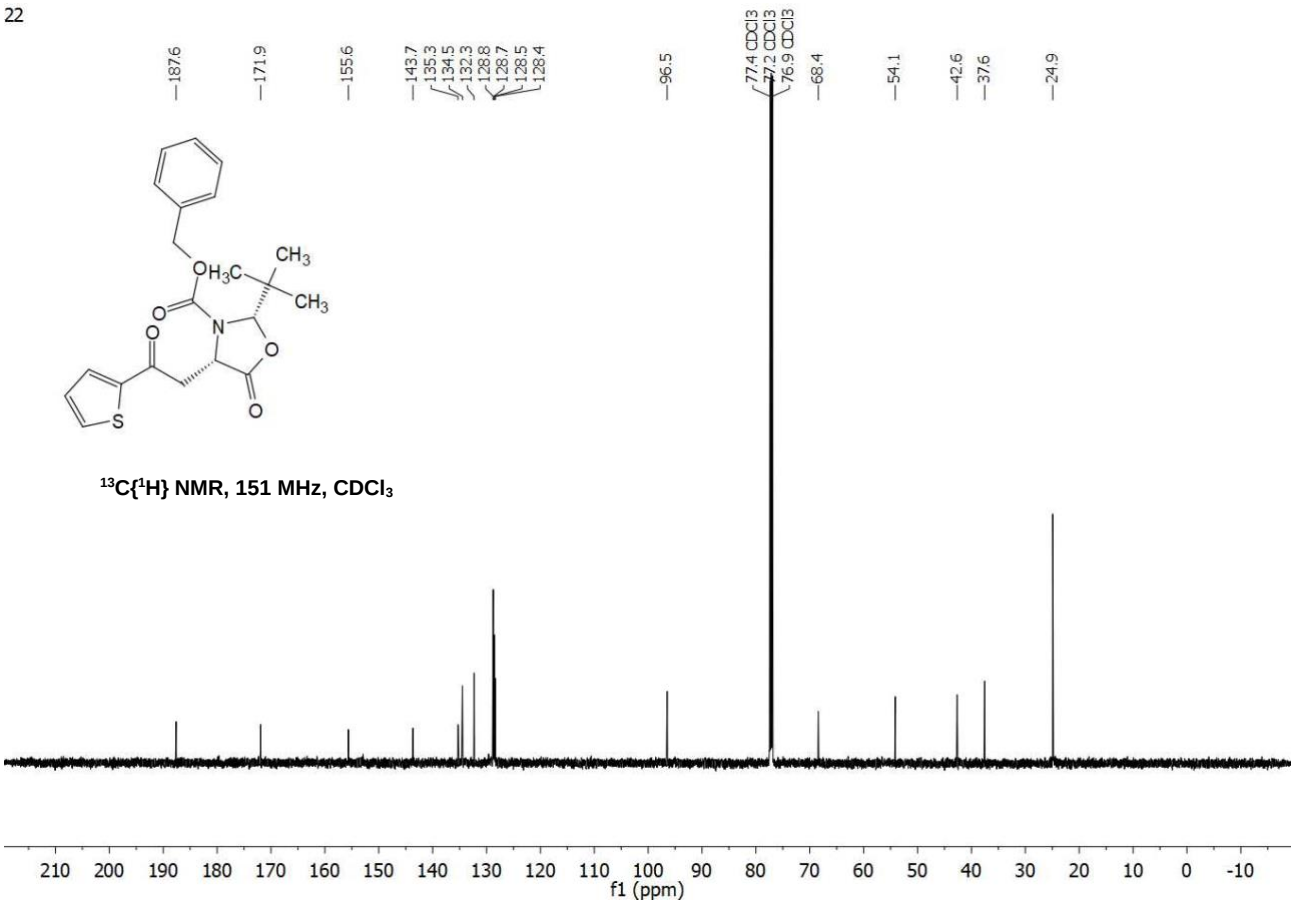


**$^{13}$C{$^{1}$H} NMR, 151 MHz, $CDCl_3$**

**Benzyl (2S,4S)-2-(tert-butyl)-4-(2-(cyclohex-1-en-1-yl)-2-oxoethyl)-5-oxooxazolidine-3-carboxylate (23)**

23

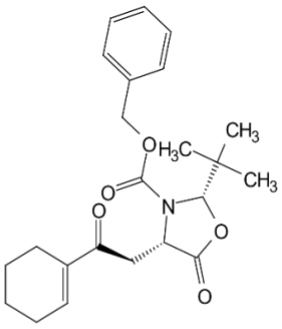

**$^{1}$H NMR, 600 MHz, $CDCl_3$**

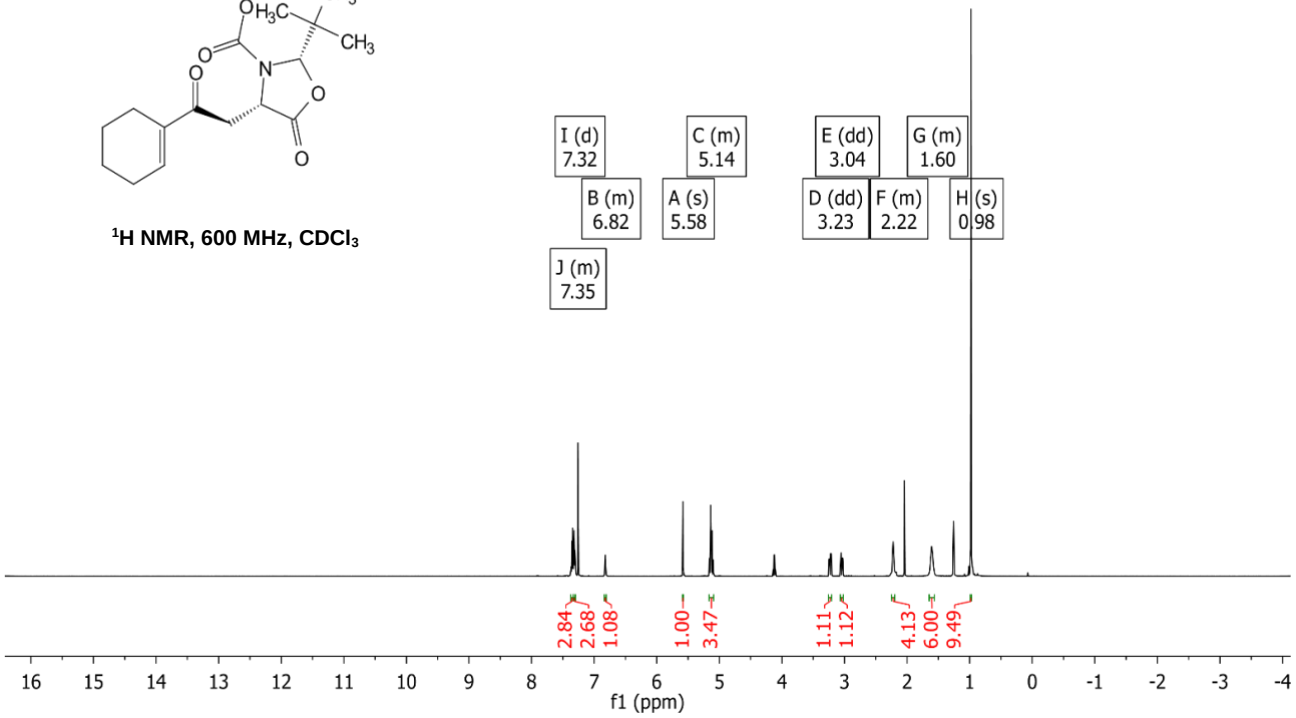


23



**$^{13}$C{$^{1}$H} NMR, 101 MHz, $CDCl_3$**

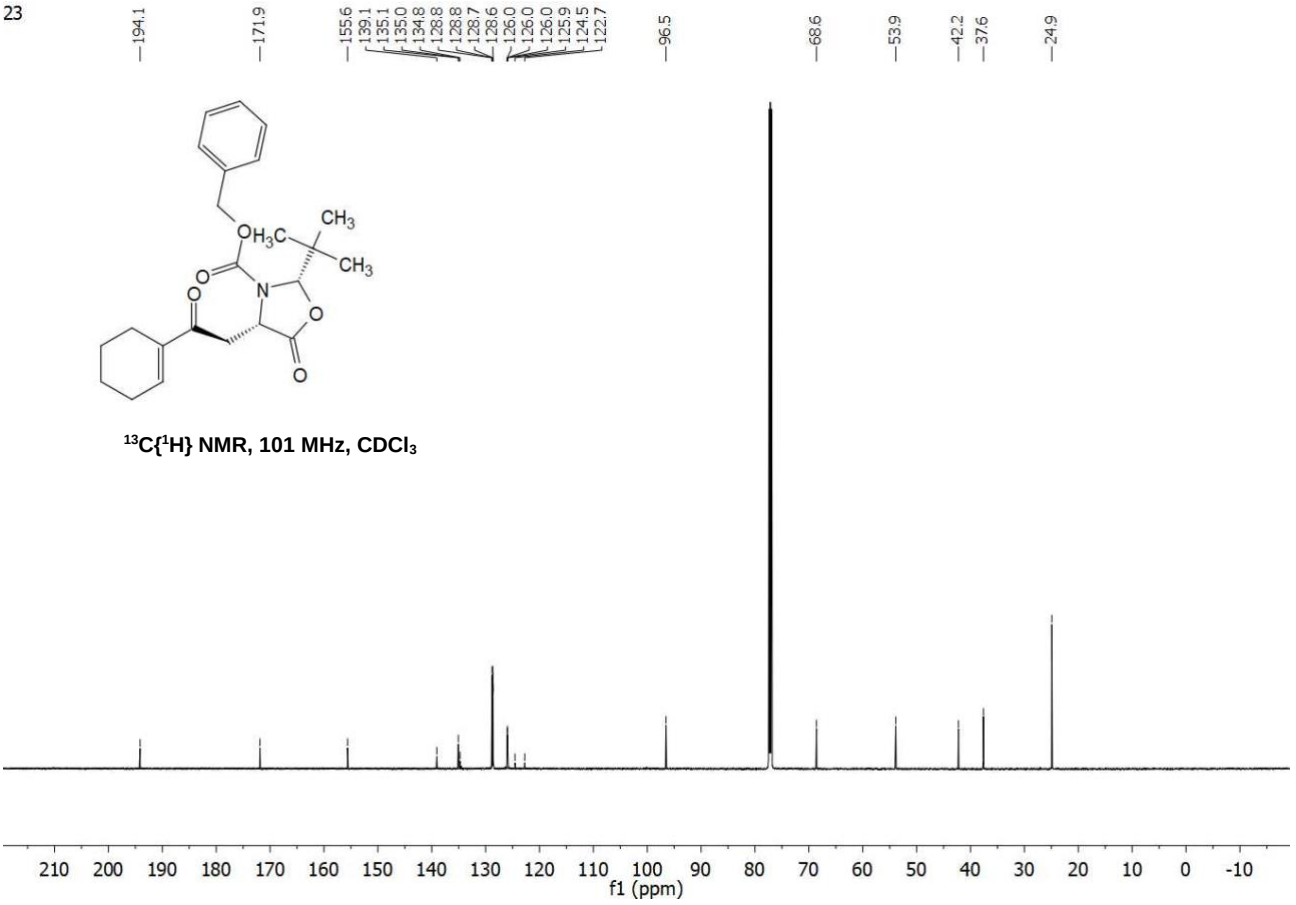

**Benzyl (2S,4S)-2-(tert-butyl)-4-(2-(3,4-dihydro-2H-pyran-5-yl)-2-oxoethyl)-5-oxooxazolidine-3-carboxylate (24)**

24



**$^{1}$H NMR, 600 MHz, $CDCl_3$**

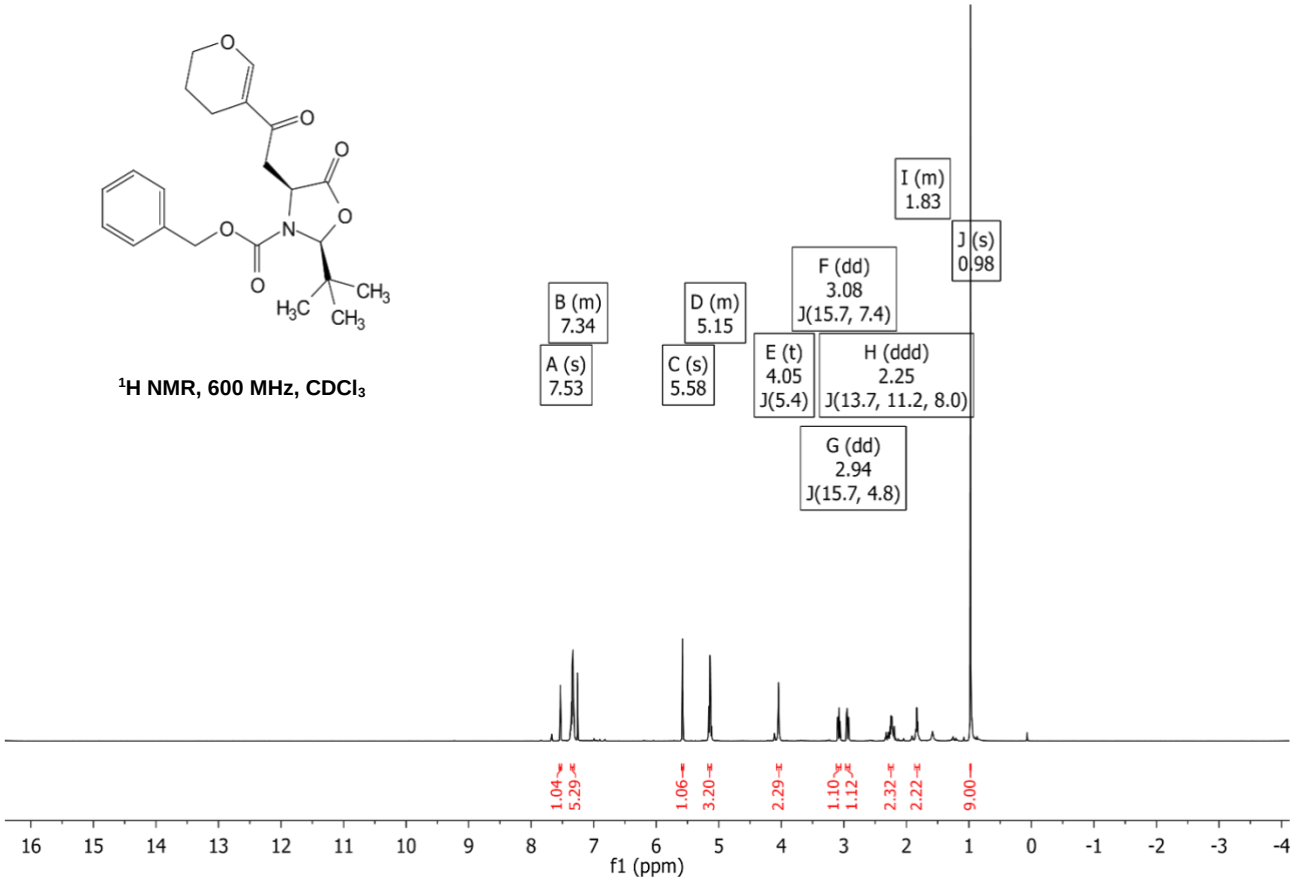


24



**$^{13}$C{$^{1}$H} NMR, 151 MHz, $CDCl_3$**

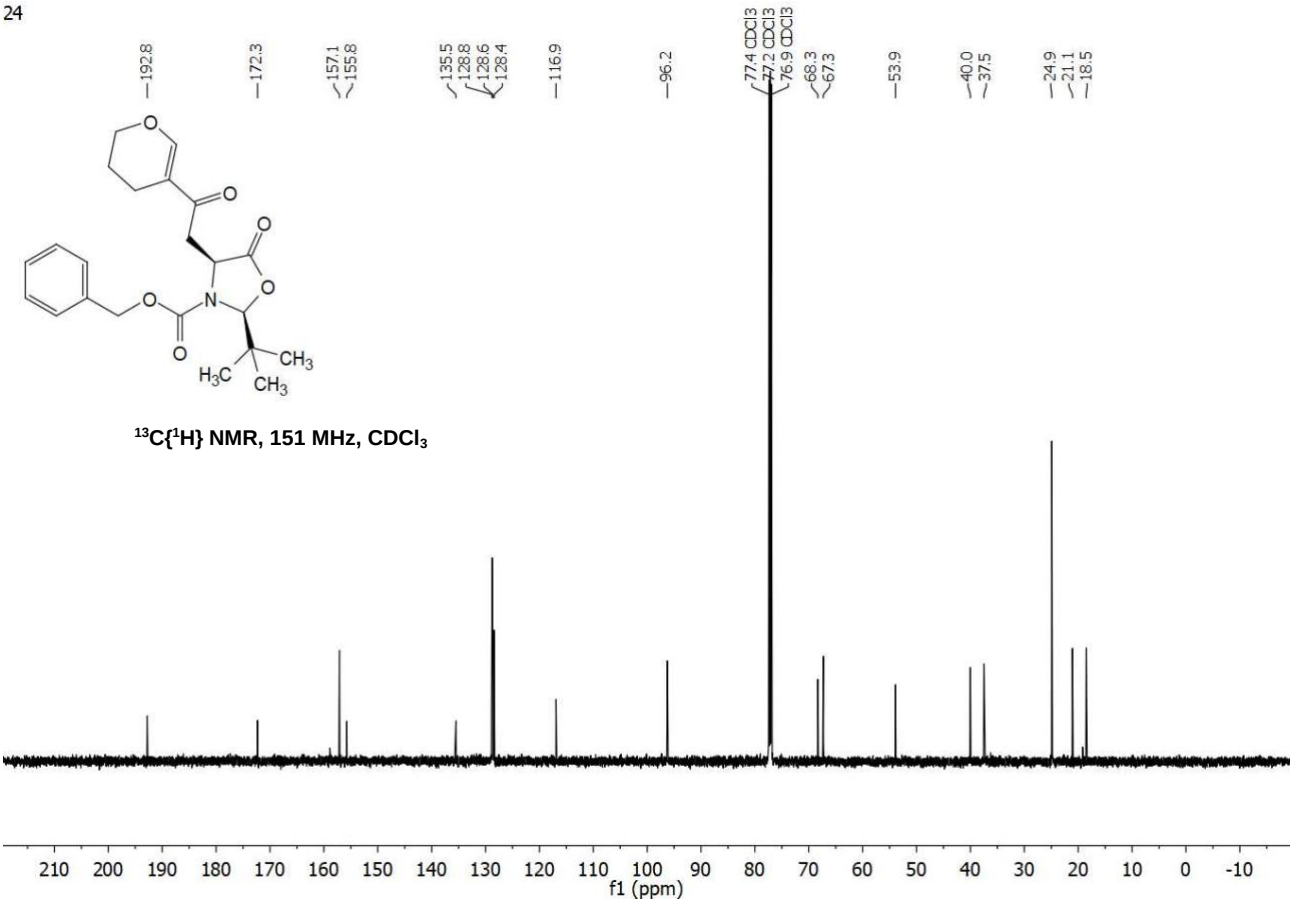

**Benzyl (2S,4S)-4-(2-(1-(tert-butoxycarbonyl)-1,2,5,6-tetrahydropyridin-3-yl)-2-oxoethyl)-2-(tert-butyl)-5-oxooxazolidine-3-carboxylate (26)**

26



**$^{1}$H NMR, 600 MHz, $CDCl_3$**

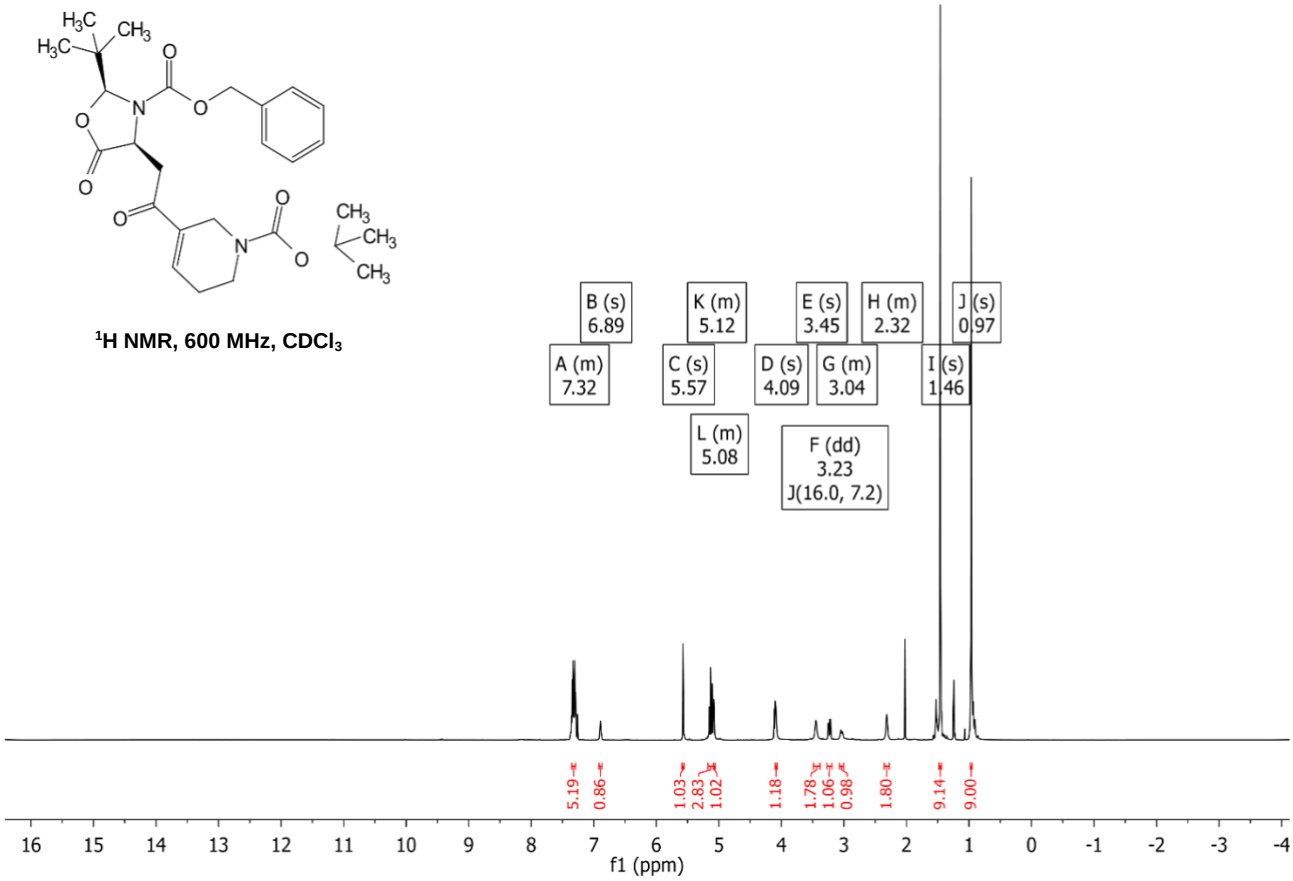


26



**$^{13}$C{$^{1}$H} NMR, 151 MHz, $CDCl_3$**

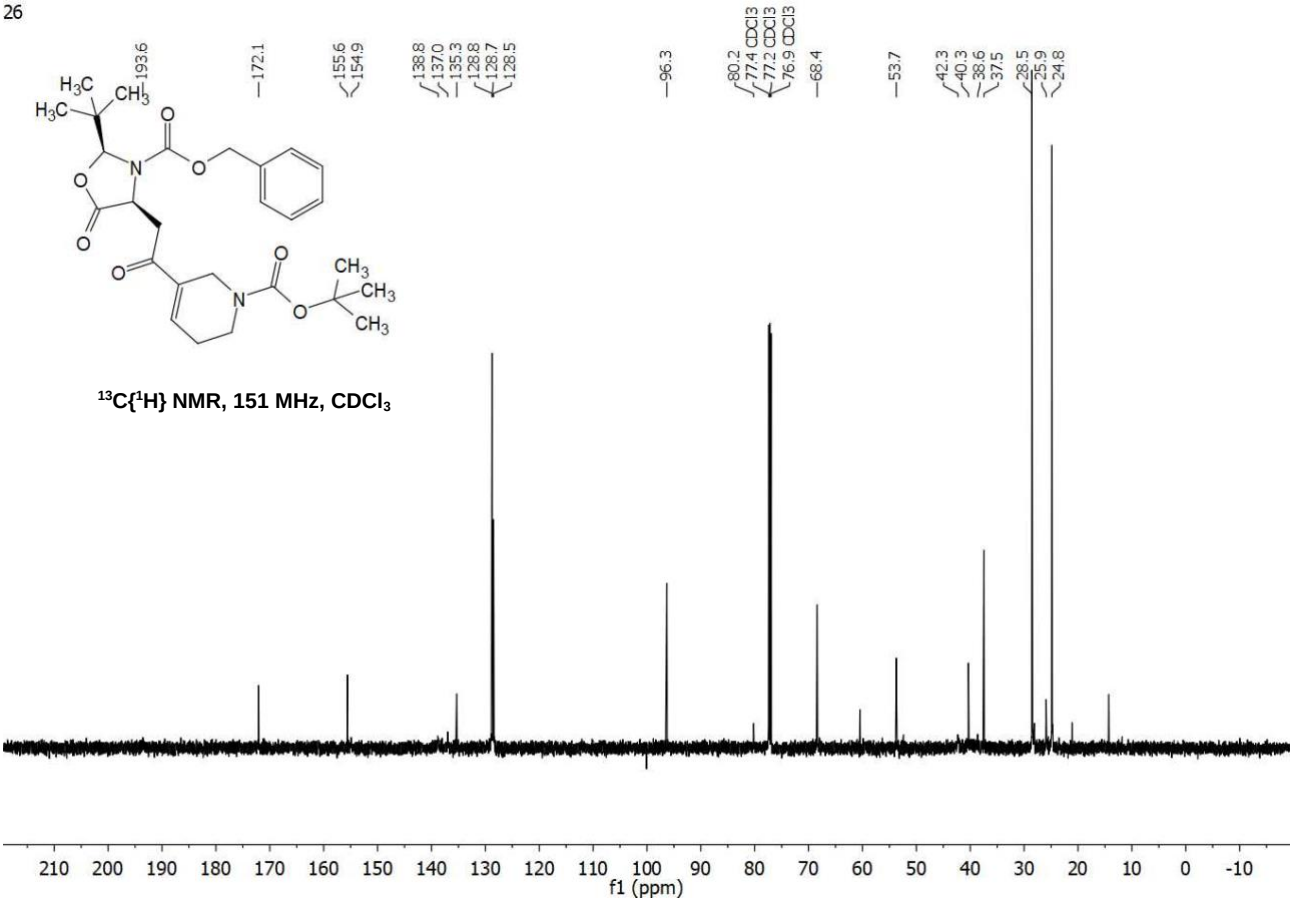

**Benzyl 2-(tert-butyl)-4-(2-(4,5-dihydrofuran-3-yl)-2-oxoethyl)-5-oxooxazolidine-3-carboxylate (27)**

27



**$^{1}$H NMR, 400 MHz, $CDCl_3$**

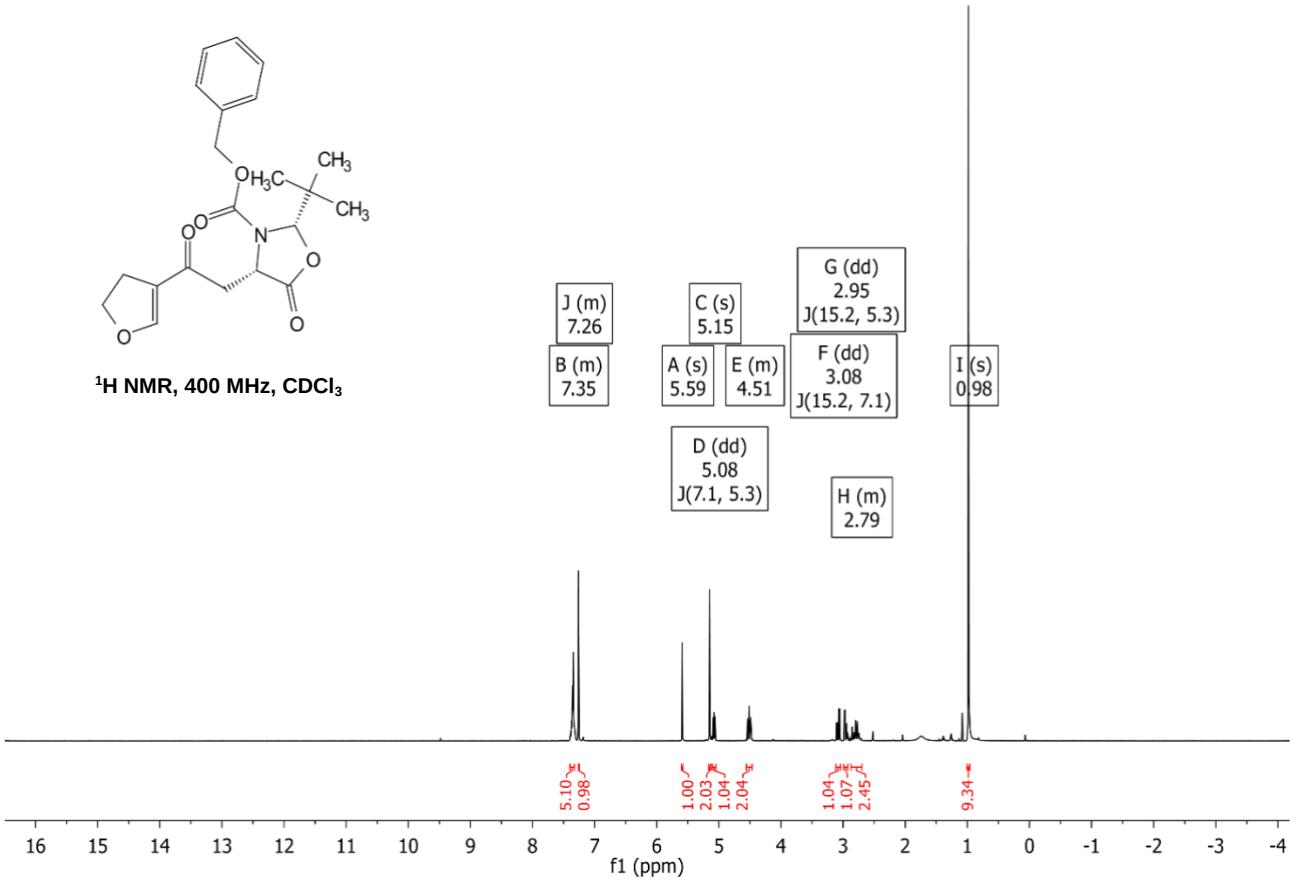


27



**$^{13}$C{$^{1}$H} NMR, 101 MHz, $CDCl_3$**

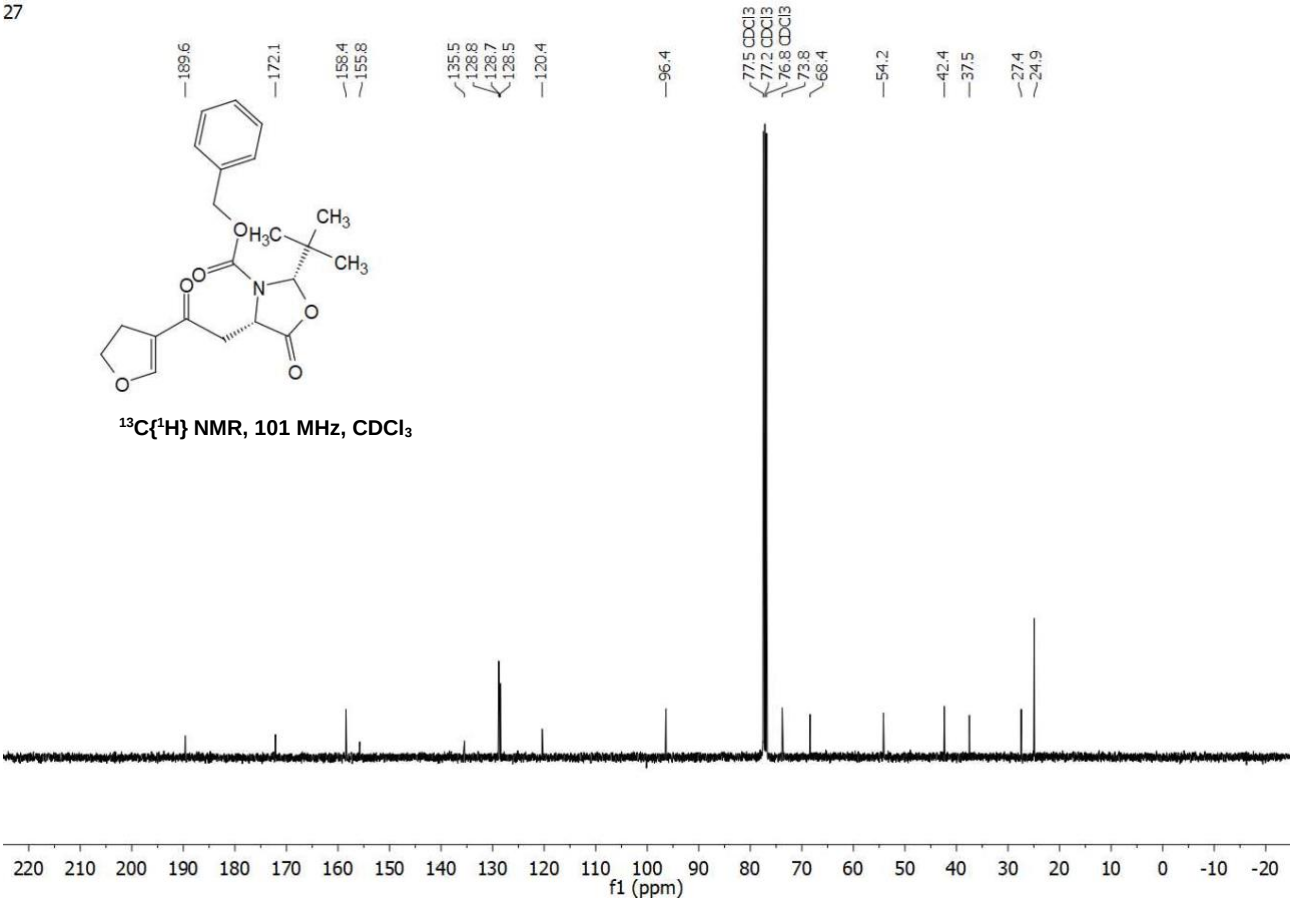

**(S)-2-amino-4-(2-hydroxyphenyl)-4-oxobutanoic acid hydrochloride salt (28)**

28




**$^{1}$H NMR, 400 MHz, $D_2O$**

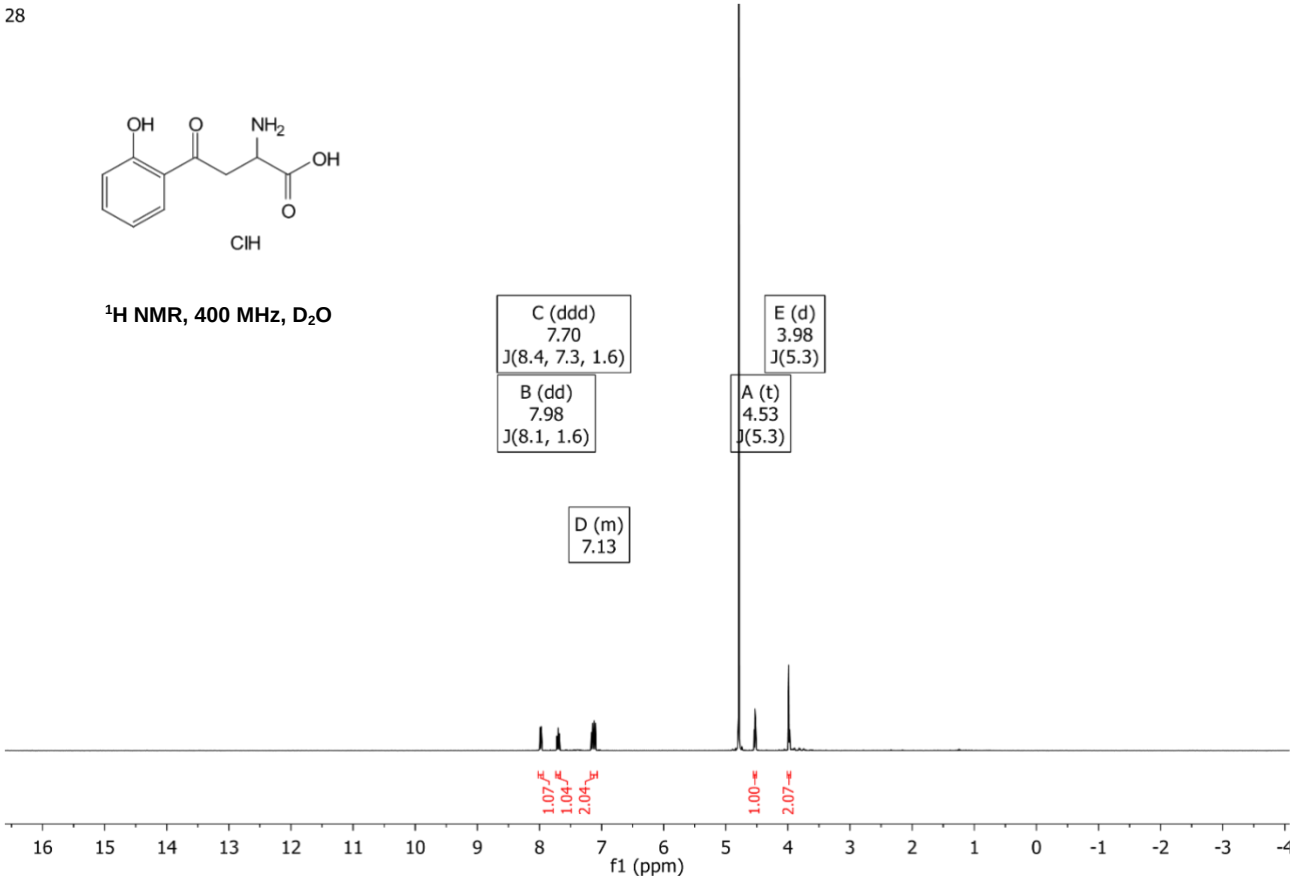


28

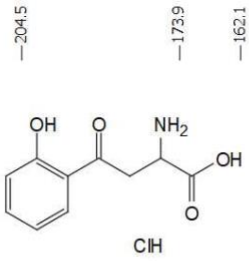


**$^{13}$C{$^{1}$H} NMR, 101 MHz, $D_2O$**

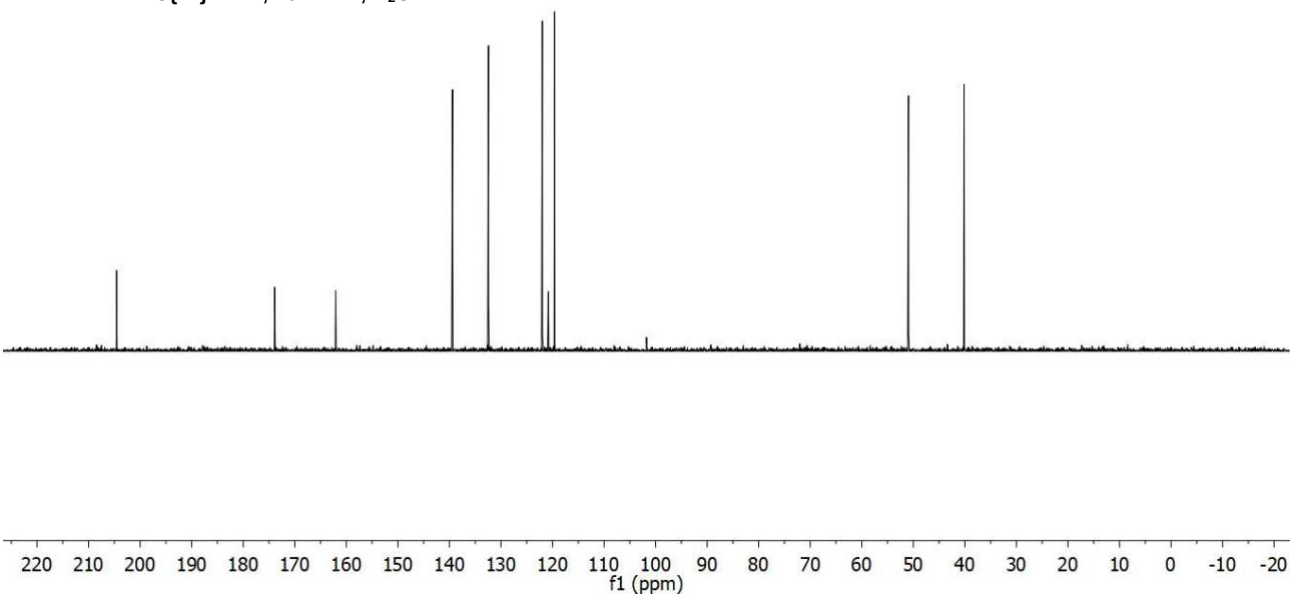

**(S)-2-amino-4-(2-chlorophenyl)-4-oxobutanoic acid hy-drochloride salt (29)**

29

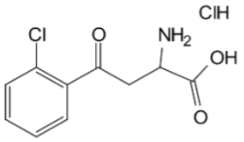


**$^{1}$H NMR, 400 MHz, $D_2O$**

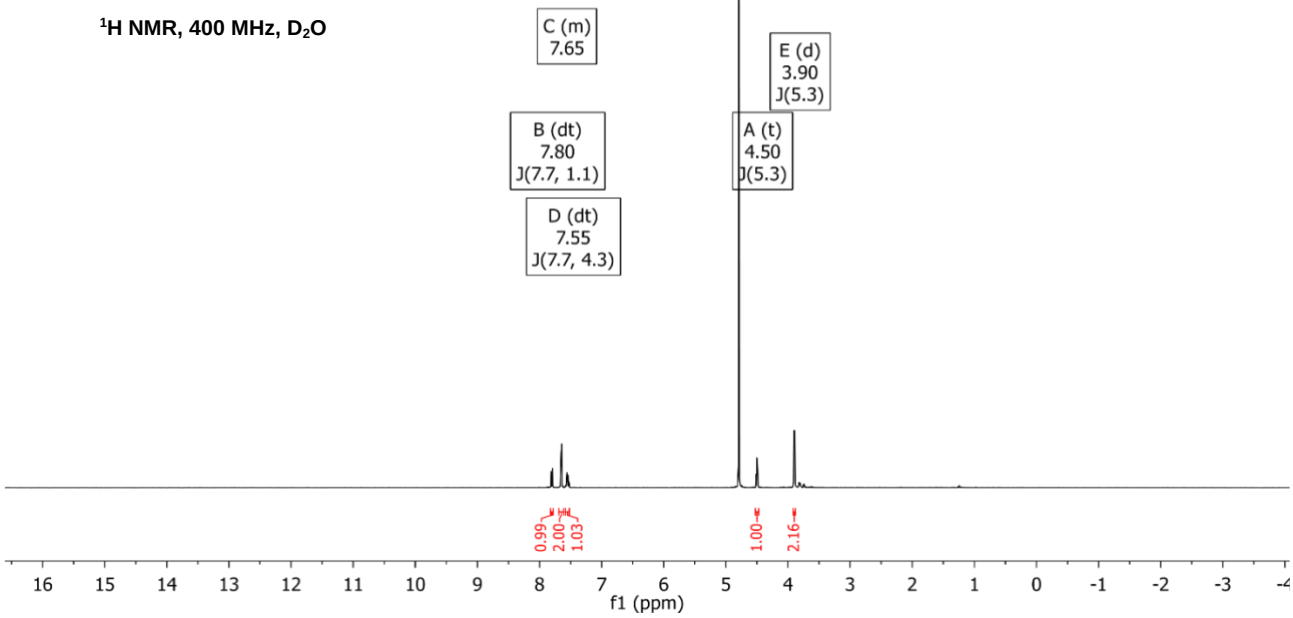


29




**$^{13}$C{$^{1}$H} NMR, 101 MHz, $D_2O$**

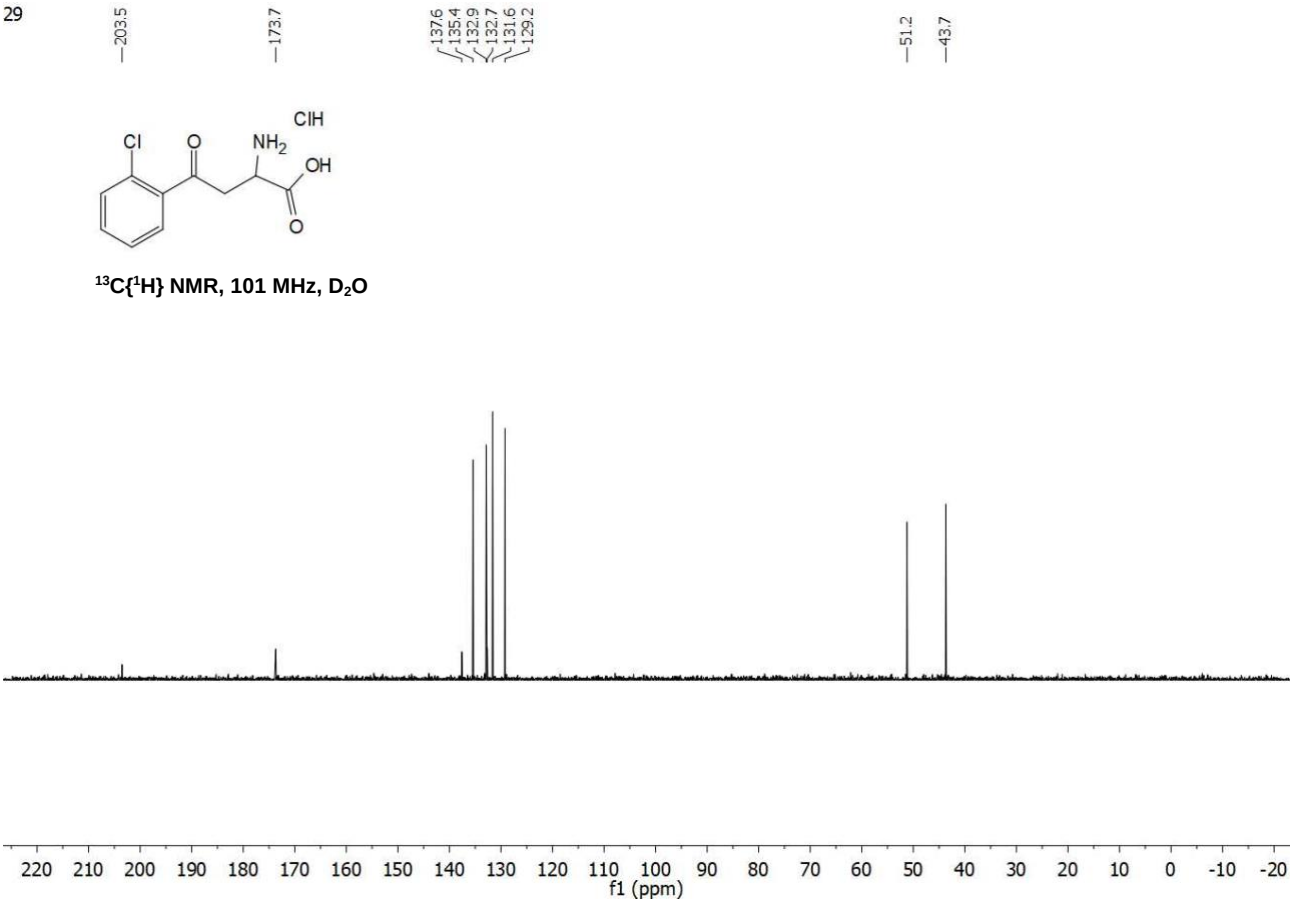

**(S)-2-amino-4-oxo-4-(pyridin-3-yl)butanoic acid hydro-chloride salt (30)**

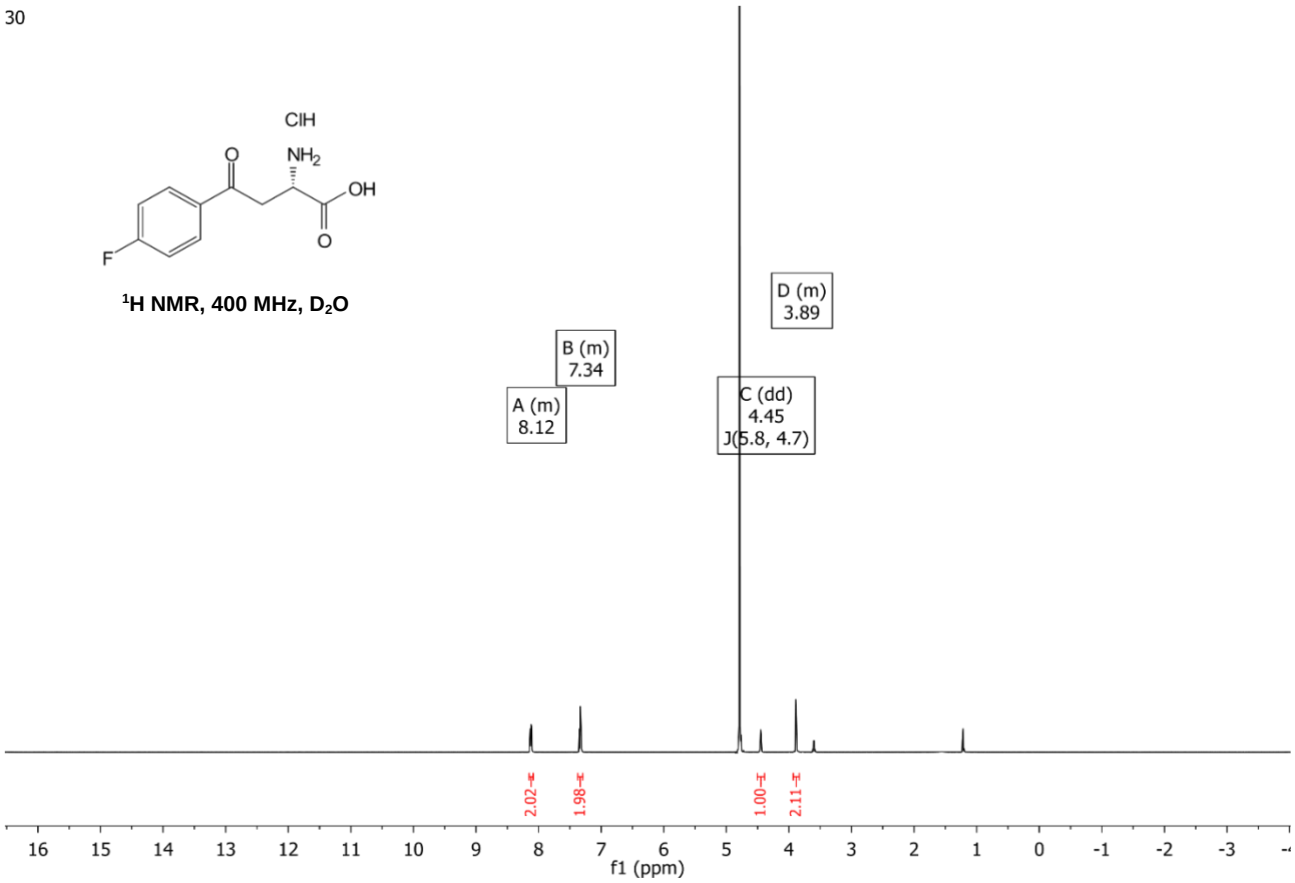

## HPLC chromatogram

HPLC analysis of Methyl 2-((tert-butoxycarbonyl)amino)-4-oxo-4-phenylbutanoate.

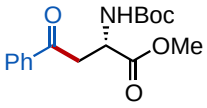


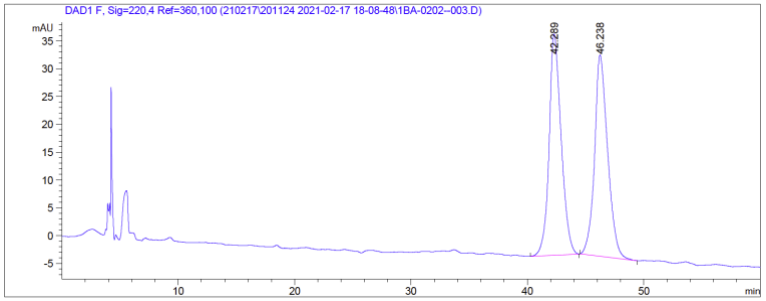


Signal 1: DAD1 F, Sig=220,4 Ref=360,100

| Peak # | RetTime [min] | Type | Width [min] | Area [mAU*s] | Height [mAU] | Area % |
|---|---|---|---|---|---|---|
| 1 | 42.289 | BB | 1.0620 | 2856.21436 | 39.76207 | 50.2073 |
| 2 | 46.238 | BB | 1.1189 | 2832.62427 | 36.19992 | 49.7927 |
| Totals : | | | | 5688.83862 | 75.96199 | |

**Figure S5.** HPLC chromatogram of racemate.

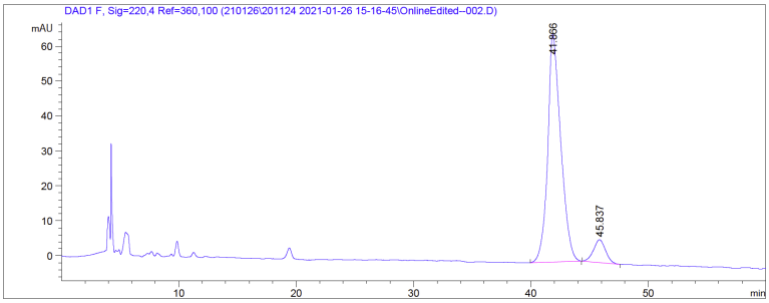


Signal 1: DAD1 F, Sig=220,4 Ref=360,100

| Peak # | RetTime [min] | Type | Width [min] | Area [mAU*s] | Height [mAU] | Area % |
|---|---|---|---|---|---|---|
| 1 | 41.866 | BB | 1.0945 | 5026.87646 | 65.12625 | 91.5371 |
| 2 | 45.837 | BB | 0.9308 | 464.74814 | 6.52664 | 8.4629 |
| Totals : | | | | 5491.62460 | 71.65289 | |

**Figure S6.** HPLC chromatogram of enantiopure compound.

## References


1. Cismesia, M. A.; Yoon, T. P. Characterizing chain processes in visible light photoredox catalysis. *Chem. Sci.* **2015,** *6*, 5426.
2. Kuhn, H. J.; Braslavsky, S. E.; Schmidt, R. *Pure Appl. Chem*. **2004**, *76*, 2105-2146.
3. Monalti, M. et. al. Chemical Actinometry. *Handbook of Photochemistry*, 3rd Ed; Taylor & Francis Group, LLC. Boca Raton, FL, **2006**, 601.
4. Hatchard, C. G.; Parker, C. A.; Bowen Edmund, J. A new sensitive chemical actinometer - II. Potassium ferrioxalate as a standard chemical actinometer. *Proceedings of the Royal Society of London. Series A. Mathematical and Physical Sciences* **1956,** *235*, 518.
5. Lowry, M. S.; Goldsmith, J. I.; Slinker, J. D.; Rohl, R.; Pascal, R. A.; Malliaras, G. G.; Bernhard, S. Single-Layer Electroluminescent Devices and Photoinduced Hydrogen Production from an Ionic Iridium(III) Complex. *Chem. Mat.* **2005,** *17*, 5712.
6. Pandey, G.; Pooranchand, D.; Bhalerao, U. T. Photoinduced single electron transfer activation of organophosphines: Nucleophilic trapping of phosphine radical cation. *Tetrahedron* **1991,** *47*, 1745.
7. Ohmatsu, K.; Nakashima, T.; Sato, M.; Ooi, T. Direct allylic C–H alkylation of enol silyl ethers enabled by photoredox–Brønsted base hybrid catalysis. *Nat. Commun.* **2019,** *10*, 2706.